LDPC CODE-BASED BANDWIDTH EFFICIENT CODING SCHEMES FOR WIRELESS COMMUNICATIONS

A Dissertation

by

HARI SANKAR

Submitted to the Office of Graduate Studies of
Texas A&M University
in partial fulfillment of the requirements for the degree of

DOCTOR OF PHILOSOPHY

August 2006

Major Subject: Electrical Engineering

LDPC CODE-BASED BANDWIDTH EFFICIENT CODING SCHEMES FOR WIRELESS COMMUNICATIONS

A Dissertation

by

HARI SANKAR

Submitted to the Office of Graduate Studies of
Texas A&M University
in partial fulfillment of the requirements for the degree of

DOCTOR OF PHILOSOPHY

Approved by:

Chair of Committee,	Krishna R. Narayanan
Committee Members,	Costas N. Georghiades
	Sunil Khatri
	Thomas E. Wehrly
Head of Department,	Costas N. Georghiades

August 2006

Major Subject: Electrical Engineering

ABSTRACT

LDPC Code-Based Bandwidth Efficient Coding Schemes
for Wireless Communications. (August 2006)
Hari Sankar, B. Tech, Indian Institute of Technology, Madras
Chair of Advisory Committee: Dr. Krishna R. Narayanan

This dissertation deals with the design of bandwidth-efficient coding schemes with Low-Density Parity-Check (LDPC) for reliable wireless communications. Code design for wireless channels roughly falls into three categories: (1) when channel state information (CSI) is known only to the receiver (2) more practical case of partial CSI at the receiver when the channel has to be estimated (3) when CSI is known to the receiver as well as the transmitter. We consider coding schemes for all the above categories.

For the first scenario, we describe a bandwidth efficient scheme which uses high-order constellations such as QAM over both AWGN as well as fading channels. We propose a simple design with LDPC codes which combines the good properties of Multi-level Coding (MLC) and bit-interleaved coded-modulation (BICM) schemes. Through simulations, we show that the proposed scheme performs better than MLC for short-medium lengths on AWGN and block-fading channels. For the first case, we also characterize the rate-diversity tradeoff of MIMO-OFDM and SISO-OFDM systems. We design optimal coding schemes which achieve this tradeoff when transmission is from a constrained constellation. Through simulations, we show that with a sub-optimal iterative decoder, the performance of this coding scheme is very close to the optimal limit for MIMO (flat quasi-static fading), MIMO-OFDM and SISO-

OFDM systems.

For the second case, we design non-systematic Irregular Repeat Accumulate (IRA) codes, which are a special class of LDPC codes, for Inter-Symbol Interference (ISI) fading channels when CSI is estimated at the receiver. We use Orthogonal Frequency Division Multiplexing (OFDM) to convert the ISI fading channel into parallel flat fading subchannels. We use a simple receiver structure that performs iterative channel estimation and decoding and use non-systematic IRA codes that are optimized for this receiver. This combination is shown to perform very close to a receiver with perfect CSI and is also shown to be robust to change in the number of channel taps and Doppler.

For the third case, we look at bandwidth efficient schemes for fading channels that perform close to capacity when the channel state information is known at the transmitter as well as the receiver. Schemes that achieve capacity with a Gaussian codebook for the above system are already known but not for constrained constellations. We derive the near-optimum scheme to achieve capacity with constrained constellations and then propose coding schemes which perform close to capacity. Through linear transformations, a MIMO system can be converted into non-interfering parallel subchannels and we further extend the proposed coding schemes to the MIMO case too.

To my family

ACKNOWLEDGMENTS

I feel that two pages are insufficient to fully thank all the people who inspired me in making this dissertation a reality. If I have missed any of your names here, I apologize and am indebted to you for all your help.

First and foremost, I want to thank my advisor, Dr. Krishna R. Narayanan, who has been a very inspiring role-model, teacher, supporter (both monetarily as well as mentally!) and friend. Without his knowledge and inspiration, this work would never have been possible. Both on bad days and good, he has been a very patient supporter and I cannot fully express my gratitude to him in words. I have learned many important qualities from him, which are required in a successful researcher, such as being methodical, hard-working, being inquisitive and patient. I thank you, Dr. Narayanan, for all your help.

I would like to thank all the members of my committee, Dr. Georghiades, Dr. Khatri and Dr. Wehrly, who have supported me in my research. I took courses under them which strengthened my concept of communications, hardware design and statistics. They also provided me with valuable feedback on my research which helped in improving my work.

I want to thank all my teachers, past and present, for instilling inquisitiveness in me and enriching my knowledge base. Dr. Miller was very patient and clarified many of my basic doubts in communications, all through the five years of my graduate study. I wish to thank him for all his time and effort. Dr. Bhaskar Ramamurthi from IIT-Madras, who was my undergraduate project advisor, shaped my communication fundamentals and was a big inspiration in my pursuing graduate study in this area. I wish to thank him for his guidance and support. I am also grateful to my mathematics teacher in high school, Ms. Chandragupta, who shaped my interest in mathematics.

I wish to thank my supervisors at Qualcomm Inc., (where I interned for close to a year), Juan Montojo, John Ketchum and Bhushan. They were very good mentors and inspired me in my research and are very good friends too. I also wish to thank Tao Luo, Byoung-Hoon, Vinay, Sharad, Kee-Bong, Durga, Avinash, Amal and Shrenik, all of whom work for Qualcomm.

I also wish to thank all my friends at Texas A&M who have made my graduate years so enjoyable and exciting: Angelos, Adriana, Kim, Nitin, Trupti, Janath, Dilani, Zoong, Vivek, Kapil, Abhiram, Argon, Burcu, Sharif, Yakut, Benat, Ezgi, Murray, Jing, Taner, Insilay, Wenyan, Yi, Yongzhe, Hicham, Murat and the list goes on. Thank you for all those wild parties we had, guys!

Words can never express the gratitude that I feel for my parents, my sister and my brother-in-law who have been pillars of support for me through good times and bad times. I thank my parents for all the sacrifices they made in bringing me up, and for providing me with all the opportunities, a very promising future and most importantly, supporting me in all my decisions. I remain indebted to them always!

Last, but not least, I wish to thank my girlfriend, Arzu, for being with me through all the tough times as well as the good ones. She has been a big source of support and inspiration and urged me on in my graduate study during times when I was feeling really low about my research. She has made me a better individual and brought new meaning to my life, and I feel very lucky to have met her.

TABLE OF CONTENTS

CHAPTER Page

CHAPTER Page

LIST OF TABLES

LIST OF FIGURES

FIGURE Page

FIGURE Page

FIGURE Page

CHAPTER I

INTRODUCTION

In the past two decades, the popularity of wireless communication systems has exploded. Wireless devices have shifted from being a luxury to a necessity in every household. The bandwidth allocated to commercial wireless communications, however, has not followed the same trend as the demand for these devices. Hence there is a pressing need to design bandwidth-efficient communication systems over the wireless channel to accommodate this ever-increasing demand. The ultimate limit to the number of users or data-rates that can be supported, for a given bandwidth and a given power constraint, is dictated by the Shannon limit [2]. If power is not constrained, theoretically infinite capacity is possible. However, in practice, the power of transmission is constrained by the battery life of the wireless device and also the interference to other cells. The problem can then be stated as follows: given the Shannon limit for the bandwidth and power constraints, what is the best practical channel coding scheme that can approach this limit. We will answer this question for the wireless channel in this dissertation.

A. Overview of the Dissertation

Typically, a wireless channel is characterized as a dynamic channel where the signal-noise ratio (SNR) fluctuates with time, space and/or frequency. Fluctuation of SNR translates to a different channel condition over time, space and frequency. This characteristic leads to the notion of parallel channels to transmit data through. Thus,

---

The journal model is *IEEE Transactions on Information Theory*.

designing codes for the wireless channel presents us with the problem of designing codes for a set of parallel channels. This work broadly falls under the category of code-design for parallel channels and it can be applied to any system with parallel channels to communicate with.

There are three important scenarios to be considered while designing coding schemes for wireless channels. These scenarios are given by:

1. Channel State Information (CSI) is available to only the receiver (CSIR).
2. CSI is not available to either the transmitter or the receiver and it has to be estimated from pilots which we denote as Partial CSI (PaCSI).
3. CSI is available to both the transmitter and the receiver (CSITR).

Code-design for each of these scenarios can be drastically different and they are considered separately in each chapter of this dissertation.

1. CSI at the Receiver: Higher Constellations

Chapter III considers the case where CSI is known perfectly to the receiver [3]. In addition, assume that a bandwidth efficient constellation such as QAM is chosen for transmission over the wireless channel. There are up to m different types of bits in 2^{2m}-QAM or 2^m-PAM, which are protected differently from one another in terms of bit-error rate (BER). In order to achieve the capacity of this channel, it is well-known that multiple code-books (up to m different ones) are required. If the code-rates are chosen carefully, a multi-stage decoder (MSD) is sufficient to achieve capacity [4]. A multi-stage decoder functions as follows: decoding of the k-th stage (bit-position) takes into account the output of the all the other $k-1$ bit-positions decoded so far. This scheme is known as a multi-level coding with multi-stage decoding (MLC/MSD).

This scheme follows directly from the chain-rule of mutual information. Suboptimal schemes such as MLC with parallel independent decoding (PID), where decoding of different stages is performed independently, and bit-interleaved coded modulation (BICM) [5], where multiple code-books are replaced by a single code-book, have also received attention since they are more pragmatic. It has been shown that if the constellation applied is Gray mapping, the penalty from capacity for these schemes is negligible.

The above discussion is valid with respect to capacity *i.e.* MLC has a distinct advantage over BICM for infinite code-word length. However, for practical schemes, which require codes of length of a few thousands, through our research, we show that this is not the case. For the same latency and complexity, multi-level coding must apply a component code which is $1/m$ times the length of an overall BICM code if there are m different levels in the constellation. Now consider a scheme where a Low-Density Parity-Check (LDPC) or turbo code is used for error-correction with the higher-order constellation. It is well-known that LDPC and turbo codes improve their performance drastically with the length of the code especially over lengths ranging from hundreds to thousands. In such a case, a BICM scheme with a single code of m times the length of each component code of MLC will perform much better in terms of bit-error rate (BER) than MLC. Hence, in this scenario, BICM is not merely a pragmatic scheme but a better scheme in terms of bit-error rate. The advantage of BICM becomes more prominent when m is large.

In the presented work, the properties of an LDPC code are further utilized (these properties are discussed in detail in Chapter II). An irregular LDPC code is applied with the above BICM scheme. Since different coded bits (same as bit nodes) of an LDPC code are protected differently due to the irregularity of the LDPC code, the connections of coded bits to different bit-positions of the modulated word can be

optimized. In this way, a different sub-code is provided to different levels of the modulated word. Since the check nodes are common to all the coded bits, it is still a single code. Hence, a multi-level coding scheme (MLC) within a BICM framework has been incorporated thus providing the best of both approaches. Through simulations, we show that this scheme can provide gains over a conventional BICM scheme as well as MLC schemes.

2. CSIR with Multiple Transmit Antennas: Rate-Diversity Tradeoff

In Chapter IV, a multiple-input multiple-output (MIMO) system with quasi-static fading is considered. In order to circumvent the harmful effects of fading, especially quasi-static fading, various forms of diversity techniques are used in practice. One such technique is to use multiple transmit and receive antennas which provide gains in diversity and outage probability over a single-antenna system. As mentioned in Section 2, diversity and transmit rate are inversely proportional to each other for a constrained constellation such as QAM. Hence, there is tradeoff between diversity and rate for a constrained constellation which defines the ultimate limits of diversity for variable-rate coding schemes [6]. We present schemes that use Low-Density Parity-Check (LDPC) codes and perform close to the rate-diversity tradeoff. In this chapter, we consider both flat-fading (MIMO) as well as frequency-selective fading (MIMO-OFDM), where OFDM is used to convert the frequency-selective fading channel into flat-fading subchannels. We show that a system with LDPC codes as the outer-code and a simple serial-parallel converter as an inner code achieves the rate-diversity trade-off over MIMO and MIMO-OFDM systems for a constrained constellation (QAM). Through simulations, we show that the presented scheme performs better than all MIMO-OFDM systems proposed so far in literature [7].

3. Partial CSI at the Receiver

In Chapter V, we discuss a scheme where perfect CSI is not available to the receiver and the receiver derives CSI through estimation with the aid of pilots [8] [9]. Use of pilots can be conserved if a differential detector is used to kick start the iterations without the knowledge of the channel. In the subsequent iterations, information from the channel code along with the pilots can be used to improve the channel estimates. This results in savings in the number of pilots without much penalty in performance. In order to guarantee differential detection in the first iteration, the inner code of the coding scheme must be an accumulator. Hence a special class of LDPC codes known as Irregular Repeat Accumulate (IRA) codes is used where the inner code is an accumulator. However, the challenge with IRA codes is that the systematic part is transmitted as such and for our scheme to work, the systematic part must also be differentially encoded. Hence, non-systematic IRA codes are required.

Given a channel estimation algorithm and ratio of pilots, the amount of irregularity can be optimized for the best performance. Extrinsic Information Transfer (EXIT) chart based optimization [10] [11] for the irregularity profile is applied to obtain optimum performance. Though simulations, we prove that the performance of this scheme can be close to the performance with perfect CSI at the receiver. This is possible because of the powerful IRA code which improves CSI apart from protecting against errors on the fading channel.

4. Perfect CSI at the Transmitter and Receiver

Chapter VI considers code-design and signal-processing for CSITR [12]. CSI estimated at the receiver can be fed back to the transmitter to improve the performance of the wireless system. In certain communication systems, for example, in TDD

systems, reciprocity can be assumed between the forward channel and the reverse channel whereby the forward and reverse channel coefficients are the same. In this case, CSI can be easily obtained at both the transmitter as well as the receiver. In terms of capacity, CSI at both transmitter and receiver (CSITR) makes a difference only at low SNRs as compared to CSI at only the receiver. However, the main advantages of CSITR are that it simplifies the decoder design significantly and prevents the occurence of outage over slow-fading channels. CSI at only the receiver however results in outage over slow-fading channels.

Consider a system with parallel subchannels for transmission of data with an overall power constraint. In practice, OFDM systems, a set of power controlled channels, or MIMO systems with CSITR fall under the category of systems with parallel subchannels. Given a power constraint at the transmitter, the problem can be stated as follows: what is the best power and rate allocation for this system which maximizes the sum-information-rate? For the Gaussian constellation, this problem is already solved and it yields the familiar water-filling power allocation [13]. In practice, however, signalling is always constrained (like QAM, QPSK etc.). Given this additional constraint, the rate and power allocation has to be derived. Furthermore, for practical systems, the CSITR changes from block to block and the power allocation must be a simple closed form expression which can be derived quickly for each block.

We approximate the constrained capacity of QAM systems and derive a closed-form power allocation expression that maximizes sum-rate. If a separate code-book is allocated to each of the subchannels (code-rate is chosen corresponding to the rate the subchannel supports), the constrained capacity of this system can be achieved. If a single code-book is assigned to all the subchannels, an ML decoder can still achieve the capacity, however, this ML decoder could be very complex. Yet, it is more practical to use one code-book for all the subchannels which is an assumption

we make in this work.

It is difficult to design a code which performs well over all code-rates between 0 and 1 (through puncturing). It is only possible for a code to perform well over a smaller range of rates as for example, between 0.3 and 0.7. Hence an algorithm is derived which allocates different constellation to each subchannel such that the overall code-rate is in a chosen range. This algorithm will derive the best constellation for each subchannel based on the subchannel state. Through simulations with LDPC codes, we show that the presented scheme performs very close to the maximum constrained sum-information-rate and also to the unconstrained capacity.

5. Memory-Saving LDPC Codes

For any communication system, hardware complexity of each of the components must be as minimal as possible. LDPC codes are decoded by a soft-decision decoding algorithm known as sum-product decoding (discussed in Chapter II). The main problem with sum-product decoding of LDPC codes of lengths longer than a few thousand, is that the memory required on the chip is huge. In Chapter VII, a new strain of sum-product decoding of LDPC codes is devised which results in lower hardware complexity and memory requirement than a conventional sum-product decoding algorithm [14]. An extension of this work is now being considered for many state-of-the-art wireless systems including IEEE 802.11n and IEEE 802.16.

Conventional sum-product decoding algorithm is usually implemented as a parallel decoding algorithm where all the bit node operations are carried out in one time-instant and all the check node updates in another time-instant. This scheme promises very high decoding speeds as all the operations are in parallel. However, in this case, the complete bipartite graph of the LDPC code has to be built in hardware which can make the chip-size huge as well as lead to congestion problems. In our re-

search, a solution to this problem is presented by dividing the graph into two halves, with each half very similar to the other in structure. In this manner, only one half of the graph needs to be built in hardware and the decoding can be done for the two different halves at different time-instants. This results in savings in hardware and chip-size but the penalty is in decoding speed. Decoding speed is roughly halved due to the above operation. However, for today's applications the speed provided by the presented scheme will be much more than sufficient.

The performance of this scheme is analyzed using a technique known as density evolution and the best code is designed with the given decoding schedule. From simulations, it is shown that the proposed scheme performs as well as the conventional sum-product decoding algorithm on the corresponding optimized LDPC code. Thus there is no penalty as a result of splitting the bipartite graph.

We finally present the conclusion and future work in Chapter VIII.

CHAPTER II

BACKGROUND

In this chapter, we discuss the fundamentals of a communication system. We describe a communication channel and the special characteristics of a wireless channel. We also discuss a popular technique known as Orthogonal Frequency-Division Multiplexing (OFDM) [15]. We finally present a relatively new class of channel codes known as Low-Density Parity-Check (LDPC) codes [16].

A. Communication Channel

Communication systems transmit information through a medium which is known as a channel. The channel distorts the transmitted signal in one or more of the following ways: (1) as the signal propagates through the medium, its power attenuates (path loss), (2) the medium often distorts the signal in time or frequency or both, (3) the channel often distorts the signal in a non-linear fashion in which case the analysis of such a system becomes very difficult. Apart from these deleterious properties of the channel, noise is added at the receiver which can be modelled as a Gaussian random process [17]. A practical communication scheme has to encode the information to be transmitted in a suitable way, in order for the receiver to decode the signal successfully and overcome the shortcomings of the channel. Since the focus of this dissertation is on wireless communication systems, we discuss some key properties of the wireless channel below.

1. Wireless Channel

When messages are transmitted over a wireless medium, the signal undergoes a phenomenon known as *fading* [18]. Assume that $s[k]$ is the discrete baseband representation of a phase- or amplitude-modulated digital signal that is transmitted. Throughout this dissertation, we consider only phase- and amplitude-modulated signals which are represented as follows:

$$s[k] = A[k] + jB[k] \tag{2.1}$$

where $A[k]$ is the real part of the transmitted signal, $B[k]$ is the imaginary part of the transmitted signal and j represents $\sqrt{-1}$. $\sqrt{A^2[k] + B^2[k]}$ is the amplitude of $s[k]$ and is constant if the signal is phase-modulated and varying if the signal is amplitude-modulated. In wireless transmission, the transmitted signal is often reflected from a number of obstacles before arriving at the receiver. Each of these reflected paths undergoes a different phase shift and can arrive at the receiver at different time-instants. There may or may not be a line-of-sight component in the received signal. The signals from different reflections might also add constructively or destructively at the receiver. Thus the received demodulated signal can be represented as:

$$y[k] = \sum_{i=0}^{L-1} h[i]s[k-i] + n[k] \tag{2.2}$$

where $y[k]$ is the received signal at the k-th time instant, $s[k-i]$ is the signal transmitted at the $k-i$-th time instant, $h[i]$ is the fade coefficient which can be modelled as a complex Gaussian random variable and $n[k]$ is the additive white complex Gaussian noise added at the receiver. The validity of the assumption that $h[i]$ is complex Gaussian, is based on the fact that there are large number of reflected paths and the central limit theorem applies. If there is a line-of-sight path, the complex Gaussian

random variable has a non-zero mean and the magnitude of $h[i]$ is Ricean distributed, and if there is no line-of-sight component, the magnitude is Rayleigh distributed. All through this dissertation, we assume that the magnitude of fading is Rayleigh distributed, *i.e.* there is no line-of-sight component. For a fading channel, $h[k]$s are usually referred to as the channel state information (CSI).

Note that Eqn. (2.2) assumes that there are L taps in the channel which results in Inter-Symbol Interference (ISI). ISI is caused when the variance of the delay associated with different reflected paths arriving at the receiver, known as *delay-spread*, is significant compared to the symbol interval. The fading channel is said to be *frequency-selective* when it causes ISI. In Eqn. (2.2), it is usually assumed that $h[i]$ are independent for different i. The relative powers of the $h[i]$ $i = 0, 1, \ldots, L-1$ is given by the power-delay profile. In this dissertation, for frequency-selective fading channel, we assume that the power-delay profile is uniform *i.e.* the power of each of the taps in the channel, $h[i]$ is equal. Eqn. (2.2) does not provide any information on how the channel taps $h[i]$ change with time. *Coherence time* is a measure of the time-correlation of the fading taps of the channel. If the coherence time is significant (>100 times) compared to the symbol interval, fading is supposed to be *slow*. If coherence time is relatively small, fading is *fast*. *Doppler spread*, f_d, is defined as the inverse of the coherence time and is the maximum dispersion in frequency that a pure sinusoid will undergo when transmitted over the channel. It is defined as:

$$f_d = \frac{v}{\lambda} \tag{2.3}$$

where v is the velocity of the receiver and λ is the wavelength of transmission.

If the delay spread of the channel is very small compared to the symbol interval, the channel will not cause ISI and and the signal is said to undergo *flat fading*. If the

channel is flat, Eqn. (2.2) can be re-written as follows:

$$y[k] = h[k]s[k] + n[k]. \tag{2.4}$$

2. Effects of Fading: Design Challenges

The effects of fading are always deleterious and special coding and signal processing methods need to be employed to overcome these effects. There are three situations under which one must consider coding for fading channels (later in this chapter, we will present a scheme known as Orthogonal Frequency Division Multiplexing (OFDM), which transforms the frequency-selective channel into a set of parallel flat-fading channels; hence consideration of coding schemes for flat-fading is sufficient):

1. Channel State Information (CSI) is available to only the receiver (CSIR).
2. CSI is not available to either the transmitter or the receiver and it has to be estimated from pilots which we denote as Partial CSI (PaCSI).
3. CSI is available to both the transmitter and the receiver (CSITR).

Designing coding schemes for the first two cases again depends on whether the fading is fast or slow. If fading is fast, many realizations of the channel will be present over a single code-word and law of large numbers can be applied. The capacity of this scheme is the expectation of the information-rate for a given channel realization over the probability distribution of the channel realization. For this case, code-design is not that challenging as codes which are designed for the AWGN channel are sufficient with the code-rate determined by the capacity of the channel.

However, if fading is very slow, there will only be finite number of channel realizations over a code-word. We will use the terms *slow fading* and *quasi-static fading* interchangeably in this dissertation to represent this scenario. For the first two cases

(CSIR and PaCSI), under slow fading, the information-rate that the channel supports is a random variable. The absolute capacity of this channel is zero as there is a non-zero probability that the rate chosen for transmission is not supported by the channel. Whenever the channel does not support the transmitted rate, the channel is said to be in *outage*. The probability of being in outage is denoted as *outage probability*. There is only the notion of *outage capacity* which is defined as the maximum rate supported for a given probability of outage, p (*p-outage-capacity*).

Since outage probability is the ultimate limit for these schemes, the aim of the coding scheme is to improve the outage probability as much as possible for the given resource constraints. Outage probability can be improved through providing diversity and coding gain. Diversity is defined as follows [19]:

$$D = \lim_{SNR \to \infty} \frac{10 \log \frac{P_1}{P_2}}{\Delta SNR(dB)} \tag{2.5}$$

where D is the diversity, SNR is the Signal-Noise Ratio, and P_1, P_2 are the probabilities of error (frame or bit) of the system at two different SNRs separated by ΔSNR which is in dB scale. The three main sources of diversity are time, frequency and space. Assume that the term *multiplexing rate* denotes the rate of increase of transmission rate with SNR. For a codebook derived from Gaussian distributed symbols (popularly known as Gaussian codebook), diversity has a relationship with the multiplexing rate, which is known as the *diversity-multiplexing tradeoff* [20]. This tradeoff suggests that the multiplexing rate, which is defined as the rate of increase of transmission rate with SNR, is inversely proportional to the diversity provided by the system. This property stems from the fact that diversity and multiplexing rate are the two factors that use up the degrees of freedom present in the system and hence they are inversely proportional. The number of degrees of freedom in a Gaussian constellation increases with SNR, hence the rate of transmission can scale with SNR

for a fixed diversity.

When the transmitted signal is constrained to be from a finite-size constellation to transmit from, such as QAM, there is a relationship between the transmission rate (note that here the rate is fixed and does not increase with SNR) and diversity provided by the system [6]. For SNRs higher than a particular value, the number of degrees of freedom in the system does not increase with SNR for a constrained constellation and hence there is a diversity-rate tradeoff. Hence, for a quasi-static fading system with a constrained constellation to transmit from, the optimality of a coding scheme is determined by how close the scheme performs to the diversity-rate tradeoff.

For CSIRT (case three), when using a Gaussian codebook subject to an overall power constraint, waterfilling across different channel realizations [13] is optimal to achieve the capacity of the system. Waterfilling pours more power into the "good" channels and less power into the "bad" channels. The number of channel realizations can be finite (slow-fading) or infinite (fast-fading) and waterfilling can be performed easily for both cases. Note that there is no outage for these cases, as the channel state is already known to the transmitter, and the transmitter can change the rate of transmission to prevent outage. Gaussian codebooks are not easily implementable in practice and signaling is always constrained. With a constrained constellation, waterfilling is not the optimal method to achieve the overall capacity of the system and other optimal design methods have to be derived.

B. Orthogonal Frequency Division Multiplexing

A frequency-selective fading channel can be converted into a set of parallel flat-fading channels without loss of any information. Orthogonal Frequency-Division Multiplex-

ing (OFDM) [15] is a popular linear technique which achieves this end. Assume that Eqn. (2.2) represents the frequency-selective fading channel. It is well-known that convolution in the time domain is equivalent to multiplication in the frequency domain. For the discrete case (*i.e.* discrete in the time and frequency domains), multiplication in the frequency domain is equivalent to circular convolution in the time domain. ISI is discrete convolution in the time domain. If the discrete convolution due to ISI can be made to mimic circular convolution, an ISI channel can be transformed into multiplication in the frequency domain which corresponds to a parallel flat-fading channel.

1. Single-Input Single-Output OFDM System

The mathematical model of the single-input single-output (SISO) OFDM system is given in Figure 1. Assume that a vector of transmit values of length N, $\mathbf{X}$, is incident

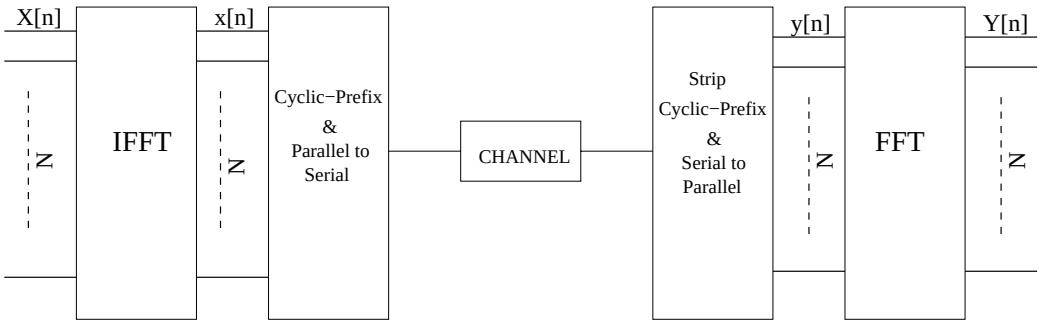

Fig. 1. Block diagram of an OFDM system

at the input of an OFDM system [21]:

$$\mathbf{X}[\mathbf{k}] = \sqrt{E_s}\,[X_0[k]X_1[k]\ldots X_{N-1}[k]] \tag{2.6}$$

where $X_i[k]$ are complex numbers representing the symbol to be transmitted satisfying $E(X_i^H[k]X_i[k]) = 1$ and k represents the time index. $E(.)$ denotes expectation of the random quantity over its probability distribution. Since each of the i represents a particular sub-frequency, X_i is said to be transmitted in subcarrier i. The OFDM system, as shown in Figure 1 applies an Inverse Fast Fourier Transform (IFFT) [22] module which can be represented as:

$$\mathbf{x}[\mathbf{k}] = \mathbf{F}_{N\times N}\mathbf{X}[\mathbf{k}] \tag{2.7}$$

where the square matrix $\mathbf{F}_{N\times N}$ of size $N \times N$ is the IFFT operator and the result $\mathbf{x}[\mathbf{k}]$ is a vector of length N representing the time-domain equivalent of $\mathbf{X}[\mathbf{k}]$. The l, m-th element of $\mathbf{F_{N\times N}}$ can be represented as:

$$F_{l,m} = \frac{1}{\sqrt{N}} \exp^{-j2\pi\frac{(l-1)(m-1)}{N}} \tag{2.8}$$

If the number of taps in the ISI (frequency-selective fading) channel is assumed to be L, as in Eqn. (2.2), a guard interval (GI) of length $L-1$ is required in an OFDM system to prevent ISI between OFDM symbols ($\mathbf{x}[\mathbf{k}]$, $\mathbf{x}[\mathbf{k}-\mathbf{1}]$ are OFDM symbols). Furthermore, a cyclic shift of the transmit vector $\mathbf{x}[\mathbf{k}]$ has to be transmitted in the guard interval in order to guarantee the orthogonality of the subcarriers. Thus the

received vector, after the removal of the guard interval, can be represented as follows:

$$\mathbf{y}[\mathbf{k}] = \mathbf{h}[\mathbf{k}]\mathbf{x}[\mathbf{k}] + \mathbf{n}[\mathbf{k}]$$

$$\mathbf{h}[\mathbf{k}] = \begin{bmatrix} h_0[k] & h_1[k] & \dots & h_{L-1}[k] & 0 & 0 & \dots & 0 \\ 0 & h_0[k] & \dots & h_{L-2}[k] & h_{L-1}[k] & 0 & \dots & 0 \\ \vdots & \ddots & \ddots & \ddots & \ddots & \ddots & \vdots & \vdots \\ h_{L-1}[k] & 0 & \dots & 0 & h_0[k] & h_1[k] & \dots & h_{L-2}[k] \\ \vdots & \ddots & \ddots & \ddots & \ddots & \ddots & \vdots & \vdots \\ h_1[k] & h_2[k] & \dots & h_{L-1}[k] & 0 & \dots & 0 & h_0[k] \end{bmatrix} \tag{2.9}$$

where $h_0[k], h_1[k], \dots, h_{L-1}[k]$ represent the L taps of the ISI channel and $\mathbf{n}[\mathbf{k}]$ represents the AWGN noise vector of size $N \times 1$ satisfying the constraint $E(\mathbf{n}[\mathbf{k}]\mathbf{n}[\mathbf{k}]^H) = 2\sigma^2\mathbf{I}_{N\times N}$. σ^2 is the variance of the real and imaginary components of the noise and $\mathbf{I}_{N\times N}$ represents an identity matrix of size $N \times N$. The eigen-value-decomposition (EVD) of the Toeplitz matrix $\mathbf{h}[\mathbf{k}]$ can be represented as follows:

$$\mathbf{h}[\mathbf{k}] = \mathbf{F}_{N\times N}\mathbf{D}\mathbf{F}^H_{N\times N} \tag{2.10}$$

where $\mathbf{F}_{N\times N}$ is the IFFT matrix as in Eqn. (2.2), $\mathbf{F}^H_{N\times N}$ is Fast-Fourier Transform (FFT) matrix (since $\mathbf{F}_{N\times N}\mathbf{F}^H_{N\times N} = \mathbf{I}_{N\times N}$). Also $\mathbf{D}$ is an $N \times N$ diagonal matrix whose diagonal entries are given by the vector which is the product of $\mathbf{F}^H_{N\times N}$ and $[h_0[k], h_1[k], \dots, h_{L-1}[k]]^T$. $\mathbf{D}$ can be written as:

$$\mathbf{D} = diag\left[\mathbf{F}^H_{N\times N}\left[h_0[k], h_1[k], \dots, h_{L-1}[k]\right]^T\right] \tag{2.11}$$

At the OFDM receiver, FFT is performed on the received sequence, $\mathbf{y}[\mathbf{k}]$, to obtain:

$$\begin{aligned}\mathbf{Y}[\mathbf{k}] &= \mathbf{F}_{N\times N}^{H}\mathbf{y}[\mathbf{k}] \\ &= \mathbf{F}_{N\times N}^{H}\left(\mathbf{F}_{N\times N}\mathbf{D}\mathbf{F}_{N\times N}^{H}\mathbf{x}[\mathbf{k}] + \mathbf{n}[\mathbf{k}]\right) \\ &= \mathbf{D}\mathbf{X}[\mathbf{k}] + \tilde{\mathbf{N}}[\mathbf{k}] \end{aligned} \tag{2.12}$$

where $E(\mathbf{N}[\mathbf{k}]\mathbf{N}[\mathbf{k}]^{H}) = 2\sigma^2\mathbf{I}_{N\times N}$. Thus the frequency-selective channel has been converted into a set of parallel flat-fading channels.

2. MIMO-OFDM System

In a multiple-input multiple-output-OFDM (MIMO-OFDM) system, there are multiple antennas (say N_T) to transmit from and multiple receiver antennas (say N_R). Apart from this, the physical SISO channel between any two transmit-receive antenna pairs (say t-th transmit antenna and r-th receive antenna) is an ISI channel with taps $h_{t,r}[l] \quad l = 0, 1, \ldots, L-1$. Assume that L is the maximum channel length of all the $N_T N_R$ SISO channels. The MIMO channel can then be represented as a sequence of matrices $\mathbf{h}[\mathbf{l}] \quad l = 0, 1, \ldots, L-1$ whose elements are $h_{t,r}[l] \quad t = 1, 2, \ldots, N_T \quad r = 1, 2, \ldots, N_R$.

Instead of a transmit vector as in Eqn. (2.6), we have a transmit matrix $\mathbf{S}$ which is of size $N_T \times N$, where N is the number of subcarriers as in the previous section. Assuming the cyclic prefix is inserted at the transmitter and stripped at the receiver (ideally), what is obtained at each of the antennas over the n-th tone, $n = 0, 1, \ldots, N-1$, is as follows:

$$y_r[n] = \sqrt{\frac{E_s}{N_T}}\sum_{t=1}^{N_T} H_{t,r}[n]S_{t,n} + \tilde{N}_r[n], \quad r = 1, 2, \ldots, N_R \tag{2.13}$$

where the noise $\tilde{N}_r[n]$ is white and complex (circularly symmetric complex Gaussian

and zero mean) and

$$H_{t,r}[n] = \sum_{l=0}^{L-1} h_{t,r}[l] \exp^{-j2\pi \frac{ln}{N}} \tag{2.14}$$

Denote:

$$\begin{aligned} \mathbf{y}[\mathbf{n}] &= [y_1[n] y_2[n] \dots y_{N_R}[n]]^T, \\ \mathbf{S}[\mathbf{n}] &= [S_{1,n} S_{2,n} \dots S_{N_T,n}]^T, \\ \tilde{\mathbf{N}}[\mathbf{n}] &= \left[\tilde{N}_1[n] \tilde{N}_2[n] \dots \tilde{N}_{N_R}[n]\right]^T, \end{aligned} \tag{2.15}$$

then the system equation of a MIMO-OFDM can be stated as follows:

$$\mathbf{y}[\mathbf{n}] = \sqrt{\frac{E_s}{N_T}} \mathbf{H}[\mathbf{n}] \mathbf{S}[\mathbf{n}] + \tilde{\mathbf{N}}[\mathbf{n}] \tag{2.16}$$

with $\mathbf{H}[\mathbf{n}]$ being a $N_R \times N_T$ matrix given by:

$$\mathbf{H}[\mathbf{n}] = \sum_{l=0}^{L-1} \mathbf{h}[\mathbf{l}] \exp^{-j2\pi \frac{ln}{N}} \tag{2.17}$$

C. Low-Density Parity-Check Codes

Low-density parity check (LDPC) codes [23], discovered by Gallager and rediscovered by MacKay [16], perform close to capacity on most memoryless channels. LDPC codes have been proved to achieve capacity on binary erasure channels (BEC). Unlike turbo codes, they can be optimized for good bit-error rate performance over a given channel and for a given code-rate.

1. LDPC Code Representation

LDPC codes can be represented in terms of a bipartite graph [24] as shown in Figure 2. LDPC codes consist of two kinds of nodes - *variable* nodes, and *check* nodes. The *variable* nodes correspond to the coded bits in a codeword. The *check* nodes cor-

respond to the parity-check constraints satisfied by the *variable* nodes. The degree of a variable node [25] is the number of checks it participates in, while the degree of a check node is the number of variable nodes that are connected to the check. If all variable nodes have the same degree and so do the check nodes, it is a *regular* LDPC code. Otherwise, it is an *irregular* LDPC code. The irregularity is typically specified by a polynomial called variable (check) node degree profile. That is,

$$\lambda(x) := \sum_{i=1}^{d_v} \lambda_i \; x^{i-1}, \qquad \rho(x) := \sum_{i=1}^{d_c} \rho_i \; x^{i-1} \tag{2.18}$$

where λ_i (ρ_i) represents the fraction of edges that are connected to the variable nodes (check nodes) of degree i. If λ'_i represented the fraction of nodes instead of edges, $\lambda'(x)$ is the degree profile from the node perspective. Similarly, $\rho'(x)$ represents the check node profile from the node perspective. Note that a given degree profile represents an ensemble of LDPC codes, as these nodes can be connected in any random fashion in the bipartite graph.

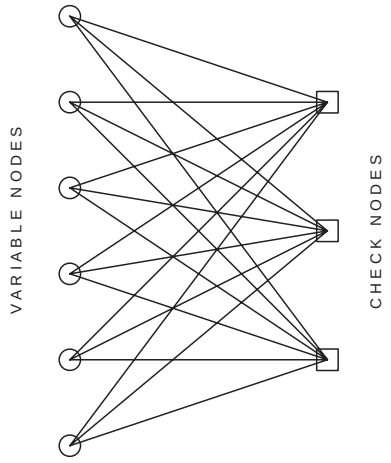

Fig. 2. Bipartite graph of an LDPC code

2. Sum-product Decoding Algorithm of LDPC Codes

Assume that a binary phase shift keying (BPSK) modulation is used and an additive white Gaussian noise (AWGN) channel is present. If $\underline{X} = (x_0, x_1, \ldots, x_{n-1})$ is the transmitted codeword (after modulation) and $\underline{Y} = (y_0, y_1, \ldots, y_{n-1})$ is the received word, then clearly,

$$y_k = x_k + n_k \tag{2.19}$$

where n_k is the noise sample which is a zero-mean, Gaussian random variable with variance σ^2. Soft information is represented in terms of log-likelihood-ratios (LLRs), which is defined as:

$$L(x_i) = \log \frac{P(y_i|x_i = 1)}{P(y_i|x_i = -1)} \tag{2.20}$$

Sum-product decoding algorithm is an iterative message passing algorithm that passes messages between variable and check nodes along each edge. Let us consider the qth stage of decoding:

3. Update at the Variable Nodes

Consider the ith variable node and assume that it is of degree V (Figure 3). It gets extrinsic information $L_{ch}(x_i) = -2y_i/\sigma^2$ from the channel and incoming edge-LLRs $L^{(q-1)}_{c\to v,l}(x_i)$ for $l = 1, 2, \ldots, V$ along each of the V edges. The outgoing LLR on the jth edge at the qth iteration, $L^{(q)}_{v\to c,j}(x_i)$, is:

$$L^{(q)}_{v\to c,j}(x_i) = L_{ch}(x_i) + \sum_{l=1, l\neq j}^{V} L^{(q-1)}_{c\to v,l}(x_i) \tag{2.21}$$

At the beginning of the first iteration, all the incoming edge-LLRs are assumed to be zero i.e.

$$L^{(0)}_{c\to v,l}(x_i) = 0 \quad l = 1, \ldots, V \tag{2.22}$$

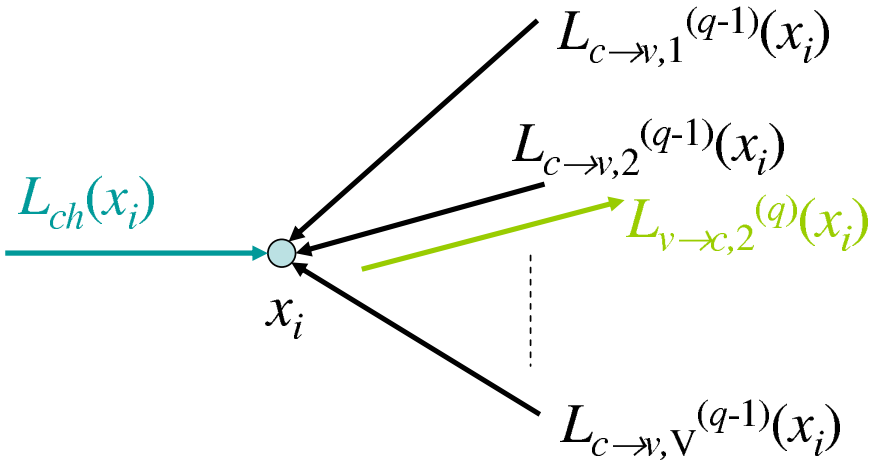

Fig. 3. Sum-product decoding at the variable node

4. Update at the Check Nodes

Consider the kth check node with degree C at the qth iteration (Figure 4). If $L^{(q)}_{v\to c,j}(y_k)$ for $j = 1, 2, \ldots, C$ represent the LLRs incident on this check node, then the output LLR on the lth edge is governed by:

$$\tanh\left(\frac{|L^{(q)}_{c\to v,l}(y_k)|}{2}\right) = \prod_{j=1, j\neq l}^{C} \tanh\left(\frac{|L^{(q)}_{v\to c,j}(y_k)|}{2}\right) \tag{2.23}$$

This completes the iteration.

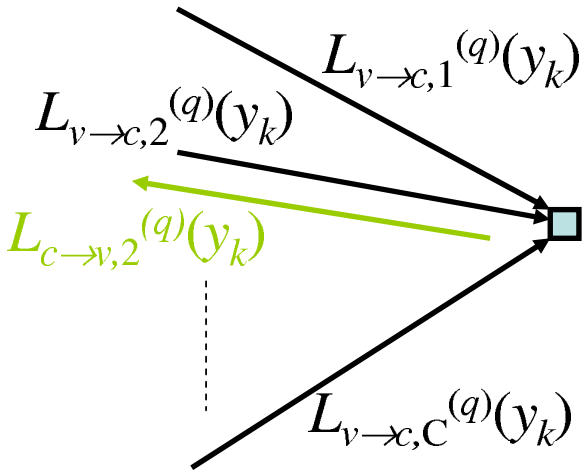

Fig. 4. Sum-product decoding at the check node

5. Decision

Soft output on the ith bit at the end of Q iterations is given as:

$$L(x_i) = L_{ch}(x_i) + \sum_{l=0}^{\nu_i - 1} L_{c\to v,l}^{(Q)}(x_i) \tag{2.24}$$

Hard decision on the bit is obtained as follows:

$$\hat{x_i} = \begin{cases} 1 & \text{if } L(x_i) < 0 \\ 0 & \text{if } L(x_i) \geq 0 \end{cases} \tag{2.25}$$

The *threshold* of an LDPC code is σ^*, which is the maximum noise standard deviation, σ for which bit error rate, P_e tends to zero as number of iterations increases.

6. Density Evolution

Density Evolution [25] is the technique which keeps track of the probability density functions (*pdf*s) of the messages (usually LLRs) passed from variable to check nodes or check to variable nodes in an iteration. It is a very useful tool which aids in

predicting the bit-error rate performance of a given code-ensemble represented by the degree profiles under sum-product decoding and also in designing optimal code-book ensembles. Since we use Gaussian Approximation (GA) based density evolution for designing LDPC codes throughout this dissertation, our focus will be on GA which is discussed in the following section.

A channel is said to be symmetric if:

$$p(y|x = 1) = p(-y|x = -1), \tag{2.26}$$

where $p(.)$ is the pdf function, y is the received signal and x is the transmitted signal. When the channel is symmetric, then Bit-error rate(BER) or Frame-error rate(FER) is independent of the transmitted codeword. In such a case, it suffices to transmit the all-zero codeword for analysis.

a. Consistency

A *pdf*, f, is *consistent* if it satisfies $f(x) = f(-x)e^x$ for all $x > 0$. Suppose a channel is symmetric and if P_0 is the distribution of LLRs of the received signal. Under the assumption that the all-zero codeword is transmitted, P_0 is consistent. Consistency condition simplifies the density evolution considerably.

7. Gaussian Approximation (GA) on Density Evolution

For an AWGN channel with BPSK/QPSK modulation (QPSK with Gray mapping), assuming that the all-zero codeword is transmitted, the LLR of the received signal has a Gaussian distribution. In addition, assume that the distribution of the messages (LLRs) passed on any of the edges of the graph, in any given iteration, is Gaussian or a mixture of Gaussians. Then, density evolution simplifies to tracking the means(m) and variances(σ^2) of the Gaussian mixtures. This is called *Gaussian*

approximation [26]. *Consistency* condition for Gaussians simplifies the variance to $\sigma^2 = 2m$. Hence, in GA, we just have to keep track of the means over iterations to see how the densities evolve. With GA, optimization for thresholds is a linear problem. Let us take a brief look at the evolution of means under GA.

a. Variable Node

Sum-product decoding at the variable node is merely sum of the LLRs, which translates to convolution of the densities of LLRs. Since the incident LLRs on each of the edges of a variable node from the check nodes are independent Gaussians, the pdf of the LLR that is passed on an edge from variable to check in the next iteration is the sum of the means and the variances. Hence,

$$m_{v,i}^{(l)} = m_{u_0} + (i-1)m_u^{(l-1)}, \tag{2.27}$$

where $m_{v,i}^{(l)}$ is the mean of the o/p message on an edge of degree-i variable node at the lth iteration, m_{u_0} is the mean of the channel LLR and $m_u^{(l-1)}$ is the mean of the message from check in the $(l-1)$th iteration.

Since the code can be irregular, the means of the Gaussians emanating from different degree variable nodes will be different, hence on an average we have to assume that the message, v at the check node is a mixture of Gaussians rather than a single Gaussian. That is:

$$f_v^{(l)} = \sum_{i=1}^{d_l} \lambda_i \mathcal{N}(m_{v,i}^{(l)}, 2m_{v,i}^{(l)}) \tag{2.28}$$

b. Check Node

From sum-product decoding of check node it is easy to observe that:

$$E\left[\tanh\frac{u_j^{(l)}}{2}\right] = E\left[\tanh\frac{v^{(l)}}{2}\right]^{j-1}, \tag{2.29}$$

where $u_j^{(l)}$ is the message from a j-degree check node to the variable nodes in the lth iteration and $v^{(l)}$ is the message from variable node to check.

If $u \sim \mathcal{N}(m_u, 2m_u)$, $E\left[\tanh\frac{u}{2}\right]$ depends only on m_u. Hence, define $E\left[\tanh\frac{u}{2}\right] := 1-\phi(m_u)$. $\phi(x)$ is a continuous, monotically decreasing function defined on $[0,\infty)$ with $\phi(0)=1$ and $\phi(\infty)=0$.

$$\Rightarrow E\left[\tanh\frac{v^{(l)}}{2}\right] = 1-\sum_{i=2}^{d_l}\lambda_i\phi(m_{v,i}^{(l)} \Rightarrow m_{u,j}^{(l)} = \phi^{-1}\left(1-\left[1-\sum_{i=2}^{d_l}\lambda_i\phi(m_{v,i}^{(l)}\right]^{j-1}\right) \tag{2.30}$$

Finally,

$$m_u^{(l)} = \sum_{j=2}^{d_r}\rho_j m_{u,j}^{(l)} \tag{2.31}$$

Threshold of an LDPC code is defined as the standard deviation (σ) of the noise at which the bit-error rate of the code goes to zero. The final problem is to optimize the profiles $((\lambda,\rho))$ to obtain the maximum possible noise threshold for a given rate which turns out to be a linear problem. [26] provides a more detailed description of the optimization. The density of message from check to variable (Eqn. (2.30)) may not be Gaussian in reality. Nevertheless, from comparison of the optimized code-profiles and noise thresholds of LDPC codes obtained through GA and actual density evolution, it can be deduced that GA is a good approximation.

CHAPTER III

CODING FOR HIGH-ORDER CONSTELLATIONS WITH CSIR*

The problem with designing codes for high order constellation schemes (e.g. QAM) is that different bits of a modulated symbol (referred to as "levels" from here on) get different amount of protection, in terms of BER. This is due to the asymmetry in bit to constellation mapping. Coding schemes must take this into account in their design. A common approach to solve this problem is to use multilevel codes (MLC), where a separate code is assigned to each of the levels, with multistage decoding (MSD) [4] (decoding the levels one after the other, assuming all the levels decoded so far are perfectly known). MLC/MSD is known to achieve capacity for these schemes. Alternative sub-optimal schemes have been considered in literature, which include MLC with parallel independent decoding (PID) of the component levels where the levels are decoded independently at the same time, and bit interleaved coded modulation (BICM) where a single code provides protection to all the levels.

MLC with MSD achieves the capacity of this system which implies it is optimal asymptotically in the length of the code. However, in the finite-length case, both MLC with MSD or with PID can have a component code of length only $1/m$ times (in 2^m-PAM or $2^{2m}-$QAM) the code-length of an equivalent BICM scheme for the same complexity and latency. Therefore, with MLC, using codes like LDPC codes and turbo codes whose performance improves significantly with length will be disadvantageous. For finite-lengths, schemes with BICM can have a distinct advantage

*

over MLC schemes as will be shown in this work. However, code-design for BICM schemes is tricky as the channel messages from the demodulator are not identically distributed due to the inherent unequal protection. In this work [3] [27], we present a simple code-design for Gray-mapped PAM schemes with LDPC codes, which possesses the advantages of both BICM, as it uses only one LDPC code, and of MLC, as it provides unequal error protection to different levels separately with LDPC subcodes. This will become clearer in the following sections. It is always possible to perform iterative demodulation to improve the BER performance of higher-order modulation schemes but with Gray mapping, it is known that the performance of iterative demodulation does not improve much [4]. Hence, in this work, we choose the demodulation to be one-shot (*i.e.* no iterations between decoder and demodulator).

The code-design presented in this work provides a separate sub-profile for each level of the modulator and optimizes the profile for minimum bit-error rate. The codes thus designed perform very well for short lengths (up to 10000 bits) which is required for most applications. Specifically, the scheme presented here performs better than MLC/PID with LDPC component codes for the same parameters (maximum variable node degree, code-length and code-rate) on additive white Gaussian noise (AWGN) and block-fading channels with CSIR. Since 2^m-PAM represents one quadrature component of 2^{2m}-QAM, the optimization holds true for QAM too. In general, this idea can be extended to other modulation schemes like M-PSK very easily.

Hou *et al.* have considered the design of LDPC codes for MLC/PID and BICM schemes [28]. However, they used differential evolution to design the codes which is very complicated. Moreover, the scheme presented here is better for shorter lengths, because as stated earlier, it is a blend of MLC/MSD and BICM.

A. Multilevel Coding

Optimization of code profiles for high order constellations such as 2^m-PAM is not as straightforward as that for BPSK. This is because bits at different levels are protected unequally by the modulator *i.e.* the average LLRs (log-likelihood ratios) of different bits from a demapped symbol are different. Hence, coding has to make up for this discrepancy by giving more protection to the bits (levels) receiving lesser protection from the modulator/demodulator. This is what MLC accomplishes [4]. MLC provides a separate component code for each of the levels. In order to achieve the constrained capacity, decoding must start with the decoder of the lowest level and proceed to the higher levels taking into account the decisions of prior decoding stages. This type of decoding is called MSD. The order in which the levels are decoded is not important. An alternative to MSD is decoding the component codes independently. This scheme is MSD/PID.

B. BICM: An Alternative to MLC

When a single code is used without differentiating the levels of the demodulator, the resulting scheme called is BICM [5]. When Gray mapping is used, the difference in capacity from MLC/MSD to BICM is negligible for one-shot demodulation [4]. This is a very promising result for practical short-medium codelength schemes. With coding schemes like turbo and LDPC codes whose power-efficiency increases tremendously with increase in length, it might be advantageous to use BICM for finite lengths. Therefore, this work implements a BICM one-shot demodulation scheme with Gray mapping where a single LDPC code is employed. At the same time, this scheme is different from the conventional BICM scheme, as each level of the demodulator is protected unequally by a subcode of the LDPC code and hence it has the good

properties of MLC as well. Note that we call it a subcode because a different variable node degree-profile is chosen for each of these levels. On the check node side, however, all these variable nodes are connected, hence it is a single code. An irregular LDPC code protects the coded-bits unequally and the inequality can be controlled through the variable-node degree profiles. This design results in better BER.

C. System Description

A channel is symmetric if:

$$p(y_k|x_k = 1) = p(-y_k|x_k = 0), \tag{3.1}$$

where $p(.)$ is the pdf function, y is the received signal corresponding to a transmitted bit of x.

For a symmetric channel, it suffices to apply density evolution assuming the all-zero codeword has been transmitted for threshold determination and code design. When high order constellations like PAM or QAM are used, the resulting binary-input channels are not symmetric. Since symmetry condition simplifies things, it is always a desirable property. We use the concept of i.i.d. channel adapters [29] [28] to symmetrize the equivalent binary-input channels. Assume the constellation in question is 2^m-PAM - Figure 5 shows our system. In this work, we consider two types of channels with 2^m-PAM as the constellation:

1. An AWGN channel for which we design the code for PAMs of different sizes -

$$y_k = x_k + n_k \tag{3.2}$$

where x_k is transmitted symbol from 2^m-PAM constellation, y_k is the received value and n_k is the AWGN noise with variance σ^2.

2. Block-fading channel with B independent block realizations over a codeword and the B values of the channel is known to the receiver (CSIR). The AWGN optimized codes are directly applied to this channel.

$$y_k = \alpha x_k + n_k \tag{3.3}$$

where x_k is transmitted symbol from 2^m-PAM constellation, y_k is the received value, α is the CSI which is available to the receiver and n_k is the AWGN noise with variance $N_o/2$.

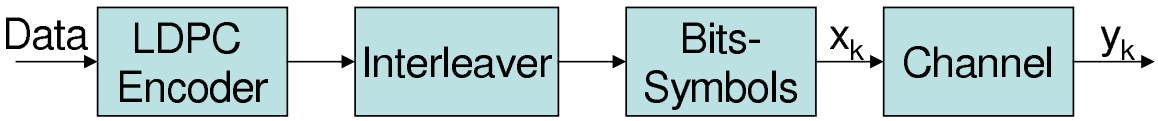

Fig. 5. LDPC BICM system

D. Code Optimization

Since differential evolution is very complex, for an AWGN or block-fading channel, Gaussian approximation can be applied to simplify the code design. But as the demodulator is not necessarily a linear system, the LLR outputs of the demodulator for different levels need not be Gaussian distributed anymore. Hence application of the Gaussian approximation might give an optimistic value for the threshold. Nevertheless, it can aid in finding good code-profiles. In this work, we consider the code-design for the plain AWGN channel. Since fading is a case of AWGN with different instantaneous SNR, we expect these codes to perform well on them too.

The code structure is as follows - a single code is designed which provides unequal error protection to different levels. Different sets of variable nodes and hence different variable-node profiles are set aside for different levels of the demodulator. But there is just one set of check nodes for all the different sets of variable nodes and hence it is a single code. This can be better understood from Figure 6. Also, the deinterleaver between demodulator and decoder must make sure that the different levels of the demodulator are transferred to the right sets of variable nodes of the decoder. If the LLRs for different levels in the constellation are assumed to be Gaussian distributed with different means (Gaussian approximation), these means can be obtained through simulations of the soft-demodulator at different SNRs. These mean-values will drive the optimization. We set aside separate λs for different levels. For example, if we have 2^m-PAM or 2^{2m}-QAM, then we have m levels of bits, hence if d_l if the maximum left degree, there are m sets of λs ($\lambda_{j,i}$ $j = 1, 2, \ldots, m$ & $i \in [1, d_l]$) satisfying the following conditions:

$$\sum_{j=1}^{m} \sum_{i=1}^{d_l} \lambda_{j,i} = 1 \tag{3.4}$$

$$\sum_{i=1}^{d_l} \frac{\lambda_{1,i}}{i} = \sum_{i=1}^{d_l} \frac{\lambda_{2,i}}{i} = \ldots = \sum_{i=1}^{d_l} \frac{\lambda_{m,i}}{i} \tag{3.5}$$

Eqn. (3.5) is due to the fact that the number of bits connected to each of the m levels are equal. The means of the LLRs at the m different levels from the demodulator is evaluated through simulations (this can be done analytically too through the approximations in [30]) and represented as $m_{u_1}, m_{u_2}, \ldots, m_{u_m}$. Optimization is then carried out with these channel means m_{u_j} for the set $\lambda_{j,i}$ for all i. So density evolution with Gaussian approximation for this case at the l-th iteration will have

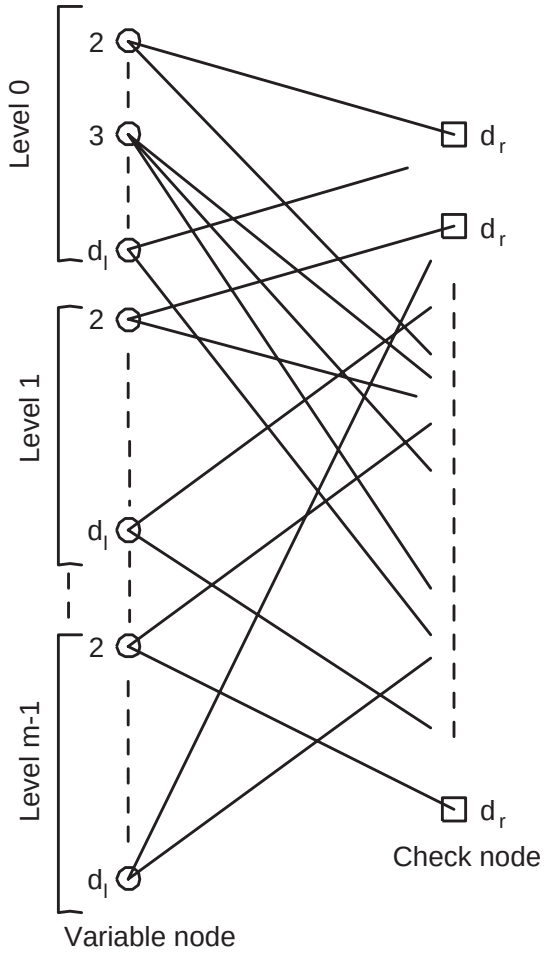

Fig. 6. LDPC coding scheme: demodulator generates LLRs of m bits for a received symbol which serve as *a priori* probability for m variable nodes each in a different level. The number on the node represents the degree of the node

the following modifications:

$$m_{v,j,i}^{(l)} = m_{u_j} + (i-1)m_u^{(l-1)} \tag{3.6}$$

where $m_{v,j,i}^{(l)}$ is the mean of the Gaussian output from a degree-i variable node at the jth level to the check node. Therefore, the outgoing message v to the check node at the lth iteration will have the following Gaussian mixture density $f_v^{(l)}$:

$$f_v^{(l)} = \sum_{j=1}^{m}\sum_{i=1}^{d_l} \lambda_{j,i}\mathcal{N}(m_{v,j,i}^{(l)}, 2m_{v,j,i}^{(l)}) \tag{3.7}$$

$$\Rightarrow E\left[\tanh\frac{m_v^{(l)}}{2}\right] = 1 - \sum_{j=1}^{m}\sum_{i=1}^{d_l} \lambda_{j,i}\phi(m_{v,j,i}^{(l)}) \tag{3.8}$$

where $\phi(m_{v,j,i}^{(l)})$ is given by [26]:

$$\phi(x) = \begin{cases} 1 - \frac{1}{\sqrt{4\pi x}}\int_{\boldsymbol{R}} \tanh\frac{u}{2} e^{-\frac{(u-x)^2}{4x}} du, & \text{if } x > 0 \\ 1, & \text{if } x = 0 \end{cases} \tag{3.9}$$

The mean of the output of a check node of degree k, $m_{u,k}^{(l)}$ is given by:

$$m_{u,k}^{(l)} = \phi^{-1}\left[1 - \left(1 - \sum_{j=1}^{m}\sum_{i=1}^{d_l} \lambda_{j,i}\phi(m_{v,j,i}^{(l)})\right)^{k-1}\right] \tag{3.10}$$

Note that the check nodes are shared by all the levels as there is just a single code. Proceeding further, we obtain the mean of the message passed from check to variable $m_u^{(l)}$ as:

$$m_u^{(l)} = \sum_{k=1}^{d_r} \rho_j \phi^{-1}\left[1 - \left(1 - \sum_{j=1}^{m}\sum_{i=1}^{d_l} \lambda_{j,i}\phi(m_{v,j,i}^{(l)})\right)^{k-1}\right] \tag{3.11}$$

Threshold of the LDPC code is the standard deviation of the noise, σ^*, below which $m_v^{(l)}$ and $m_u^{(l)} \to \infty$ as $l \to \infty$. Note that (3.11) is similar to (10) in [26]. The only difference is that here there are more variables, $\lambda_{j,i}$s. Proceeding in the

same manner as in [26], the problem of optimizing the profiles, λ and ρ, for the best threshold for a given rate of the code reduces to a linear optimization problem. This is certainly a much simpler scheme compared to actual density evolution, which involves keeping track of actual pdfs of the messages between variable and check nodes.

E. Simulations and Results

By applying the optimization based on the Gaussian approximation [26], we obtained the degree-profiles of the rate-1/2 LDPC code for a 4-PAM scheme (equivalent to a 16-QAM scheme) over an AWGN channel. The left maximum degree, d_l was fixed at 15. The optimized code-profile is shown in Table I. Our code has a threshold of $E_b/N_o = 2.52$dB (for the given scheme of rate-1/2 4-PAM E_b/N_o is same as E_s/N_o). The channel capacity is 2.11dB and the PID capacity is 2.27dB.

In order to characterize the advantages of our proposed scheme, we have simulated the rate 0.5, 4-PAM BICM scheme for an overall code-length of 1000 bits and compared this performance to the best optimized rate-0.5 4-PAM MLC/PID and MLC/MSD schemes respectively (code-profiles for MLC obtained from [28], variable-node degree, d_l constrained to 15) on an AWGN channel. It must be noted that these MLC codes were designed with actual density evolution. Overall code-length of 1000 implies that the length of the BICM code is 1000 and lengths of the MLC component codes are 500 each (for the same complexity and latency requirement). As can be seen from Figure 7 and Figure 8, our proposed scheme has gains of over 1dB at a FER of 0.01. This gain will be higher for higher-order constellations as the length of the component codes will further reduce. Hence BICM is not merely a pragmatic scheme but a more optimal scheme at short-medium block-lengths even though MLC/MSD achieves capacity (infinite-length code-words). Also it is also more practical to main-

Table I. Degree profiles

i	$\lambda_{1,i}$	$\lambda_{2,i}$	j	ρ_j
2	0.1587	0.1262	7	1
3	0.0569	0.2113		
4	0.0257	0.0192		
5	0.0228	0.0098		
6	0.0230	0.0062		
7	0.0243	0.0038		
8	0.0264	0.0024		
9	0.0290	0.0017		
10	0.0323	0.0014		
11	0.0358	0.0011		
12	0.0395	0.0007		
13	0.0433	0.0004		
14	0.0469	0.0006		
15	0.0489	0.0016		

tain a single code (BICM) for all the bit-positions as used in our scheme.

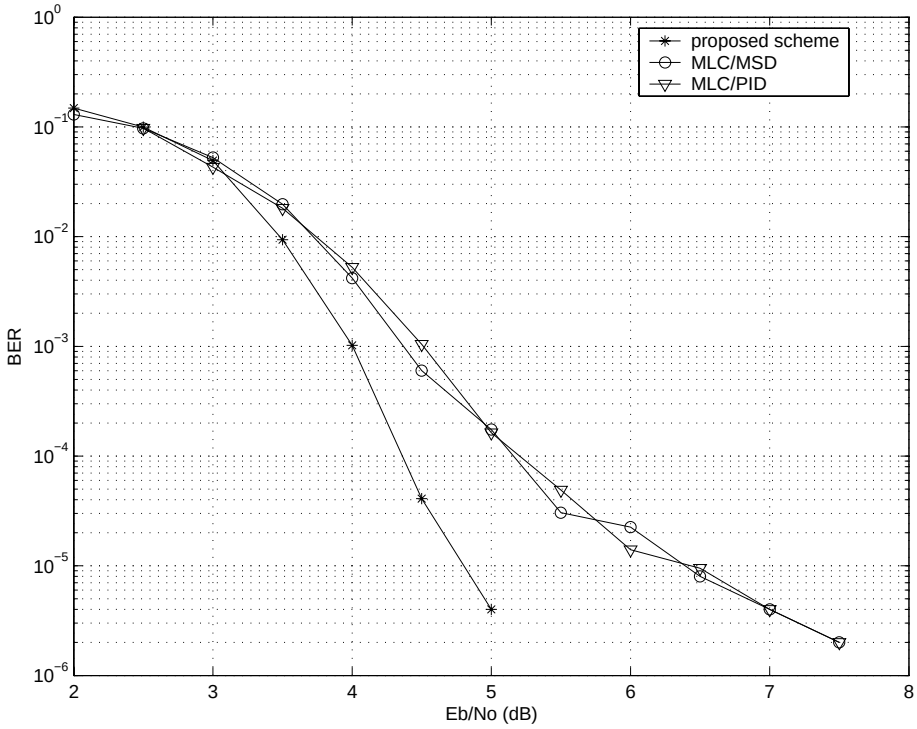

Fig. 7. Comparison of our scheme (BER) to the best MLC/MSD and MLC/PID schemes for gray-mapped 4-PAM R=0.5 (1000,500) LDPC and $d_l = 15$ for AWGN

Over a block-fading channel, even for a longer code-length of 16200 (comparable to 2 irregular component codes of length 8100 in [31] with d_l =15), the proposed BICM scheme achieves a gain of over 2.5dB at an FER of 0.02 as can be seen from Figure 9 and Figure 10 (BER and FER respectively). There are 16 independent block realizations of fading over one block (16200) of the code.

Figure 11 compares the performance of the proposed scheme with 4-PAM to a BICM scheme also with 4-PAM but with an LDPC rate 0.5 code optimized for AWGN channel with BPSK constellation. As can be seen, the BPSK-AWGN optimized LDPC code performance is around 0.4 dB away from the proposed BICM scheme which

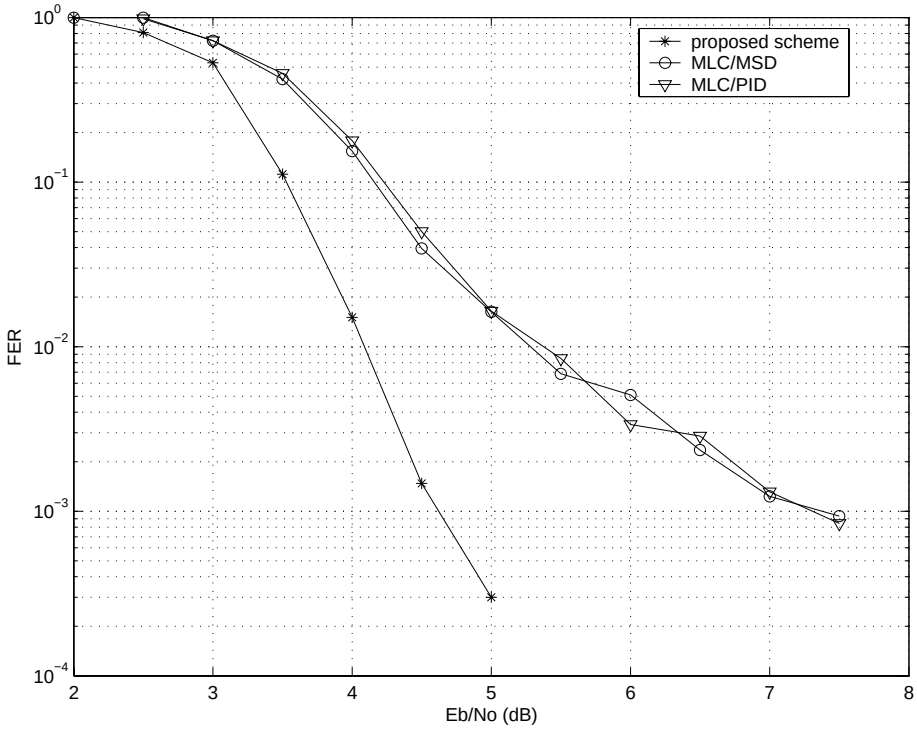

Fig. 8. Comparison of our scheme (FER) to the best MLC/MSD and MLC/PID schemes for gray-mapped 4-PAM R=0.5 (1000,500) LDPC and $d_l = 15$ for AWGN

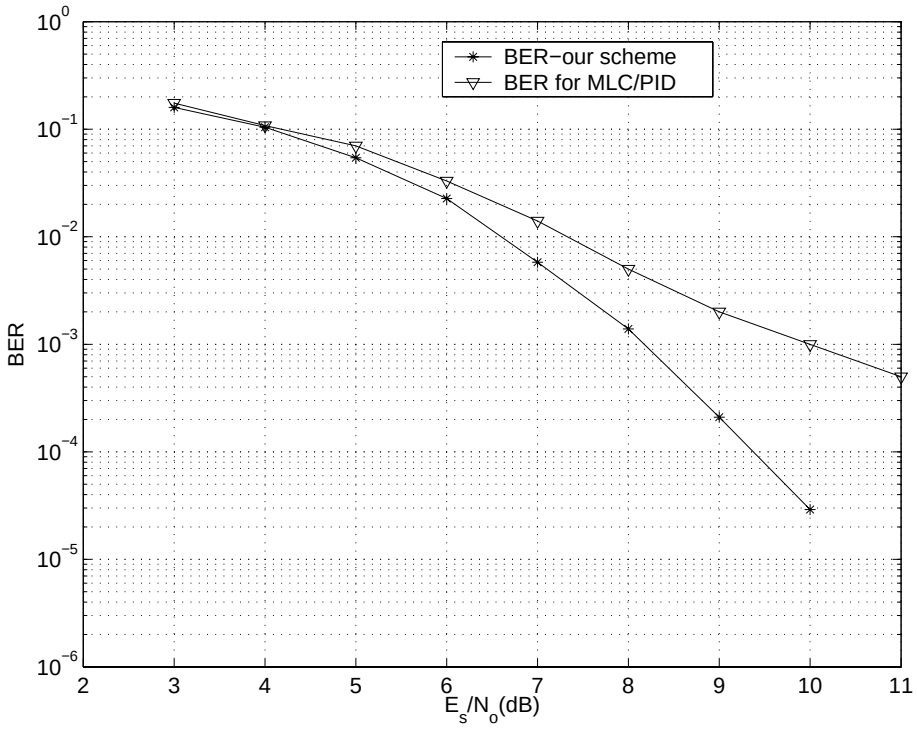

Fig. 9. Comparison of BER of our scheme to the best MLC/PID scheme for gray-mapped 4-PAM R=0.5 (16200,8100) LDPC and $d_l = 15$ for block-fading

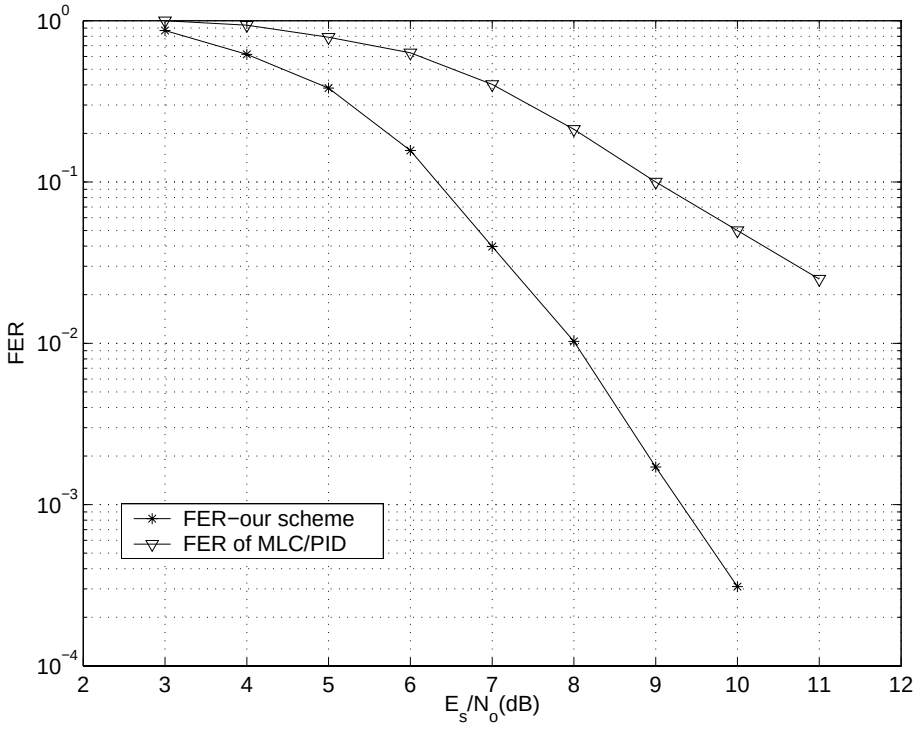

Fig. 10. Comparison of FER of our scheme to the MLC/PID scheme for gray-mapped 4-PAM R=0.5 (16200,8100) LDPC and $d_l = 15$ for block-fading

underlines the fact that special BICM code-design schemes (as the one proposed) are required for better performance. In all the optimizations, we have assumed the right

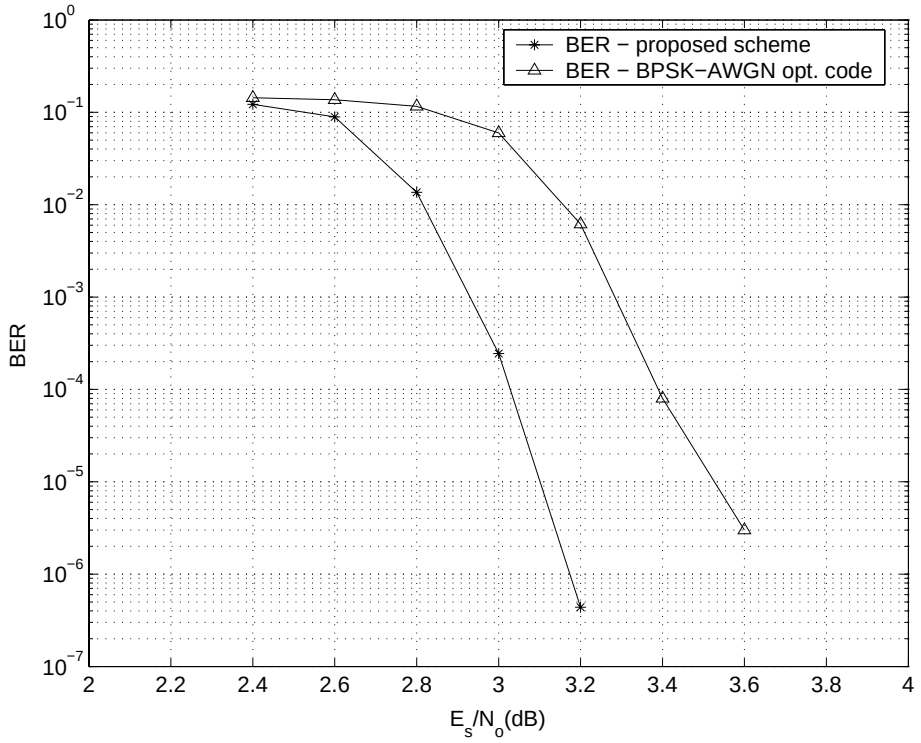

Fig. 11. Comparison of the proposed scheme to a BICM scheme with BPSK/AWGN optimized LDPC code and gray-mapped 4-PAM R=0.5 (16200,8100) and $d_l = 15$ for AWGN

nodes are concentrated in one degree. This scheme can be extended to mixture of right degrees in which case we expect even better performance. All simulations were run for 100 iterations.

In summary, we designed a simple power and bandwidth efficient scheme (blend of MLC/BICM) with LDPC codes. The optimization technique for the design of code-profiles follows a simple linear programming method and can be implemented very easily as opposed to differential evolution. Even though this work deals with

PAM/QAM case, it can be easily extended to other constellations too. Simulation results show that for practical short and medium block-lengths, the proposed scheme achieves much better BER performance than MLC/MSD and MLC/PID schemes over AWGN and block-fading channels. This is so in spite of the fact that the MLC schemes were designed with exact density evolution.

CHAPTER IV

SPACE-TIME AND SPACE-FREQUENCY CODING WITH LDPC CODES

Quasi-static fading with the channel state (fade) known only to the receiver (CSIR) is an adverse system to design channel codes for. The capacity of this system is zero as there is a non-zero probability that the transmitted rate is not supported by the channel (this event is defined as *outage* and its probability is called *outage-probability*). Diversity of some form such as space, frequency or time is required to improve the outage probability of this system. Some forms of diversity (*e.g.* receive diversity) come for free, while others like transmit diversity do not.

In practice, signalling is always constrained to a maximum constellation-size. In this case, beyond a certain SNR, the degrees of freedom available from the channel is fixed and cannot increase (*e.g.* with 64-QAM and 2 transmit antennas, the total degrees of freedom is fixed by the constellation). These degrees have to be shared between transmit diversity and transmission rate. For this case, there is a rate-diversity tradeoff [6], where the "rate" is the actual transmission rate and not the rate of increase of transmission rate as before. Consider a scheme with random-like linear codes such as Low-Density Parity-Check codes as the outer-code and a simple serial-parallel converter as the inner-code. The number of parallel streams at the output of this system is equal to the number of transmit antennas, N_T. It has been shown that this scheme achieves the rate-diversity tradeoff with a Maximum-Likelihood (ML) decoder [32]. In this work, we derive the rate-diversity tradeoff of MIMO-OFDM system (Multiple-Input Multiple-Output system with Orthogonal Frequency Division Multiplexing) and prove that random-like codes such as LDPC codes or turbo-codes achieve the tradeoff with an ML decoder. Furthermore, we show

that for a single-input single-output (SISO) OFDM system, all the frequency diversity is achievable with a channel code which has a large-enough minimum-distance (d_{min}). Thus, for a SISO-OFDM system, we show that full-diversity is achievable for code-rates tending to 1.

Finally through simulations, we demonstrate that the coding gain of the proposed scheme is good. Thus, the contribution of this work is as follows:

1. Characterization of rate-diversity tradeoff of MIMO-OFDM and SISO-OFDM systems

2. Achievability of rate-diversity tradeoff of MIMO-OFDM and SISO-OFDM systems with random-like codes such as LDPC with an ML decoder

3. Achievability of rate-diversity tradeoff of MIMO-OFDM, SISO-OFDM and MIMO systems with LDPC codes and sub-optimal iterative sum-product decoder

We also make comparisons to some schemes presented in literature for MIMO-OFDM [1] [33]. In comparison to these schemes presented in literature, our scheme has the following advantages:

1. Our scheme performs very close to the rate-diversity tradeoff while the schemes presented in [1] and [33] are far away from the tradeoff. In fact the schemes presented in these references require a penalty in code-rate of the precoder for every additional degree of frequency-diversity that can be guaranteed. This is not the case with our scheme where we show that rate-diversity tradeoff exists only for the transmit diversity and that frequency-diversity can come for free.

2. These schemes in literature require a re-design of the precoder to maximize the transmission rate for different frequency-diversity to be guaranteed (this maximum rate is still far from the rate our scheme guarantees for the same

frequency diversity achieved) while our proposed scheme requires only a single code which can be punctured to obtain different code-rate which will provide different diversity depending on the rate-diversity tradeoff.

3. Our scheme applies the use of sum-product decoder (turbo decoder for turbo codes) which have very practical complexity compared to the ML decoder required for the block-coded precoder which is very complex.

4. Since the codes we use are more random in nature, the coding gain obtainable can be much higher (this is shown through simulations but is difficult to be proved).

A. System Description

Consider a system as shown in Figure 12. The output of the LDPC encoder is converted from serial into N_T parallel streams where N_T is the number of transmit antennas. The incumbent bits on each of the streams is mapped to symbols of a

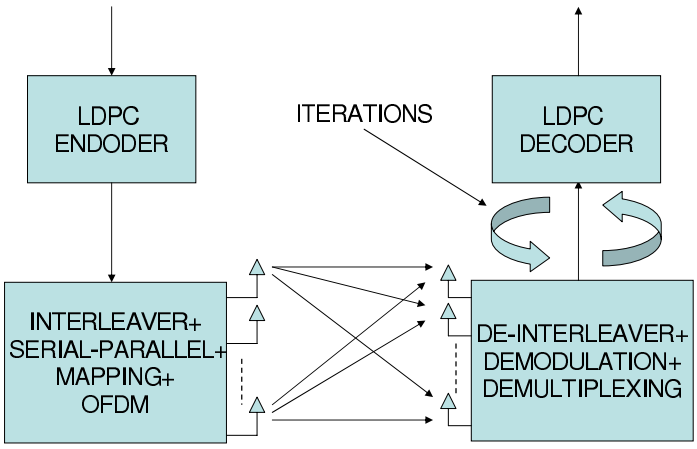

Fig. 12. System description of a MIMO-OFDM system

fixed constellation, say QPSK, 16-QAM etc. (constellation remains the same across antennas). In this work, we consider two cases: (1) where frequency-selective fading is present and OFDM is used to circumvent ISI, and (2) when fading is flat and there is no ISI present - for this case, we present simulation results directly. In both cases, we assume that the fading is slow and remains constant over the block of the LDPC codeword transmitted and that only the receiver has access to the fade coefficients (CSIR). With respect to outage, this is the worst-case scenario and most difficult to code for, as inherently the amount of diversity is fixed and small and there is a non-zero probability that the rate transmitted is not supported by the channel. Let us first consider the case where OFDM is applied to take care of frequency-selective fading and there are N_T transmit antennas.

B. OFDM with Multiple Antennas

Throughout this work, we assume that the OFDM system is ideal with a long-enough guard interval and no Inter-Carrier Interference (ICI) and thereby it converts the frequency-selective fading channel into parallel flat-fading channels. Assume that over a given tone, i, of the OFDM system, a vector:

$$\mathbf{x_i} = \left[x_i^{(1)} x_i^{(2)} \dots x_i^{(N_T)}\right] \tag{4.1}$$

is incident on the OFDM modulator. If the IFFT operation at the transmitter and the FFT operation at the receiver are ideal, $x_i^{(l)}$ is the symbol transmitted from the l-th antenna at the i-th tone. This vector passes through a flat-faded MIMO channel and is obtained at the receiver as:

$$\mathbf{r_k} = \sqrt{\frac{E_s}{N_T}}\mathbf{H}(\exp^{j\frac{2\pi i}{N}})\mathbf{x_i} + \mathbf{n_i} \quad i = 0, 1, \dots, N-1 \tag{4.2}$$

where $\mathbf{r_k}$ is a vector of size $N_R \times 1$, N_R is the number of receive antennas, N is the number of subcarriers, $E(||\mathbf{x_i}||^2) = N_T \Rightarrow E(||x_i^{(l)}||^2) = 1 \quad l = 0, 1, \ldots, N_T - 1$, and $\mathbf{n_k}$ is the complex Gaussian received noise vector of the same size as $\mathbf{r_k}$ satisfying:

$$E(\mathbf{n_i}\mathbf{n_l}^H) = \sigma^2 \mathbf{I}_{N_R \times N_R} \delta[i-l] \tag{4.3}$$

with $(.)^H$ being the Hermitian operator, $\mathbf{I}_{N_R \times N_R}$ being an identity matrix of size $N_R \times N_R$ and σ^2 is the variance of the noise. The channel transfer function, $\mathbf{H}(\exp^{j\frac{2\pi i}{N}})$ is of size $N_R \times N_T$ and is defined as follows:

$$\mathbf{H}(\exp^{j\frac{2\pi i}{N}}) = \sum_{k=0}^{L-1} \mathbf{h}(k) \exp^{j\frac{2\pi ik}{N}} \tag{4.4}$$

where L is the total number of taps in the channel and $\mathbf{h}(k)$ is a $N_R \times N_T$ random complex-matrix representing the k-th tap of the MIMO-ISI channel (in the time domain). As is evident, there is the notion of data being transmitted in the frequency domain in a MIMO-OFDM system similar to a single-antenna OFDM system and the channel transfer function is a Fourier transform of the time-domain MIMO-ISI channel as given by Eqn. (4.4). We further assume that $\mathbf{h}(k)$ is complex Gaussian with variance $1/2L$ in the real and imaginary parts (uniform power delay profile), and $\mathbf{h}(k)$, $\mathbf{h}(n)$ are independent, if $k \neq n$.

1. Code Design

Assume that a codeword of the LDPC code is transmitted in one OFDM symbol from N_T antennas. In other words, $N_T \times N$ symbols of the higher-order constellation span a single codeword of the LDPC code. N can be chosen to satisfy this condition. For the time being, assume that an ML decoder is available at the receiver for this system. The ML decoder must choose the $N_T \times N$ codesymbol, $\tilde{\mathbf{X}} = [\tilde{\mathbf{x_1}}\tilde{\mathbf{x_2}} \ldots \tilde{\mathbf{x_{N-1}}}]$

which maximizes the likelihood probability or minimizes the Euclidean distance:

$$\tilde{\mathbf{X}} = \arg\min_{\mathbf{X}} \sum_{i=0}^{N-1} ||\mathbf{r_i} - \sqrt{\frac{E_s}{N_T}}\mathbf{H}(\exp^{j\frac{2\pi i}{N}})\mathbf{x_i}||^2 \tag{4.5}$$

A standard approach to the problem of code-design is to consider the pair-wise error probability (PEP) between any two code-symbols (we define a code-symbol as a code-word of the LDPC code, which is a set of coded-bits, mapped to their corresponding symbols in the constellation that is transmitted). We follow the steps in [1] in this section. For the sake of completeness, the steps in [1] are retraced here. Assume that $\mathbf{X_1}$ and $\mathbf{X_2}$ are two code-symbols which correspond to codewords $\mathbf{C_1}$ and $\mathbf{C_2}$ respectively of the LDPC code. For a given channel realization which is fixed over the duration of the code-symbol and which is known to the receiver, the PEP in choosing $\mathbf{X_2}$ while $\mathbf{X_1}$ was transmitted, can be written as [19]:

$$P\left(\mathbf{X_1} \rightarrow \mathbf{X_2}|\mathbf{H}\right) = Q\left(\sqrt{\frac{E_s}{2N_T\sigma^2}d^2(\mathbf{X_1}, \mathbf{X_2}|\mathbf{H})}\right) \tag{4.6}$$

where

$$d^2(\mathbf{X_1}, \mathbf{X_2}|\mathbf{H}) = \sum_{i=0}^{N-1} ||\mathbf{H}(\exp^{j\frac{2\pi i}{N}})(\mathbf{X_{1,i}} - \mathbf{X_{2,i}})||^2 \tag{4.7}$$

Applying Chernoff bound, $Q(x) \leq \frac{1}{2}\exp^{-\frac{x^2}{2}}$,

$$P\left(\mathbf{X_1} \rightarrow \mathbf{X_2}|\mathbf{H}\right) \leq \frac{1}{2}\exp^{-\left(\frac{E_s}{4N_T\sigma^2}d^2(\mathbf{X_1}, \mathbf{X_2}|\mathbf{H})\right)} \tag{4.8}$$

Denote $\mathbf{E} = \mathbf{X_1} - \mathbf{X_2}$. With a uniform power delay profile, the expectation of PEP over the distribution of the channel transformation matrix yields the following upper-bound [34]:

$$P\left(\mathbf{X_1} \rightarrow \mathbf{X_2}\right) \leq \frac{1}{2}\prod_{k=0}^{\mathrm{Rank}(\mathbf{Z})-1} \frac{1}{\left(1 + \frac{E_s}{4N_T\sigma^2}\lambda_k(\mathbf{Z})\right)^{N_R}} \tag{4.9}$$

where $\mathbf{Z} = \mathbf{T}(\mathbf{E})\mathbf{T}^H(\mathbf{E})$ and:

$$\mathbf{T}(\mathbf{E}) = [\mathbf{E}^T \ \mathbf{R}\mathbf{E}^T \dots \ \mathbf{R}^{L-1}\mathbf{E}^T] \tag{4.10}$$

with $\mathbf{R} = (\exp^{-j\frac{2\pi i}{N}}) \quad i = 0, 1, \dots, N-1$ and $\lambda_k(\mathbf{Z})$ is the k-th eigen-value of $\mathbf{Z}$ in Eqn. (4.9).

Hence, the order of diversity of a coding scheme is the minimum rank over all pairwise difference matrices of code-symbols following the definition in [19]. In the next sub-section, we will take a more careful look at the rotated difference matrix $\mathbf{T}(\mathbf{E})$ in order to maximize the diversity.

2. SISO-OFDM System

In this sub-section, we show that all the frequency-diversity can be achieved at no expense of code-rate when transmission occurs through a SISO system. Consider the matrix $\mathbf{Z}$ derived in the previous sub-section. When $N_T = 1$, the difference code-symbol parameter, $\mathbf{E}$ is a vector and not a matrix anymore. $\mathbf{T}(\mathbf{E})$ becomes:

$$\mathbf{T}(\mathbf{E}) = \begin{bmatrix} \mathbf{e_0} & \mathbf{e_1} & \dots & \mathbf{e_{N-1}} \\ \mathbf{e_0} & \exp^{-j\frac{2\pi 1}{N}}\mathbf{e_1} & \dots & \exp^{-j\frac{2\pi N-1}{N}}\mathbf{e_{N-1}} \\ \vdots & \vdots & \ddots & \vdots \\ \mathbf{e_0} & \exp^{-j\frac{2\pi L-1}{N}}\mathbf{e_1} & \dots & \exp^{-j\frac{2\pi (L-1)(N-1)}{N}}\mathbf{e_{N-1}} \end{bmatrix}^T \tag{4.11}$$

Assume that a code exists with minimum distance $d_{min} > mL$, where m is the number of bits mapped to a constellation symbol (e.g. $m = 2$ for QPSK and $m = 4$ for 16QAM) and L is the number of taps in the ISI channel. In such a case, atleast L non-zero rows of $\mathbf{T}(\mathbf{E})$ will be present for each set of difference symbols, $\mathbf{E}$. Let us consider the matrix with the first L non-zero rows of $\mathbf{T}(\mathbf{E})$. Denote these rows as

$i_1, i_2, \ldots, i_L$ and the truncated matrix as $\mathbf{T'(E)}$. $\mathbf{T'(E)}$ is given as:

$$\mathbf{T'(E)} = \begin{bmatrix} \mathbf{e_{i_1}} & \mathbf{e_{i_2}} & \ldots & \mathbf{e_{i_L}} \\ \exp^{-j\frac{2\pi i_1}{N}}\mathbf{e_{i_1}} & \exp^{-j\frac{2\pi i_2}{N}}\mathbf{e_{i_2}} & \ldots & \exp^{-j\frac{2\pi i_L}{N}}\mathbf{e_{i_L}} \\ \vdots & \vdots & \ddots & \vdots \\ \exp^{-j\frac{2\pi}{N}i_1(L-1)}\mathbf{e_{i_1}} & \exp^{-j\frac{2\pi}{N}i_2(L-1)}\mathbf{e_{i_2}} & \ldots & \exp^{-j\frac{2\pi}{N}i_L(L-1)}\mathbf{e_{i_L}} \end{bmatrix}^T \tag{4.12}$$

In order to determine the rank of this matrix, let us apply an elementary transformation to this matrix. Multiply each row of $\mathbf{T'(E)}$ by the corresponding $\mathbf{e_{i_l}}$ $l = 1, 2, \ldots, L$. This results in $\mathbf{T''(E)}$ given by:

$$\mathbf{T''(E)} = \begin{bmatrix} 1 & 1 & \ldots & 1 \\ \exp^{-j\frac{2\pi i_1}{N}} & \exp^{-j\frac{2\pi i_2}{N}} & \ldots & \exp^{-j\frac{2\pi i_L}{N}} \\ \vdots & \vdots & \ddots & \vdots \\ \exp^{-j\frac{2\pi}{N}i_1(L-1)} & \exp^{-j\frac{2\pi}{N}i_2(L-1)} & \ldots & \exp^{-j\frac{2\pi}{N}i_L(L-1)} \end{bmatrix}^T \tag{4.13}$$

which is a *Vandermonde* matrix and is full-rank. Hence, all the diversity in a single-antenna OFDM system can be obtained by merely using a channel code with a minimum distance larger than a factor of the number of taps in the channel and an ML decoder for the system, irrespective of the rate of the code (as length of the code-word can be made as large as required to increase d_{min}).

$$d_{min} > mL \tag{4.14}$$

is the required condition and will guarantee the full frequency-diversity. However, this condition is not always required to obtain the full diversity (when d_{min} codebits are distributed to more than d_{min}/m code-symbols, which is usually more probable, d_{min} can be slightly less than mL and $\mathbf{T''(E)}$ can still be full-rank). It must also be noted that in order to obtain the full frequency-diversity, an interleaver is not

required. However, without an interleaver, the coding gain might be small as the rows of the *Vandermonde* matrix, $\mathbf{T}''(\mathbf{E})$, might be very similar to each other and hence the determinant will be of small magnitude. An interleaver will ensure that the rows are not similar and guarantee a high coding gain.

3. MIMO-OFDM

It has already been proved that a random code such as an LDPC code achieves the rate-diversity tradeoff [6] over a basic MIMO system [32] with BPSK constellation. For higher-order constellations, it has been conjectured that LDPC code achieves the rate-diversity tradeoff for long lengths of the code. Based on this previous work, we make the assumption that the rate-diversity tradeoff for a basic MIMO system is achievable for any fixed constellation by random codes to prove the achievability of the tradeoff for a MIMO-OFDM system.

Theorem 1: If a long random code of a given code-rate, R, achieves a transmit diversity of d in its basic MIMO mode of operation (*i.e.* no frequency diversity, receive diversity equal to N_R is always available), then it will achieve dL order diversity as a result of the presence of frequency diversity of order L given that the code-rate R remains the same.

Proof: We present arguments which are true asymptotic in length of the LDPC code:

When there are multiple antennas to transmit from, the matrix $\mathbf{T_O}(\mathbf{E})$ takes the

following form:

$$\mathbf{T_O(E)} = \begin{bmatrix} \mathbf{e_0^1} & \mathbf{e_1^1} & \dots & \mathbf{e_{N-1}^1} \\ \vdots & \vdots & \ddots & \vdots \\ \mathbf{e_0^{N_T}} & \mathbf{e_1^{N_T}} & \dots & \mathbf{e_{N-1}^{N_T}} \\ \mathbf{e_0^1} & \exp^{-j\frac{2\pi 1}{N}}\mathbf{e_1^1} & \dots & \exp^{-j\frac{2\pi N-1}{N}}\mathbf{e_{N-1}^1} \\ \vdots & \vdots & \ddots & \vdots \\ \mathbf{e_0^{N_T}} & \exp^{-j\frac{2\pi 1}{N}}\mathbf{e_1^{N_T}} & \dots & \exp^{-j\frac{2\pi N-1}{N}}\mathbf{e_{N-1}^{N_T}} \\ \vdots & \vdots & \ddots & \vdots \\ \mathbf{e_0^1} & \exp^{-j\frac{2\pi L-1}{N}}\mathbf{e_1^1} & \dots & \exp^{-j\frac{2\pi (L-1)(N-1)}{N}}\mathbf{e_{N-1}^1} \\ \vdots & \vdots & \ddots & \vdots \\ \mathbf{e_0^{N_T}} & \exp^{-j\frac{2\pi L-1}{N}}\mathbf{e_1^{N_T}} & \dots & \exp^{-j\frac{2\pi (L-1)(N-1)}{N}}\mathbf{e_{N-1}^{N_T}} \end{bmatrix}^T \tag{4.15}$$

In order to prove that all the frequency diversity is achievable in the presence of multiple transmit antennas, we apply the following lemmas:

Lemma 1 (Scaling Property): For an expurgated random code [23], the minimum distance, d_{min}, scales as:

$$d_{min} \approx \beta N_{code}, \tag{4.16}$$

where β is a non-zero constant and N_{code} is the length of an LDPC code-word.

This property was proved by Gallager in his dissertation work on LDPC codes. LDPC are a class of linear block codes which when constructed in a pseudo-random manner satisfy this lemma, especially for long lengths of the code.

Assumption 1: Proof of *Theorem 1* is simpler with a sub-class of LDPC codes with a non-zero fraction of odd-degree check nodes. For this class of LDPC codes, all-one word is not a valid code-word (all-one word being a valid codeword is disastrous

as then the maximum transmit diversity achievable in a plain MIMO system is 1 irrespective of code-rate) and furthermore, the weight of the highest Hamming weight code-word is ΔN_{code}, where Δ is strictly less than 1.

$$\Delta < 1 \tag{4.17}$$

Lemma 2: When bits of the random LDPC code is mapped to a higher-order constellation, the scaling property of the minimum distance of the codewords in terms of the symbols in the constellation (code-symbols), S_{min}, is preserved *i.e.*

$$S_{min} \approx \beta' N_{code}. \tag{4.18}$$

Proof: Since the bits are mapped one-one to symbols in the constellation, the minimum distance in terms of the constellation-symbols is atleast d_{min}/m, where m is the number of bits present in a symbol of the constellation. Hence the scaling property prevails, even though the scale factor is lower. S_{min} corresponds to the minimum number of non-zero entries in the error code-symbol, $\mathbf{E}$.

Lemma 3: When coded bits of the LDPC code in *Assumption 1* are randomly mapped to constellation symbols, the maximum number of non-zero code-symbols in the error code-symbol, $\mathbf{E}$ given by $\Delta' N_{code}/m$ is such that $\Delta' < 1$.

Proof: From Eqn. (4.17), it is evident that atleast $(1-\Delta)N_{code}$ bits are different between any two LDPC codewords, where $(1-\Delta) > 0$ strictly. Zero code-symbols occur in $\mathbf{E}$ when the bits in m consecutive positions of the error code-word (these are in bits) which make up the constellation symbol are zero. Since $(1-\Delta) > 0$, there is a non-zero probability that these m positions of the error code-word are zero (this strictly non-zero probability is atleast $(1-\Delta)^m$). Thus *Lemma 3* is true.

Denote the first N_T columns of $\mathbf{T_O(E)}$ as $\mathbf{S(E)}$.

$$\mathbf{S(E)} = \begin{bmatrix} \mathbf{e_0^1} & \mathbf{e_1^1} & \dots & \mathbf{e_{N-1}^1} \\ \vdots & \vdots & \ddots & \vdots \\ \mathbf{e_0^{N_T}} & \mathbf{e_1^{N_T}} & \dots & \mathbf{e_{N-1}^{N_T}} \end{bmatrix}^T \tag{4.19}$$

These columns represent the multiplexed LDPC codeword transmitted over N_T transmit antennas. Assume that the rank of this matrix is N_d for any set of error code-symbols, $\mathbf{E}$, which also represents the transmit diversity order achieved by the LDPC code when transmitted over a MIMO system with N_T transmit antennas and no frequency diversity. Since the LDPC code is assumed to achieve the rate-diversity tradeoff of the MIMO system, N_d depends on the code-rate of transmission chosen.

If $\mathbf{S(E)}$ is assumed to have rank N_d, it implies that $\mathbf{S(E)}$ has N_d independent columns and therefore has atleast N_d non-zero columns for every $\mathbf{E}$. Let us denote these N_d independent non-zero columns of $\mathbf{S(E)}$ for a given error code-symbol as $\mathbf{S'(E)}$. One way to prove that $\mathbf{T_O(E)}$ can have rank N_dL is to show that with non-zero probability, there are some N_dL rows in $\mathbf{S'(E)}$ with only one entry in each column. If these correspoding rows in $\mathbf{T_O(E)}$ are considered (denote this matrix as $\mathbf{T''_O(E)}$), they will be full-rank, equal to N_dL, since this matrix has a Vandermonde structure. As an example, assume that $N_d = 2, N_T = 2, L = 2$ and also that the N_dL rows of $S'(E)$ with single entries are $i_0, i_1, \dots, i_5$. Then $T''_O(E)$ can be expressed as in Eqn. (4.20).

$$\mathbf{T_O^{''(E)}} = \begin{bmatrix} \mathbf{e_{i_0}^1} & \mathbf{e_{i_1}^1} & 0 & 0 \\ \exp^{-j\frac{2\pi i_0}{N}}\mathbf{e_{i_0}^1} & \exp^{-j\frac{2\pi i_1}{N}}\mathbf{e_{i_1}^1} & 0 & 0 \\ 0 & 0 & \mathbf{e_{i_2}^1} & \mathbf{e_{i_3}^1} \\ 0 & 0 & \exp^{-j\frac{2\pi i_2}{N}}\mathbf{e_{i_2}^1} & \exp^{-j\frac{2\pi i_3}{N}}\mathbf{e_{i_3}^1} \end{bmatrix}^{\mathbf{T}} \tag{4.20}$$

As can be seen from $\mathbf{T}_{\mathbf{O}}^{''(\mathbf{E})}$, no column can be expressed as a linear combination of other columns and no row can be expressed as linear combination of other rows and hence, $\mathbf{T}_{\mathbf{O}}^{''(\mathbf{E})}$ is full-rank. Hence in order to complete the proof of *Theorem 1*, we need to show that $N_d L$ rows of $\mathbf{S}'(\mathbf{E})$ exist with single entries, with a high probability. Assume that a given error code-symbol, $\mathbf{E}$, has a weight (number of non-zero positions) given by $\delta N_{code}/m$ (for different code-symbols, δ can be different). From Eqn. (4.18), the minimum value of δ is β' and from *Lemma 3*, the maximum value of $\delta = \Delta' < 1$.

Since a random code such as LDPC code distributes the ones in its codewords randomly among the total length of the code-word (and also because of the interleaver present between the encoder and S-P converter in Figure 28, it can be safely assumed that the $\delta N_{code}/m$ non-zero symbols are independently distributed among the N_{code}/m total symbols of $\mathbf{S}(\mathbf{E})$. This implies that the probability that a given element in a column of $\mathbf{S}(\mathbf{E})$ is non-zero is

$$\begin{aligned} P &= \frac{\delta \frac{N_{code}}{m}}{\frac{N_{code}}{m}} \\ &= \delta \end{aligned} \tag{4.21}$$

Given this probability, the following is true for a given row of $\mathbf{S}'(\mathbf{E})$. In a given row of $\mathbf{S}'(\mathbf{E})$, the probability of all the elements being zero is given by:

$$P_{all-zero} = [1-\delta]^{N_d} \tag{4.22}$$

Probability of finding a single-entry in a given row, P_{se} is:

$$P_{se} = \left[(1-\delta)^{N_d - 1}\,\delta\right] \tag{4.23}$$

As $0 < \delta < 1$ strictly, P_{se} is a finite non-zero quantity. The average number of

single-entry columns, N_{se}, is proportional to:

$$N_{se} = NP_{se} \tag{4.24}$$

where N is the number of sub-carriers and is also equal to the number of rows in $\mathbf{S}(\mathbf{E})$. N_{se} is a strictly non-zero quantity and can be made greater than N_dL merely by increasing N (which implies increasing N_{code}. Hence, *Theorem 1* is proved.

Thus we show that rate and transmit diversity have a tradeoff given by the rate-diversity tradeoff but frequency diversity can come for free. If diversity of N_d is guaranteed by the basic MIMO system, it can be shown that asymptotically in length $N_{code} = NN_T$ of the code (by letting $N \rightarrow \infty$), diversity of N_dL can be achieved with no penalty in the rate of the code. Thus there is no rate-diversity tradeoff for the frequency part of the overall diversity and frequency-diversity will come for free.

C. Simulation Results

In this section, we present simulation results for an LDPC coded MIMO system with $N_T = 2$ and $N_R = 2$. We consider three lengths for the LDPC code - $N_{code} = 4096$ bits (very short), 16384 bits (short) and 131092 bits (long). The N_{code} coded bits are split into 2 ($= N_T$) streams of $N_{code}/2$ bits each and which are then Gray-mapped to $N_{code}/4$ QPSK symbols each. These symbols are transmitted over an OFDM symbol with $N = 1024$ or 4096 or 32768 subcarriers. The receiver consists of a MAP demodulator for the MIMO system with 2 receive antennas followed by the sum-product decoder for the LDPC code with 100 iterations. Iterations between the demapper and the LDPC decoder are in general helpful, however, if AWGN optimized LDPC codes are used, iterations between demapper and demodulator will not improve performance much. Unless the extrinsic characteristics of the LDPC code is matched

to that of the demapper (EXIT charts [35]), iterations between demapper and decoder will not improve performance.

We consider up to four separate code-rates for the LDPC code - 1/3, 0.5 (= 0.49 which is slightly less than rate 0.5, but for practical purposes, we will refer to the rate as 0.5), 2/3 and 0.9 to demonstrate the rate-diversity tradeoff. The profiles for these codes are the best optimized ones for AWGN channel with a maximum variable degree of 20. For all these codes, it was ensured that atleast a small fraction of check nodes have an odd degree. The SNR assumed in one of the simulation figures for comparison purposes, is defined as $SNR = E_s/\sigma^2$ which can be viewed as the transmit SNR from Eqn. (4.2). This definition of SNR is chosen as opposed to E_b/N_o, to facilitate easy comparison of simulation results with other references. Note that this definition of SNR is the same as in [1] (in [1], their E_s is $1/N_T$ times our E_s, hence overall SNR is the same). Corresponding to the code-rates of $R = 1/3, 1/2, 2/3$ and 0.9, the overall transmission rate (assuming QPSK from each transmit antenna) from across all antennas is $R \times m \times N_T$ which will be equal to 4/3, 2 (slightly less than 2), 8/3 and 3.6 bps/Hz respectively.

For the MIMO case with no OFDM, we show the simulated results in Figure 13 with length 16384 LDPC code over a quasi-static fading channel where there are only 4 channel realizations (2×2) over the entire code-word. As can be seen, for $Rate < 2$ bps/Hz, all the diversity of 4 can be achieved, but for higher rate, asymptotically only diversity of 2 is achievable. Thus, the rate-diversity tradeoff for MIMO systems is closely followed by LDPC codes [32].

Diversity is defined as a measure asymptotic in SNR given by Eqn. (2.5). In Figure 13, the highest-rate code of code-rate 2/3 can achieve a slope higher than 2 for SNRs shown, but is expected to stabilize to a diversity of 2 at high SNRs. This is merely an artifact of observing the slope at finite SNRs.

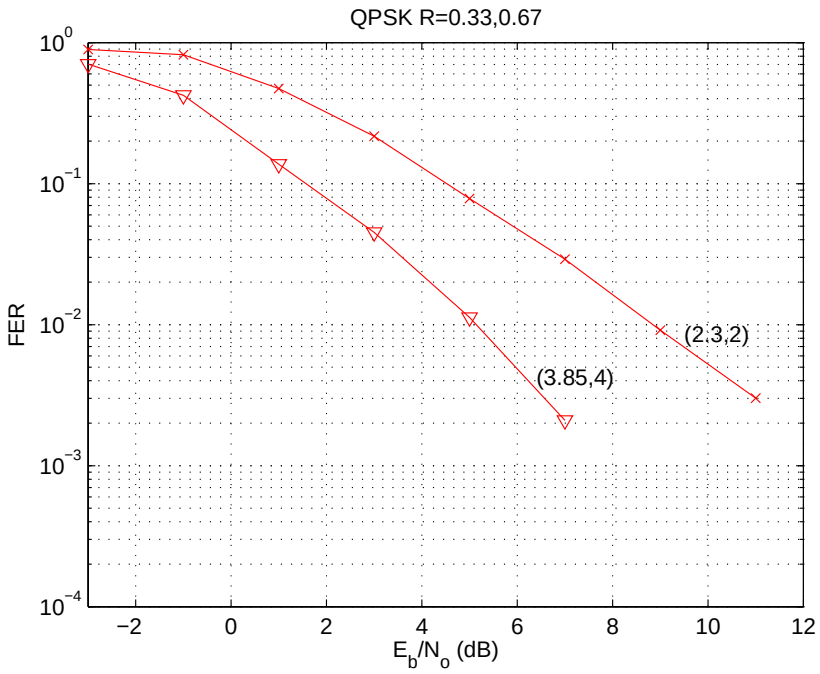

Fig. 13. Simulation results of a 2 × 2 MIMO system with QPSK and LDPC code-rate 0.5 and rate 0.67 (correspond to ≈2 b/s/Hz and 2.67 b/s/Hz respectively). The two numbers on the curve stand for the slope for that 2 dB section and the expected diversity order respectively

For the MIMO-OFDM case, we show the simulated results in Figure 14 with length 16384 LDPC code for all code-rates and Figure 15 with 131092 length LDPC code for code-rate 1/3. For both these cases, the number of taps $L = 2$. As can be seen, for code-rates given by 1/3 and 1/2, the highest diversity of 8 is achievable (it is our belief that the slope will tend to 8 as SNR increases further - some of the loss of slope can be attributed to the sub-optimal decoder used) while with code-rate 2/3, diversity of 4 is achievable as predicted by *Theorem 1*.

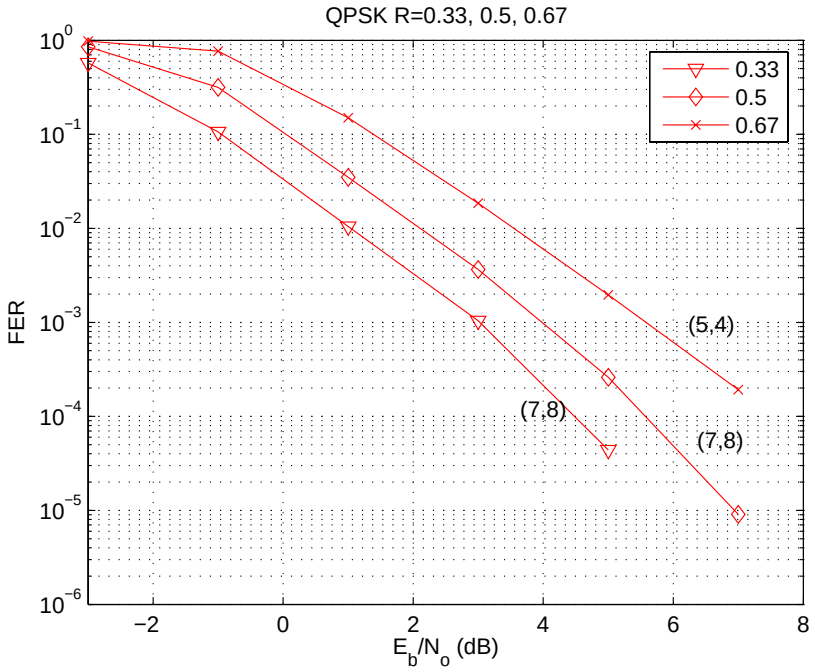

Fig. 14. Simulation results of a 2 × 2 MIMO-OFDM ($L = 2$) system with QPSK and LDPC code-rate 0.33, 0.5 and rate 0.67 (correspond to 1.33 b/s/Hz, ≈2 b/s/Hz and 2.67 b/s/Hz respectively). The two numbers on the curve stand for the slope for that 2 dB section and the expected diversity order respectively

For the MIMO-OFDM case, we also show the simulated results in Figure 16 with length 4096 LDPC code for code-rates 2/3 and 0.9. As can be seen from the

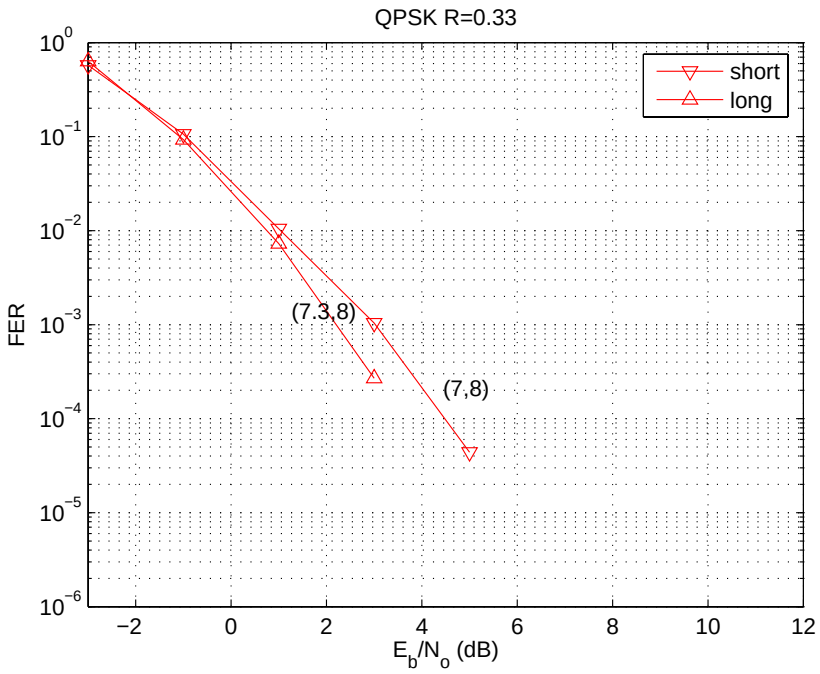

Fig. 15. Simulation results of a 2×2 MIMO-OFDM ($L = 2$) system with QPSK and LDPC code-rate 0.33 (corresponds to 1.33 b/s/Hz) and code-length 131072. The two numbers on the curve stand for the slope for that 2 dB section and the expected diversity order respectively

figure, the diversity for the 2/3 code-rate LDPC code for finite SNRs is higher than 4 (=5) but stabilizes to less than 4 at high SNRs. For code-rate 0.9, this effect is less pronounced, as for the SNRs shown, the curve stabilizes to a slope of 4.

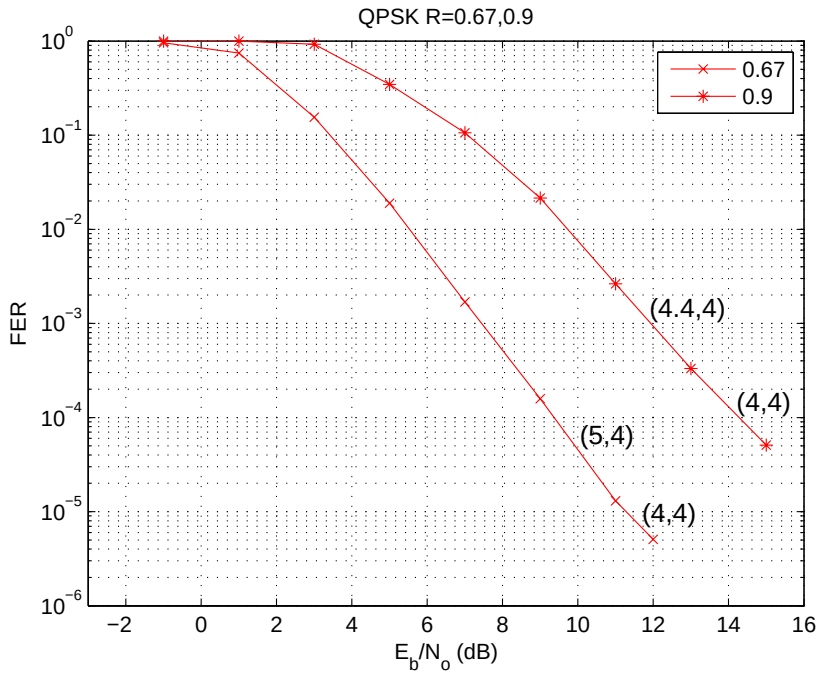

Fig. 16. Simulation results of a 2×2 MIMO-OFDM ($L = 2$) system with QPSK and LDPC code-rate 0.67 and 0.9 (correspond to 2.67 and 3.6 b/s/Hz respectively). The two numbers on the curve stand for the slope for that 2 dB section and the expected diversity order respectively

In Figure 17, we compare the proposed scheme with code-rate equal to 1/2 QPSK, $N_{code} = 16384$ and 2×2 MIMO system with $L = 2$ taps, to the simulation result for the same system given in Fig. 1(a) in [1]. The code in [1] has actually a transmission rate of 1b/s/Hz which is half our transmission rate for the same diversity, as they have to sacrifice rate to achieve the frequency diversity (the authors of [1] state that their scheme does not yield the optimal rate-diversity tradeoff). As seen from the

figure, our proposed scheme achieves better performance than the compared scheme with double the transmission rate. Our coding gain is also very good as it performs as well as a code which is half its rate in [1]. This can be attributed to the use of random-like codes such as LDPC codes. Fitz *et al.* also designed coding schemes for

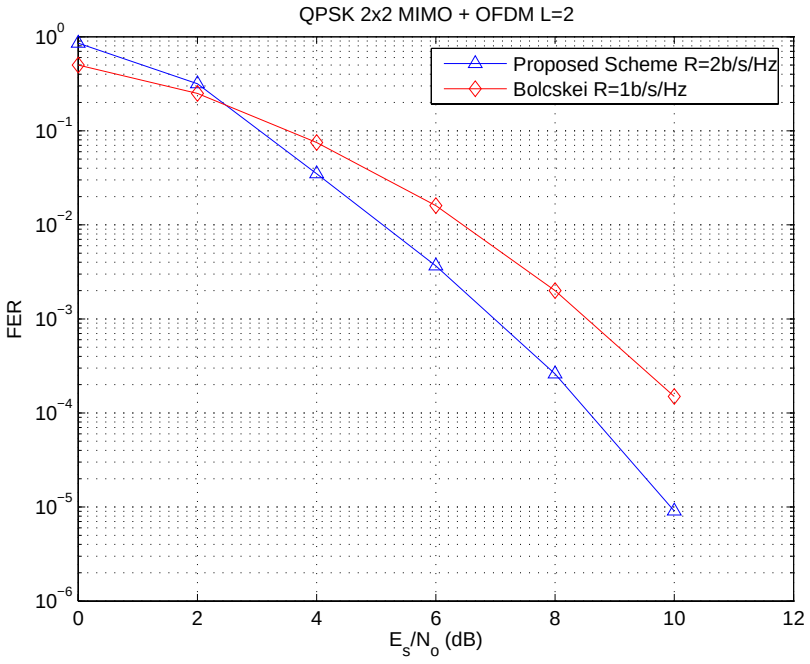

Fig. 17. Comparison of simulation results to Fig. 1(b) in [1]

MIMO-OFDM system [36], however they were unable to achieve the full-diversity of the MIMO-OFDM system (Table III in [36]) as opposed to our scheme which can achieve the full-diversity, due to the constraints on the code-rate they chose. The scheme in [36] also does not have the advantages of a variable-diversity variable-rate scheme as the one presented in this work.

For the plain SISO-OFDM case, we simulate an LDPC code of length 16384 and code-rate 0.8 over a SISO-OFDM system with $L = 2, 4$ and QPSK modulation. The

number of subcarriers is $N = 8192$. As can be seen from Figure 18, the diversities of 2 and 4 are achievable with this code-rate as proved in Section 2.

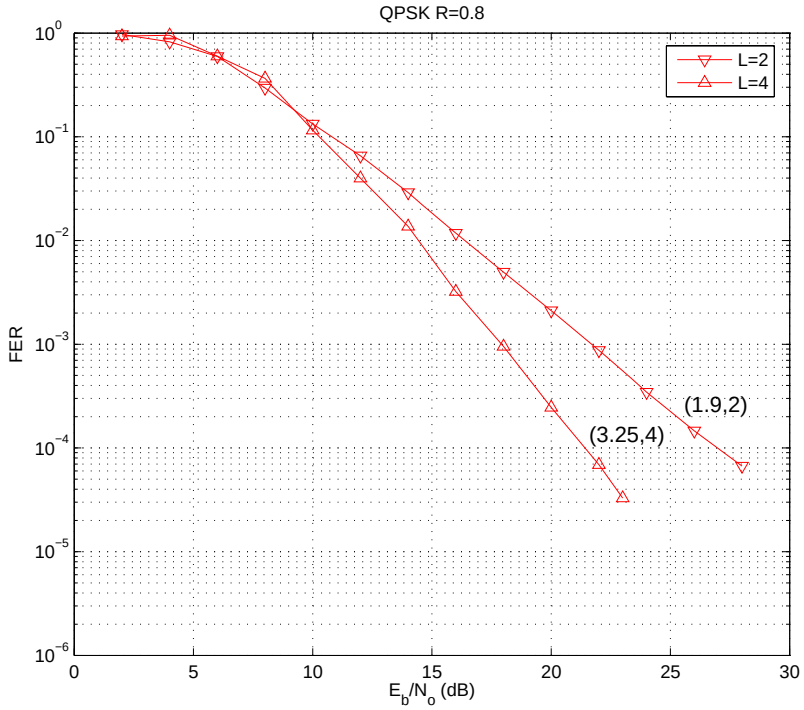

Fig. 18. Simulation results of a SISO-OFDM system with QPSK and LDPC code-rate 0.8 with L =2 and L =4

In summary, we have characterized the rate-diversity tradeoff for MIMO-OFDM and SISO-OFDM systems in this work. We show that there is no tradeoff in rate in order to obtain the frequency diversity present but only careful code-design is required. We prove that a scheme with LDPC codes as an outer-code and serial-parallel converter as an inner code achieves this rate-diversity tradeoff for MIMO-OFDM and SISO-OFDM systems with an ML decoder. We further show through simulations that the proposed scheme with a sub-optimal sum-product decoder can perform very close to this tradeoff curve with good coding gains. The presented

scheme is a very flexible scheme and can achieve different diversities as the requirement might arise by merely changing the code-rates.

CHAPTER V

DESIGN OF LDPC CODES FOR OFDM WITH PARTIAL CSI*

Irregular Repeat Accumulate (IRA) codes perform very close to capacity on most memory-less channels with coherent detection. Further, techniques are available to design good IRA codes that can be matched to a given channel for a given rate [37]. IRA codes also have the advantage of having an easily implementable encoder structure and their encoding and decoding can be done in linear time. In this work [9] [8], we design good IRA codes for Inter-symbol interference (ISI) channels when OFDM is used. The focus is on the case when CSI is not available at the receiver and has to to be estimated from a few pilots.

When CSI is available, code design for multipath fading ISI channels can be done in two ways - a soft output equalizer can be used in conjunction with a decoder and codes can be optimized [38] [39] or OFDM can be used to circumvent ISI and code design for flat-fading channels can be directly applied. The second approach is simpler and is considered in this work but perfect CSI is not assumed at the receiver.

Most of the work done on OFDM so far has assumed the availability of perfect channel information at the receiver. However, this is a very optimistic assumption and in practice some kind of estimation has to be done. Acquiring correct channel state information is a difficult problem as the complexity of an optimal channel estimator is quite high and it also requires knowledge of the statistics of the channel [40] [41].

In this work, we propose the use of IRA codes with a very simple receiver that

*

performs iterative estimation and decoding. The channel estimator does not require knowledge of the number of taps in the ISI channel or the statistics of the fading process. Similar receiver structures have been considered in [42] [43] but code design is not addressed in these papers. Low-density Parity-check (LDPC) code design for a similar scheme on correlated flat-fading channels has been considered in [44].

The key components of the technique used in this work are the use of differential encoding across sub-carriers in an OFDM system and the use of a non-systematic IRA code, which is carefully optimized. Hence, the technique can be thought of as a joint code and receiver design approach. We use EXIT charts to optimize the IRA code [10]. The basic idea is to use a simple differential detector during the first iteration (hence the use of IRA code) and then use the output of the differential detector to generate soft output from the decoder which can then be used to perform pseudo-coherent detection. A similar receiver design for Multiple-Input Multiple-Output (MIMO) ISI channels with OFDM and serial concatenated codes but with differential encoding in time (rather than across sub-carriers as is being proposed here) was considered in [45]. Consequently, the schemes considered in [45] may not be robust to faster fading and is certainly not suitable for block fading as they are differential in time rather than in frequency (our scheme). Also their scheme does not optimize the code for a given receiver structure.

A. System Description and Decoding

1. IRA Codes

IRA codes are represented in terms of a bipartite graph similar to an LDPC code. IRA codes consist of three kinds of nodes - *information* nodes, *check* nodes and *parity* nodes. The *information* nodes correspond to the information bits in a codeword.

The *parity* nodes correspond to the parity bits in the codeword. The *check* nodes correspond to the parity-check constraints satisfied by the *information* and the *parity* nodes. The degree of an information node or a parity node is the number of checks it participates in while the degree of a check node is the number of information nodes that are connected to the check. The degree of a parity node is 2 unless stated otherwise. If the information bits are transmitted along with the parity bits, it is a systematic IRA code otherwise it is a non-systematic IRA code. In this work, we are interested in non-systematic IRA codes for two reasons: one, they allow differential detection and two, the outer irregular part can be easily matched to the inner code and channel and hence code design is easier.

2. System Description

As shown in Figure 20, the data bits are repeated irregularly and then passed onto a differential encoder (accumulator). Some of the symbols (say 1 every p symbols) at the output of the accumulator are set to zero which act as pilot symbols. This can be done by setting the corresponding input bits to zero or one depending on which will give a zero output. As shown in figure 20, the coded bits are incident on the OFDM modulator. Adjacent coded bits of the IRA codeword are transmitted as BPSK symbols on adjacent sub-carriers of the OFDM symbol through the channel. An IRA codeword is assumed to span several groups of OFDM symbols. Assume that the length of the IRA codeword is $N = M_1 \times N_1$ where N_1 is the number of sub-carriers. By one group of OFDM symbols, we mean the set of N_1 symbols which is of total duration $N_1 T_s$ in the time domain (where T_s is $1/f_s$, f_s being the bit-rate) obtained after IFFT of the bits present in all the N_1 sub-carriers. The channel is assumed to have $L-$taps with uniform power distribution among them. The modulator uses an appropriate guard interval to counter ISI and a cyclic shift in the guard interval to

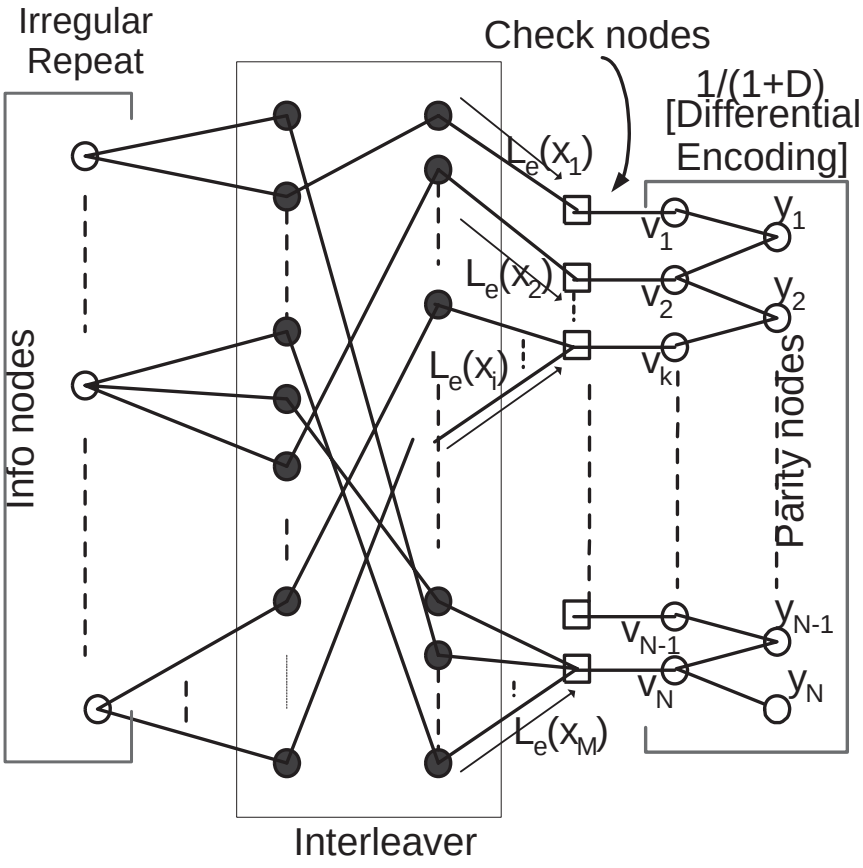

Fig. 19. Bipartite graph of an IRA code

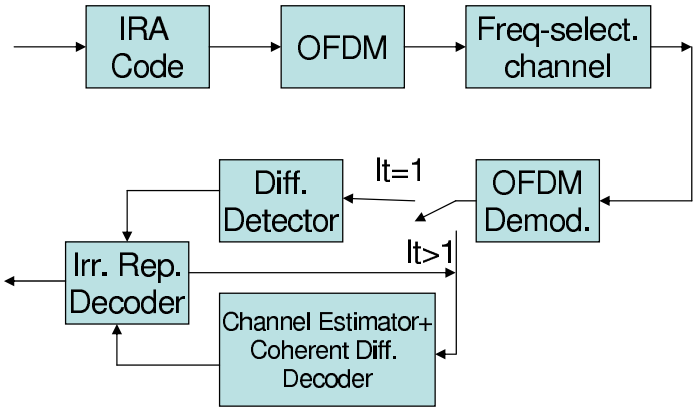

Fig. 20. System description of an IRA-OFDM system

prevent inter-carrier interference (ICI). For the time being, assume that the channel is a block fading channel i.e. over a group of OFDM symbols the fading is constant and across OFDM symbol groups, the channel is independent. This assumption of fading being constant over an OFDM symbol group shall be relaxed later when slow/fast fading is considered, the rest being the same. After demodulation of the received OFDM symbols which involves a stripping of the guard interval and an FFT operation on the received baseband signal, decoding is done in the following fashion.

3. Decoding

We consider BPSK signaling ($0 \rightarrow -1, 1 \rightarrow +1$) and assuming proper sampling of the outputs from the matched filter, the received discrete-time baseband signal corresponding to the j_2-th sub-carrier in the j_1-th OFDM symbol can be written

as:

$$r_k = h_k y_k + n_k$$

$$k = j_1 \times N_1 + j_2, \qquad j_1 = 1, \ldots, M_1, \qquad j_2 = 1, \ldots, N_1 \tag{5.1}$$

$$h_k = \alpha_k e^{j\theta_k} \tag{5.2}$$

where y_k is the DBPSK signal (± 1), $y_k = v_k y_{k-1}$, n_k is the i.i.d complex AWGN with zero mean and variance $\sigma^2 = N_0/2$ in each dimension. v_k is the input bit to the DBPSK modulator. The fading amplitude α_k is a normalized Rayleigh random variable with $E[\alpha_k^2] = 1$ and pdf $p_\alpha(\alpha) = 2\alpha_k \exp(-\alpha_k^2)$ for $\alpha_k > 0$ and the fading amplitude θ_k is assumed to be uniformly distributed in $[0, 2\pi]$. For coherent detection, θ_k is perfectly known whereas for non-coherent detection it is unknown. Also for the case where there is Doppler, we use a two-dimensional isotropic scattering land mobile Rayleigh channel model to describe the correlated Rayleigh process, α_k which has autocorrelation $R_k = 0.5 J_o(2k\pi f_d T_s)$, where $f_d T_s$ is the normalized Doppler spread, and $J_o(.)$ is the zeroth order Bessel function of the first kind.

For the proposed scheme, the first step is one-symbol differential detection on the received values which is as follows [44]:

$$u_k = \text{Real}(r_k r_{k-1}^*) \tag{5.3}$$

where $*$ represents the complex conjugate. The log-likelihood ratio (LLR) for u_k can be obtained from its pdf. The conditional pdf of u_k given α_k and v_k is [18]:

$$f_{U|\alpha,V}(u|\alpha, v) = \begin{cases} \frac{1}{2N_0} \exp\left(\frac{vu - \alpha^2/2}{N_0}\right), & -\infty < vu \leq 0; \\ \frac{1}{2N_0} \exp\left(\frac{vu - \alpha^2/2}{N_0}\right) Q\left(\sqrt{\frac{\alpha^2}{N_0}}, \sqrt{\frac{4vu}{N_0}}\right), & 0 < vu < \infty; \end{cases}$$

where $Q(a, b)$ is the Marcum Q function. Then, we can obtain the true pdf of u_k

using:

$$f_{U|V}(u|v) = \int_0^\infty f_{U|\alpha,V}(u|\alpha,v) f_\alpha(\alpha) d\alpha, \tag{5.4}$$

$$= 2\int_0^\infty f_{U|\alpha,V}(u|\alpha,v)\alpha e^{-\alpha^2} d\alpha. \tag{5.5}$$

Since this is complex to evaluate, a simpler method would be to substitute α with $E[\alpha]$, which leads to:

$$f_{U|\alpha,V}(u|\alpha,v) = \begin{cases} \frac{1}{2N_0}\exp\left(\frac{vu-\pi/8}{N_0}\right), & -\infty < vu \leq 0; \\ \frac{1}{2N_0}\exp\left(\frac{vu-\pi/8}{N_0}\right) Q\left(\sqrt{\frac{\alpha^2}{N_0}}, \sqrt{\frac{4vu}{N_0}}\right), & 0 < vu < \infty; \end{cases}$$

The corresponding LLR can then be computed as:

$$L_{ch}(v_k) = \text{sign}(u_k)\left(\frac{2|u_k|}{N_0} + \log\left(Q(\sqrt{\frac{\pi^2}{4N_0}}, \sqrt{\frac{4|u_k|}{N_0}})\right)\right). \tag{5.6}$$

In the proposed scheme, however, we have used a simpler expression [46] [44] which assumes that u_k is Gaussian distributed and is given by:

$$f_{U|V}(u|v) \approx \mathcal{N}(v, 2N_0 + N_0^2), \tag{5.7}$$

$$L_{ch}(v_k) \approx \frac{2u_k}{2N_0 + N_0^2} \tag{5.8}$$

As stated earlier, we apply non-systematic IRA codes to this system to allow differential detection and due to the ease of design. For iterations to start in a non-systematic IRA code, some check nodes must have degree 1. In the proposed design, we consider a fraction, ρ_1' $(0 < \rho_1' < 1)$, of the check nodes to have degree 1 and the rest of the check nodes have a higher degree. Once the soft decisions on v_k has been obtained, decoding is performed as follows.

In the bipartite graph of the IRA code (figure 19), the parity nodes, y_k and the edges connected to these nodes are removed. Note that $L_{ch}(v_k)$ is the *a priori*

information on v_ks. There is no a priori information on the information nodes and the LLRs on the edges of the interleaver ($L_e^{(0)}(x_i)$) are initialized to zero. Two iterations of sum-product decoding are performed at the check nodes and at the information nodes on this residual bipartite graph. Assuming the number of edges in the interleaver is M, the extrinsic edge LLRs ($L_e^{(2)}(x_i), \quad i = 1, \ldots, M$) from the information nodes to the check nodes after the two iterations can be obtained. For the edges connected to the degree-1 check nodes, define a soft output:

$$L_{e,so}^{0}(x_i) = L_e^{(2)}(x_i) + L_{ch}(v_i) \tag{5.9}$$

and for the edges connected to the higher degree check node define the same as $L_{e,so}^{0}(x_i) = L_e^{(2)}(x_i)$.

The subsequent iterations (call it $q, q \geq 0$) use $L_{e,so}^{q}(x_i)$ as a priori information on the uncoded bits to an APP decoder for the accumulator trellis and along with the presence of the pilot symbols in the trellis, extrinsic values $L_{coded}^{q}(y_k)$ on the coded bits y_k can be obtained. In order to obtain the extrinsic values, $L_{coded}^{q}(y_k)$, an estimate of the channel is required. A simple moving-average filter of length K can be used to obtain complex estimates of the channel given as:

$$\hat{h}_{j_1 N_1 + j_2}^{q} = \frac{1}{K} \sum_{i=(j_2 - K/2) \bmod N_1}^{(j_2 + K/2) \bmod N_1} r_{j_1 N_1 + i} \tanh\left(\frac{L_{coded}^{q-1}(y_{j_1 N_1 + i})}{2} \right).$$
$$j_1 = 1, \ldots, M_1 \qquad j_2 = 1, \ldots, N_1 \tag{5.10}$$

where mod is the modulo operation. Note that $\hat{h}_{j_1 N_1 + j_2}$ has to be determined separately for each OFDM symbol, as each OFDM symbol has independent fades. The moving average filter runs circularly over each OFDM symbol (due to the periodicity of FFT) to calculate the corresponding $\hat{h}_{j_1 N_1 + j_2}$. These estimates can be used to

obtain the LLRs on y_k as:

$$\hat{L_{ch}}(y_k) = \frac{2}{\sigma^2}\mathcal{R}(r_k^*\hat{h}_k) \tag{5.11}$$

where $\mathcal{R}(a)$ represents the real part of a. $L_{ch}(y_k)$ serves as *a priori* information on the coded bits and using $L_{e,so}^{q}(x_k)$ as a priori information on the uncoded bits, the APP (*a posteriori* probability) decoder for the accumulator can obtain extrinsic information on the uncoded bits. A decoding procedure similar to sum-product decoding for the variable nodes can be applied to the information nodes to obtain extrinsic information ($L_{e,so}^{q+1}(x_k)$) on the uncoded bits of the accumulator. These set of iterations of channel estimation, APP decoding of accumulator and information nodes decoding continue for a fixed number of iterations after which a hard decision is obtained from the soft values.

B. Code Design

In the system considered here, since there are several channel realizations in a single codeword, we will assume that the channel is ergodic. The problem of code design boils down to finding the optimum check and information node profiles which perform as close to capacity as possible. For the check node, we consider a fraction (ρ_1') of the nodes to be of degree 1 and the rest to be of another degree. To design the information node profile, it is easier to assume the serial concatenated structure of IRA codes and then optimize [10].

Extrinsic Information Transfer (EXIT) charts [35] are a robust measure to track the progress of the decoder in an iterative scheme. Through simulations, it has been conjectured that the EXIT curve of the outer code must lie very close to that of the inner code to maximize the rate of the outer code and for good BER performance. If

there is a gap, then it will result in rate loss. Also the EXIT curve of the outer decoder must lie completely below the EXIT curve of the inner decoder for the iterations to converge. For the proposed scheme, EXIT curve is obtained for the inner decoder (for the accumulator). The EXIT curve of the outer irregular repeat decoder must then be matched to the inner one. This method can be applied separately to the case with perfect channel knowledge at the receiver and with partial channel knowledge where a channel estimator is used, to design different codes for the two schemes.

In the case of non-systematic IRA codes with no check nodes of degree 1, the EXIT curves of both the inner and the outer decoder start from the $(0, 0)$ point and hence iterations cannot start at all. If the non-systematic code is doped with some check nodes of degree 1, however, the EXIT curve of the inner code will start from a non-zero point and the outer code which always starts from the all-zero point can be matched with the guarantee that the iterations will start. There will be a slight rate loss, the magnitude of which depends on the fraction of degree 1 check nodes. Deciding upon a good value for ρ_1' is a tricky problem for the fading channel. Even though we have assumed the channel to be ergodic for the infinite length case, for the finite length case for any given block of the IRA codeword and its associated channel realizations, it may not be ergodic. In other words, the EXIT curve of the inner decoder can shift around its average from block to block of the code.

The ergodic EXIT curve for the inner code with the above parameters can be obtained easily. Finding the optimum information node profiles for the outer code is then a curve-fitting problem which can be done as follows [10]:

Define a function $J(.)$ as the mutual information function between the random variables X and $Y = X + N$ where $\Pr(X = m) = \Pr(X = -m) = 1/2$ and N is zero mean, Gaussian noise with variance σ^2 and assume that $m = \sigma^2/2$ so that symmetry

condition is satisfied [25]. Then:

$$\begin{aligned} J(\sigma) &= H(X) - H(X|Y) \\ &= 1 - \int_{-\infty}^{\infty} \frac{e^{-\frac{(\xi-\sigma^2/2)^2}{2\sigma^2}}}{\sqrt{2\pi\sigma^2}} . \log_2(1+e^{-\xi}) d\xi \end{aligned} \tag{5.12}$$

where $H(X)$ is the entropy of X and $H(X|Y)$ is entropy of X conditioned on Y.

If $L_{i,in}$ is the LLR incident on a degree-d_v information node and $L_{j,out}$ is the extrinsic LLR on the $j-$th edge connected to the same node, then:

$$L_{j,out} = \sum_{i \neq j} L_{i,in} \tag{5.13}$$

Further, if we assume that $L_{i,in}$ is Gaussian distributed with standard deviation, $J^{-1}(I_{A,O})$, where $I_{A,O}$ is the a priori mutual information incident on the irregular repeat from the inner code. Then:

$$I_{E,O}(I_{A,O}, d_v) = J(\sqrt{d_v - 1}.J^{-1}(I_{A,O})) \tag{5.14}$$

where $I_{E,O}(I_{A,O}, d_v)$ is the extrinsic information from the irregular repeat nodes back to the inner code through an information node of degree-d_v.

Hence, owing to the linear property of mutual information, the overall extrinsic mutual information from the irregular repeat outer code can be given as:

$$I_{E,O}(I_{A,O}) = \sum_{d_v=2}^{D_v} \lambda_{d_v} I_{E,O}(I_{A,O}, d_v) \tag{5.15}$$

where λ_{d_v} is the degree profile of the information nodes from the edge perspective. Since the EXIT curve of the inner code has to be matched to the EXIT curve of the

outer code, if $(I_{E,I}, I_{A,I})$ is a point on the EXIT curve of the inner code:

$$I_{E,O}(I_{E,I}) \geq I_{A,I} \tag{5.16}$$

$$\Rightarrow \sum_{d_v=2}^{D_v} \lambda_{d_v} I_{E,O}(I_{E,I}, d_v) \geq I_{A,I} \tag{5.17}$$

Solving for λs is a constrained linear optimization problem which can be easily done. In this type of code design sufficiently long length of the code and proper interleaving is assumed to make the messages passed between the inner and outer decoder independent.

C. Capacity of the System

The capacity of the OFDM system with a frequency-selective channel given perfect knowledge of the channel is equal to the sum-capacity of parallel flat fading channels given perfect knowledge of the channel. The system is equivalent to:

$$r_k = h_k y_k + n_k \tag{5.18}$$

where y_k is the input BPSK symbol (± 1) to the OFDM modulator, r_k is the complex received value after the OFDM demodulator, h_k is the complex-valued channel which is known at the receiver and n_k is complex-valued white Gaussian noise with variance $\sigma^2 = N_0/2$ in each dimension. When h_k is known at the receiver, Eqn. 5.18 can be written as:

$$r_k h_k^* = \|h_k\|^2 y_k + h_k^* n_k. \tag{5.19}$$

Note that this operation does not change the overall capacity of the system. Since, the information about y_k is present only in the real part of LHS, the above equation

can be further simplified to:

$$w_k = \mathcal{R}(r_k h_k^*) = \|h_k\|^2 y_k + \mathcal{R}(h_k^* n_k) \tag{5.20}$$

where $\mathcal{R}(.)$ represents the real part.

Also $\mathcal{I}(R;Y|H) = \mathcal{I}(W;Y|H)$ and the capacity of the system is $E_H[\mathcal{I}(W;Y|H)]$. Since the channel is ergodic,

$$E_H[\mathcal{I}(W;Y|H)] = \frac{\sum_{i=1}^{M} \mathcal{I}(W;Y|H_i)}{M} \tag{5.21}$$

$$\mathcal{I}(W;Y|H_i) = \frac{1}{2}. \sum_{y=\pm 1} \int_{-\infty}^{\infty} p_{W|H_i}(w|h_i, Y=y) \log_2 \frac{2p_{W|H_i}(w|h_i, Y=y)}{p_{W|H_i}(w|h_i, Y=-1) + p_{W|H_i}(w|h_i, Y=1)} dw \tag{5.22}$$

A plot of the capacity against E_b/N_0 has been given in Figure 21. It has been conjectured that the ergodic capacity [35] is close to the area under the EXIT curve of the inner code + channel ($(A)_{in}$) multiplied by the rate of the inner code (R_{in}) for most of the channels i.e.

$$\mathcal{I}(R;Y) = (A)_{in} R_{in} \tag{5.23}$$

This was verified to be fairly accurate for the EXIT curve of the inner code.

D. Results

For a rate 1/2 code with perfect CSIR at the receiver, the ergodic capacity is around $E_b/N_0 = 1.9$ dB. However, the EXIT curve of the irregular part could be matched to the inner decoder EXIT curve for the given rate of 0.5 only at 2.3 dB. The EXIT curve for the inner decoder was obtained for this E_b/N_0 and the outer code was designed to match it as shown in Figure 22. For the receiver with no channel information other than from the channel estimator (CE), to obtain a rate-0.5 code, its matching could

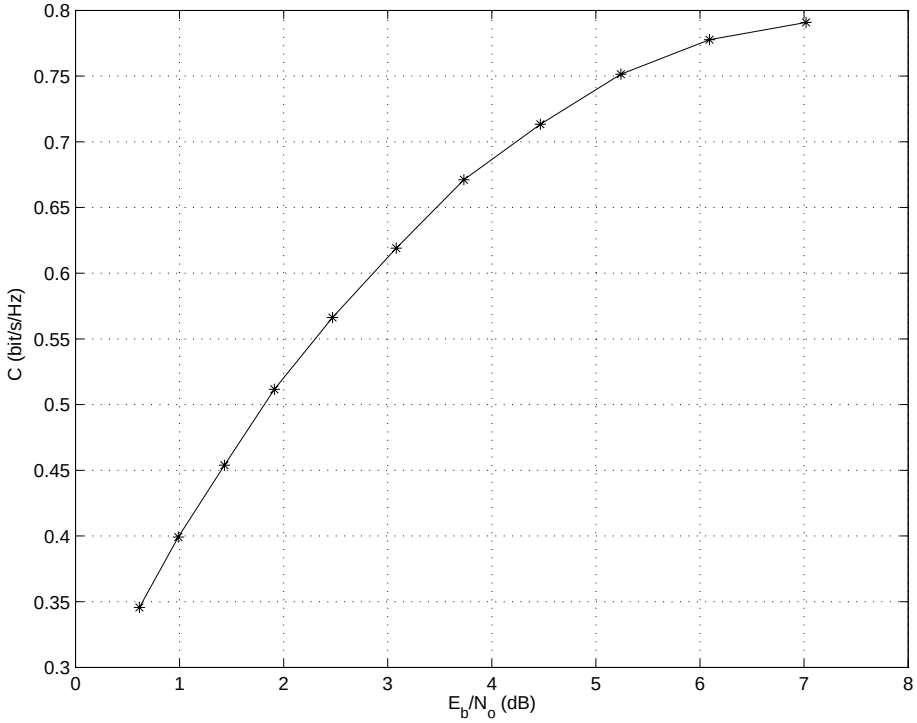

Fig. 21. Capacity of the OFDM + multipath channel system with 1024 sub-carriers and 4 multipaths with equal power distribution

be done only at $E_b/N_0 = 2.4$ dB. The profiles obtained for the two cases are:

$$\begin{aligned} \text{CSIR:} \quad & \lambda(x) = 0.3318x^2 + 0.6682x^7 \\ \text{CE:} \quad & \lambda(x) = 0.3067x^2 + 0.3148x^6 + 0.3824x^7 \end{aligned} \tag{5.24}$$

The presence of degree-2 information nodes leads to error-floors, hence, it was set to zero. For this rate, $\rho'_1 = 0.5$ and $\rho'_4 = 0.5$ was found to be a good check degree profile.

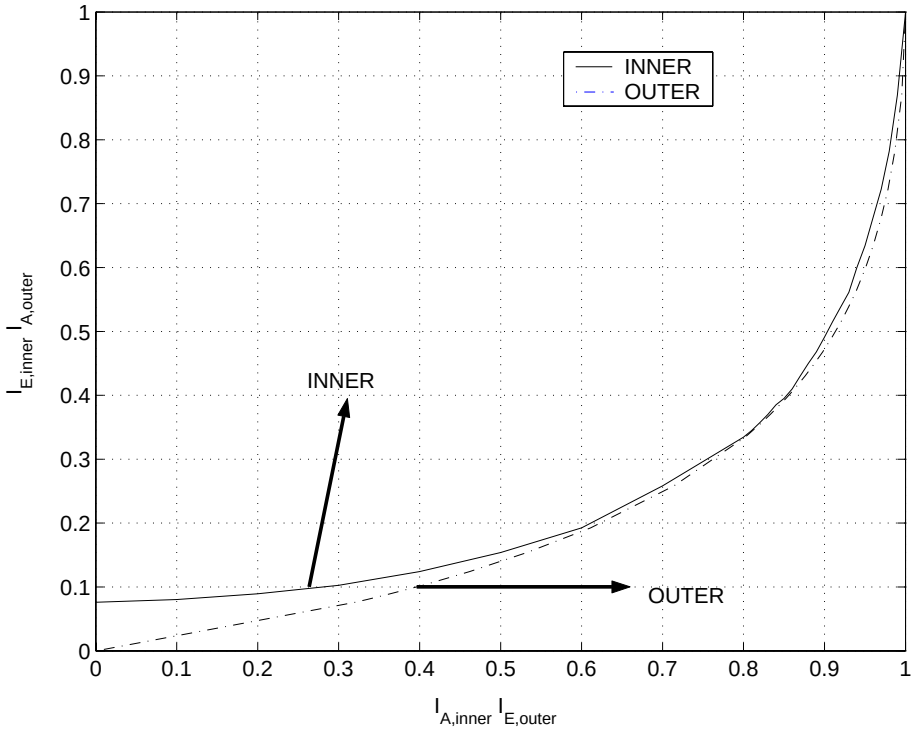

Fig. 22. EXIT chart matching for the case with perfect channel state information at the receiver

The length of the IRA codeword is chosen to be 32768 i.e. $M_1 N_1 = 32768$ and the number of sub-carriers in the OFDM is assumed to be $N_1 = 1024$ unless stated otherwise. Also, fading across OFDM symbols is assumed to be block fading so that over an OFDM symbol, the fading does not change. Fading on different multipaths

is always independent. Two cases have been considered for simulations - one with perfect channel state information at the receiver (CSIR) and another with the channel estimator. The channel estimator is a simple moving-average filter as described in Section II with $K = 150$. The number of iterations is set to 100. A small ratio of pilots is required so that the error propagation is curbed at regular intervals. Unless otherwise stated, a pilot ratio of 1 every 32 symbols is used. As stated earlier, pilots are inserted in the trellis so that they can aid in APP decoding of the accumulator also.

Simulation results comparing the optimized code for CSIR system and for the channel estimation system (CE) have been presented in Figure 23. It can be seen that the system with the channel estimator system performs within a few tenths of dB from the CSIR system. The system with channel estimation has been penalized in E_b/N_0 for the presence of pilots. The same figure also shows the CSIR and CE scheme for a longer length of 131072 coded bits and $N_1 = 256$ and the same rate. The codes turned out to have the same profile as (5.24). The CSIR code performs closer to its threshold of 2.3 dB for this length and so does the CE code to its threshold. For longer lengths, the system has more diversity and is closer to being ergodic and hence, the EXIT curve is less random and the design more exact. To show the importance of the proposed code optimization, Figure 24 compares the CE optimized code (25) to an AWGN optimized rate 1/2 systematic IRA code of the same complexity and to a (3,6) regular LDPC code in a receiver with channel estimator. The codes are of length 32768 and the number of sub-carriers in an OFDM symbol is 1024. It can be seen that code (25) performs the best followed by (3,6) LDPC code and the IRA code. This is because code (25) and (3,6) are better matched to the characteristics of the channel estimator than the AWGN optimized IRA code.

To show the robustness of the proposed scheme to different channel lengths, 2

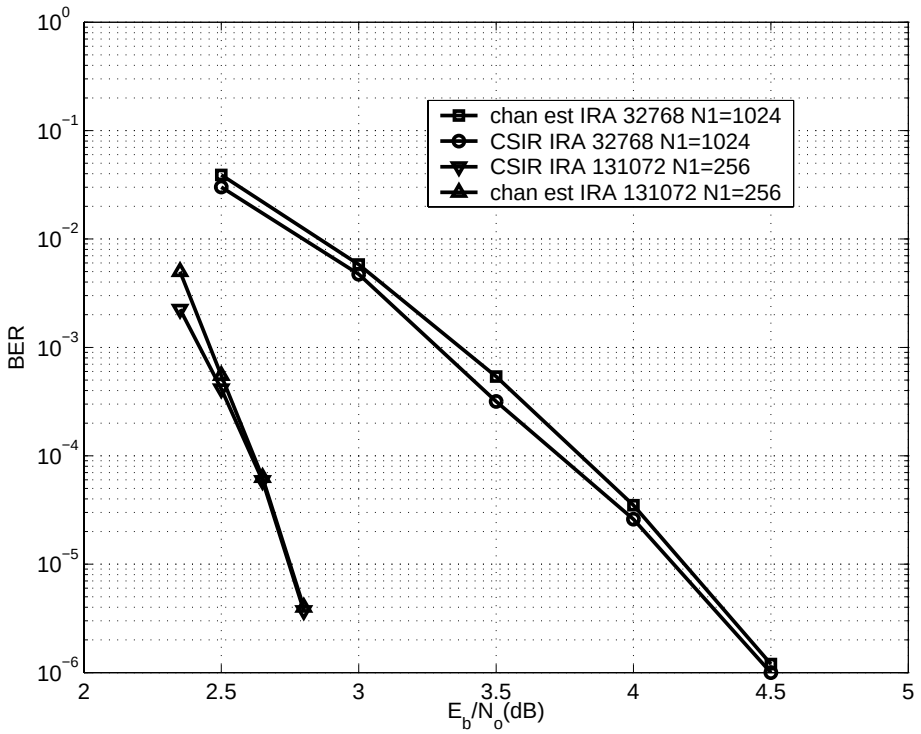

Fig. 23. BER of CSIR and NCSI with channel estimator for a rate-0.5 IRA code of length 32768 BPSK and OFDM with 1024 sub-carriers and CSIR and NCSI rate-0.5 length 131072 IRA and OFDM (256 subc.). Ergodic capacity with CSIR is $E_b/N_0 = 1.9$ dB

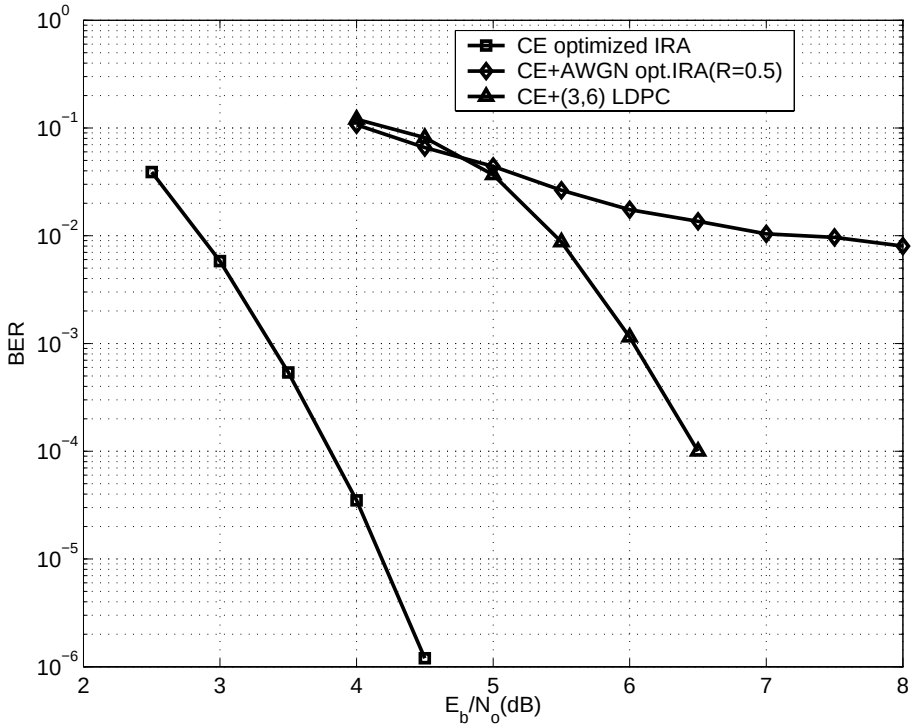

Fig. 24. Comparison of BER of (i) NCSI with channel estimator for the rate-0.5 IRA code given by (25) of length 32768 BPSK and OFDM with 1024 sub-carriers, (ii) AWGN optimized rate-0.5 IRA code of same decoding complexity, and (iii) (3,6) LDPC code

different channel lengths of 4 and 10 have been compared in Figure 25. For length 10, the CSIR system has also been simulated in the same figure for comparison. The codes have the same profiles as (5.24) for the CE and CSIR system. It can be seen that the proposed scheme performs very close to the coherent system under the case of 10 multipaths too and hence the proposed scheme is not sensitive to the number of taps. An optimum Weiner filter on the other hand would be sensitive to the number of taps in the channel.

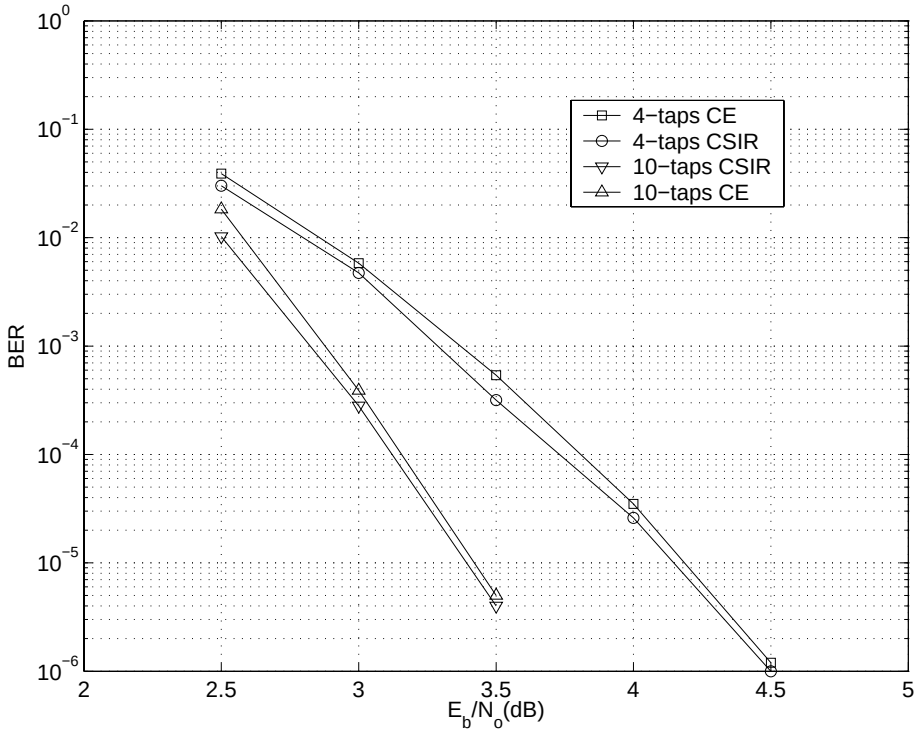

Fig. 25. BER of a rate-0.5 length 32768 IRA code BPSK and OFDM with 1024 sub-carriers and 4, 10 multipaths on an NCSI system with channel estimator and with CSIR

To show the sensitivity of the proposed scheme to the ratio of pilots introduced in the trellis, 3 different pilot ratios of 1/32, 1/64 and 1/128 were simulated for

the 4-tap channel and the results are presented in Figure 26. The proposed system performs well for all these pilot ratios. The pilot separation is however a function of the coherence bandwidth - coherence bandwidth is roughly 256 bits for the 4-tap channel.

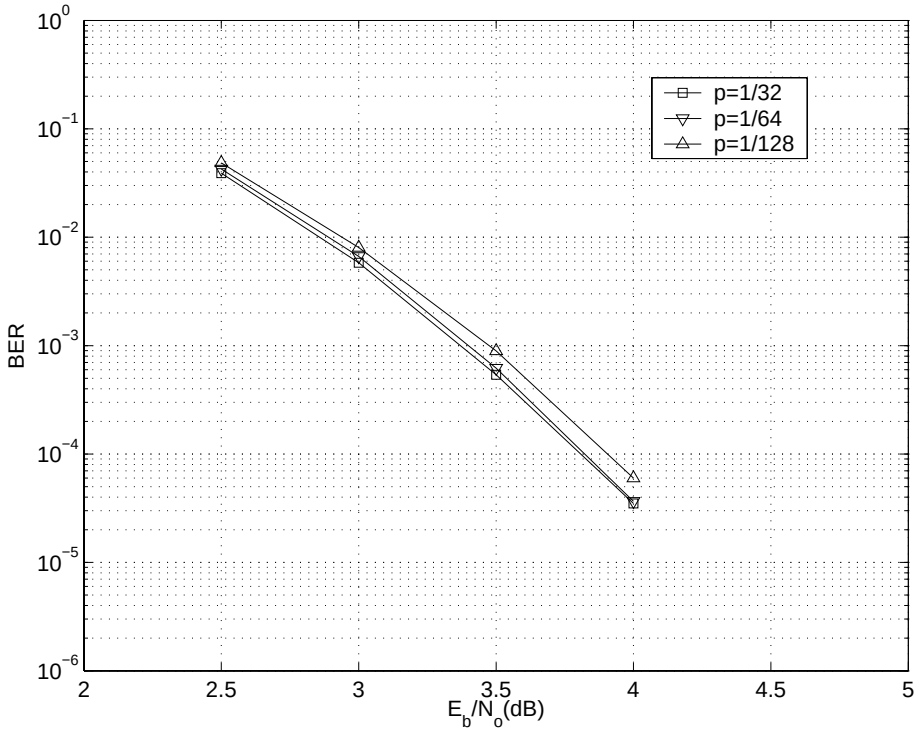

Fig. 26. BER of NCSI with channel estimator for a rate-0.5 length 32768 IRA code BPSK and OFDM with 1024 sub-carriers and p=1/32, 1/64 and 1/128 and channel with 4 multipaths. Ergodic capacity with CSIR is $E_b/N_0 = 1.9$ dB

To show the robustness of the proposed scheme to fading over an OFDM symbol, simulation results are shown when there is a Doppler of $f_d = 100, 400$Hz in Figure 27. The bit-rate is assumed to be $f_s = 1$ Mbps. It can be seen that $f_d = 100$ performs well but $f_d = 400$ has a floor effect due to the fading. However, the OFDM symbol can still withstand this much of Doppler if the number of sub-carriers is reduced to

256 as shown in the same figure.

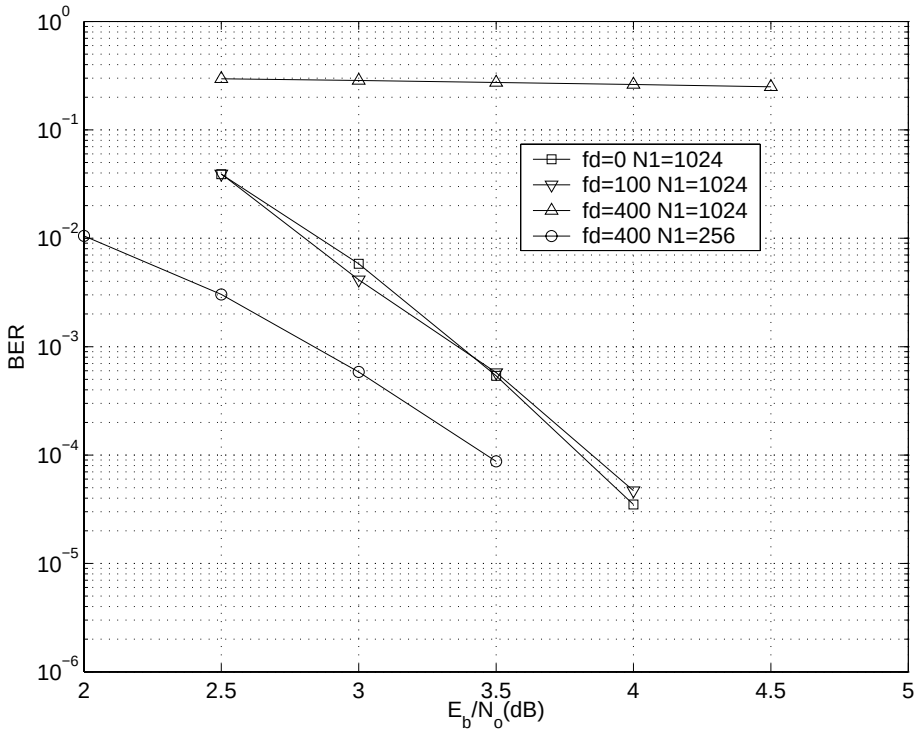

Fig. 27. BER of NCSI with channel estimator for a rate-0.5 length 32768 IRA code BPSK and OFDM with N1=1024 sub-carriers and Doppler over an OFDM symbol of 0,100 and 400 and 256 sub-carriers with Doppler 400. Ergodic capacity with CSIR is $E_b/N_0 = 1.9$ dB

In summary, a novel scheme with IRA codes on a frequency-selective block fading channel with partial CSI is proposed in this work. Non-systematic IRA codes were designed for the proposed scheme. It performs within a few tenths of a dB of the coherent detection case with the channel parameters. The scheme is robust to changes in number of taps and time-delay profile of the channel and requires a very simple channel estimator.

CHAPTER VI

LDPC CODE DESIGN FOR ADAPTIVE MODULATION

Communication systems with channel state information at both the transmitter and the receiver (CSITR) are becoming increasingly common owing to the higher data rates these systems can support. Capacity-achieving coding schemes for CSITR systems have only been derived assuming Gaussian constellations at the transmitter (waterfilling) [47] [48]. Gaussian constellations are not practical and hence trasmit signals have to be constrained (for example QAM). So capacity-achieving schemes for constrained constellations have to be derived and it is still an open problem.

In the first part of this work [12] [49], we derive the constrained capacity and the capacity-achieving power allocation algorithm for a single-antenna system with parallel flat-fading subchannels and CSITR assuming transmission of constrained constellation symbols such as QAM. In practice, this is similar to a multicarrier system (for example, OFDM) with CSITR. The resulting power-allocation for the constrained constellation system is different from waterfilling obtained for Gaussian constellations. Information theory suggests that a single ideal (capacity-achieving) code with ML decoding and having a code-rate given by the average of the code-rates supported on each of the parallel subchannels achieves the capacity of this system. However, achieving performance of ML decoding with practical codes such as LDPC codes [25] is a difficult problem and ML performance can only be approached. If practical codes are used, a dedicated codebook for each of the subchannels will be required to perform close to the constrained limit. However, it is very impractical to maintain multiple codebooks/decoders at the transmitter and receiver. So we design the power/rate allocation algorithm with a single mother-code whose coded bits will

be transmitted from all the different subchannels. Since only one code is used, it is a Bit-Interleaved Coded Modulation (BICM) system [5]. Let this one code (which we call mother-code) have a code-rate R_{min}. Depending on the average code-rate supported over all subchannels, the mother code has to be punctured to obtain code-rates higher than R_{min}. Rate-adaptation across subchannels for given subchannel states is then obtained by transmitting different QAM constellations (2-QAM, 4-QAM, 16-QAM or 64-QAM) from different subchannels in spite of using a single code. In practice, it is very difficult to obtain good BER performance over the whole spectrum of code-rates with a single code through puncturing. Hence, the mother-code is assumed to perform well within the code-rate range R_{min} to R_{max}. There is also an overall power constraint on a single code-word transmitted. This proposed method can however be extended easily to a case where the power constraint is over multiple codewords. In summary, we derive the capacity of the system with parallel flat-fading channels and CSITR under the following constraints:

1. Transmission is from a constrained constellation such as BPSK, QPSK, 16-QAM or 64-QAM.

2. A single code is used for all the subchannels together. Rate allocation is obtained by transmitting different constellations from different subchannels.

3. Power constraint on a single codeword transmitted. Proposed method can be easily extended to more relaxed power constraints.

4. The average code-rate is constrained between R_{min} and R_{max}.

In the second part of this work, a multiple antenna system is considered with CSITR. Through linear transformation, a Multiple-Input Multiple-Output (MIMO) system can be resolved into a set of parallel subchannels. We then apply the princi-

ples discussed earlier for multicarrier transmission directly to obtain the constrained capacity and the capacity-achieving power/rate allocation. All of the constraints discussed above (1-4) hold for this case too. The LDPC mother-code is designed for an AWGN channel with a fixed code-rate, R_{min}. If the average code-rate supported on all the subchannels is higher than the rate of the mother-code, the mother code is punctured. Finally through simulations with this LDPC code, we show that the proposed allocation algorithm is very robust and performs within 1.5-2dB of the unconstrained capacity limit.

Since the subchannel states change from one codeword block to the next, it is a must for the power/rate allocation algorithm to be simple enough to enable fast implementation for each codeword block. The proposed power-allocation and rate-determination satisfies this condition and it can be implemented on-the-fly at the transmitter to keep track of the changes in the subchannel states. The power-allocation algorithm proposed is also near-optimal in terms of information rate and it provides a practical coding scheme to achieve the capacity of the constrained multi-channel system. Some of the conventional bit-loading schemes optimize power-allocation for multicarrier and ADSL systems [50] [51], however, they either do not consider coding or do not maximize the sum-information rate as proposed in this work. Also the computational complexity of the proposed method here is lower than bit-loading algorithms which are more numerically intensive and hence may not be very friendly to fast implementation.

Some other schemes in literature [52] [53] have considered the constrained signaling power/rate allocation problem. [52] does not consider coding and hence, it is far from capacity. [53] considered adaptive modulation with coding but this method suffers from the following shortcomings: this scheme is subject to the characteristics of a particular code that is going to be employed for this system. It is not a

very general design and the optimization procedure has to be applied every time a different code is employed. This scheme employs multiple codebooks to maximize throughput. It is not very obvious if such a system can be easily implemented for practical systems. This scheme also performs further away from capacity than our proposed scheme in spite of employing multiple codebooks. [54] considered capacity of BPSK OFDM systems, however, their work does not look into higher constellations and coding schemes to approach capacity when using higher constellations.

A. System Description

1. System Model

The system considered here is as follows (Figure 28): assume that there are M flat-

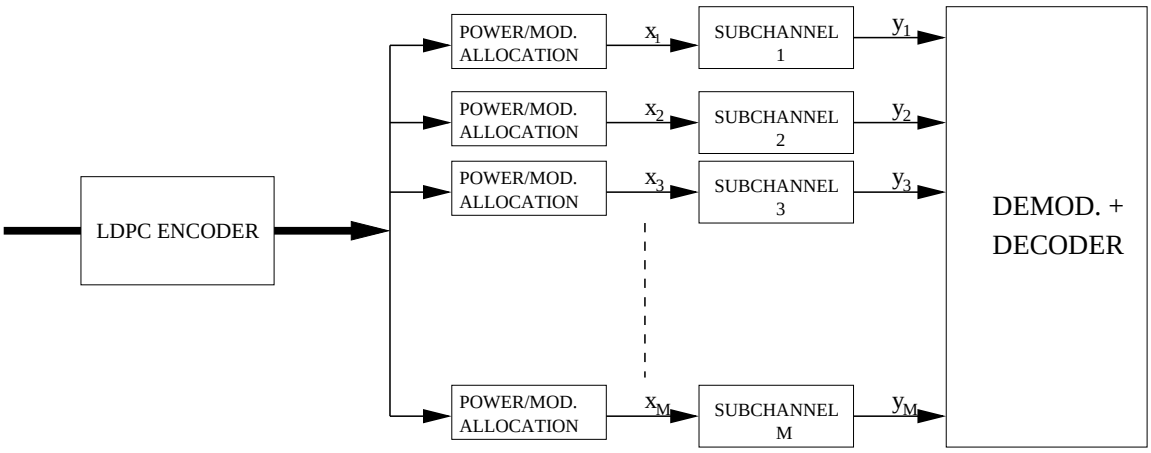

Fig. 28. Adaptive modulation system description

fading parallel subchannels over which data is to be transmitted. Channel state information (CSI) is known to the receiver and the transmitter perfectly. The output of a channel encoder is modulated into symbols of different constellations (BPSK (2-QAM), QPSK (4-QAM), 16-QAM or 64-QAM) at each of the subchannels depending

on the subchannel state. Due to practical constraints, a single LDPC mother-code with code-rate R_{min} is used and is punctured to obtain higher code-rates if the code-rate supported by the subchannels is higher than R_{min}. (This scheme can be very easily extended to a system with a dedicated codebook for each subchannel.) Different rates of transmission from different subchannels is obtained by changing the constellation in the different subchannels. The channel is assumed to be static over the length of a codeword and it changes from one codeword to the next. A single codeword of the LDPC code spans multiple symbols from each subchannel, and the fade remains constant on all subchannels for the whole duration of the codeword (quasi-static fading). With this channel model, the received samples can be expressed as:

$$y_m = \alpha_m x_m + n_m, \qquad m = 1, 2, \ldots, M \tag{6.1}$$

where y_m is the received value, α_m is the magnitude of the channel gain of the m-th subchannel and x_m can belong to one of the following constellations - BPSK, QPSK, 16-QAM or 64-QAM. Note that y_m has already been compensated for any phase rotation that might occur at the receiver (so that the fade value α_m is real) and n_m is the complex AWGN noise with variance of one dimension σ^2 ($\sigma^2 = N_o/2$). Modulation schemes other than the above ones for x_m can be easily incorporated into the system, however, for the sake of simplicity, we consider only these constellations here. There is a short-term power constraint on x_m i.e. each codeword (which will occupy all the subchannels and multiple time-slots) is constrained to have a given power, $\mathbf{P}$. This scheme can be easily extended to a power constraint on more than one codeword.

This power, $\mathbf{P}$, is allocated among the subchannels depending on the state of the subchannel. For the simplicity of analysis, the number of symbols transmitted from

each subcarrier (can be from any of the constellations mentioned above) is assumed to be the same corresponding to a codeword from the LDPC code. That is, one single codeword of the LDPC code will be multiplexed into M or lower streams, one for each of the subchannel transmitting signals, in such a way that the total number of symbols (refers to modulation symbols and not bits) from each subchannel is equal. Mapping codewords to subchannels is considered in more detail in Section V-A. The problem then is to maximize the sum-rate of these subchannels subject to the constraints 1)-4) in Section 1. It is assumed that depending on the state of the subchannel, different constellations can be used for different subchannels. The system model can be better understood from Figure 28.

B. Sum Information Rate for Gaussian Signaling

Define $\Gamma = (\gamma_1\gamma_2 \dots \gamma_M)$ where γ_i is the power allocated to the i-th subchannel and $\alpha = (\alpha_1\alpha_2 \dots \alpha_M)$. The sum information rate with Gaussian signaling for the above system, for a given α is given below [55]:

$$I_M(\Gamma|\alpha) = \sum_{m=1}^{M} \log(1 + \frac{\alpha_m^2 \gamma_m}{\sigma^2}) \tag{6.2}$$

where $I_M(\Gamma|\alpha)$ is the sum-rate, γ_m is the power allocated to the m-th subchannel, subject to the power constraint:

$$\frac{1}{M} \sum_{m=1}^{M} \gamma_m \leq \mathbf{P}. \tag{6.3}$$

Maximizing the information rate is then an optimization problem, which has the following solution [13]:

$$\gamma_m = \left(\mu - \frac{\sigma^2}{\alpha_m^2}\right)^+ \tag{6.4}$$

where $(.)^+$ is zero if $(.)$ is less than zero and μ is such that Eqn. (6.3) is satisfied.

C. Capacity of Constrained Constellations

The capacity of constrained modulation schemes over AWGN channel with noise variance σ^2 can be evaluated as follows. If $\mathbf{X}$ is the transmitted symbol and $\mathbf{Y}$ is the received symbol, then:

$$\begin{aligned} I(\mathbf{X};\mathbf{Y}) &= H(\mathbf{Y}) - H(\mathbf{Y}|\mathbf{X}) \\ &= H(\mathbf{Y}) - \log(2\pi e\sigma^2) \end{aligned} \tag{6.5}$$

where $H(\mathbf{Y})$ can be obtained from $p_{\mathbf{Y}}(y)$ which is given as [56]:

$$p_{\mathbf{Y}} = \sum_{k=1}^{N} p_{\mathbf{Y}|x_k} P(x_k) \tag{6.6}$$

where N is the number of points in the transmit constellation that x belongs to ($N = 16$ for 16-QAM). Eqn. (6.6) can be evaluated only through simulations and closed-form expressions cannot be obtained for the constrained capacity in Eqn. (6.5). Then it is not a straightforward problem to optimize the power distribution for constrained constellations. Hence, we need to look at approximations for the capacity of constrained modulation schemes which can be manipulated easily in the corresponding optimization to yield good power distributions. Also the resulting power-allocation expression has to be very simple so that it can be implemented on-the-fly at the transmitter to keep up with the changes in the fade values. (Time-consuming methods as numerical optimization techniques will not be very useful here).

The capacity obtained for schemes like BPSK, QPSK, and 16-QAM have shapes similar to exponential curves. Also, as will become obvious in the next part of this section, assuming an exponential function for the capacities can help in solv-

ing the optimization problem analytically. Exponential functions of the form $f(x) = a(1 - \exp(-bx))$ [57] have similar shapes as the constrained capacity curve, where a, b are constants that depend on the constellation and x is the SNR Curve-fitting with minimum mean-squared error as the criterion provides the best values for the parameters a and b for different constellations as tabulated in Table II. The actual capacities and their corresponding approximations for BPSK, QPSK, 16-QAM and 64-QAM are shown in Figure 29. As can be seen the two curves match very well for BPSK, QPSK and 16-QAM and fairly well for 64-QAM over the whole range of SNRs.

Table II. Optimum values for a and b

Const.	a	b
BPSK	1	1.325
QPSK	2	0.657
16QAM	4	0.202
64QAM	6	0.0714

D. Optimization of Power Profiles

In the previous section, we described how to obtain approximate expressions for the constrained capacity of BPSK, QPSK, 16-QAM and 64-QAM. These can be written as:

$$C(SNR) \approx a\left(1 - \exp^{-bSNR}\right) \tag{6.7}$$

where SNR is the signal to noise ratio (E_s/N_o) and E_s is the energy available at the transmitter to send a constellation symbol. Assume that transmitting symbols

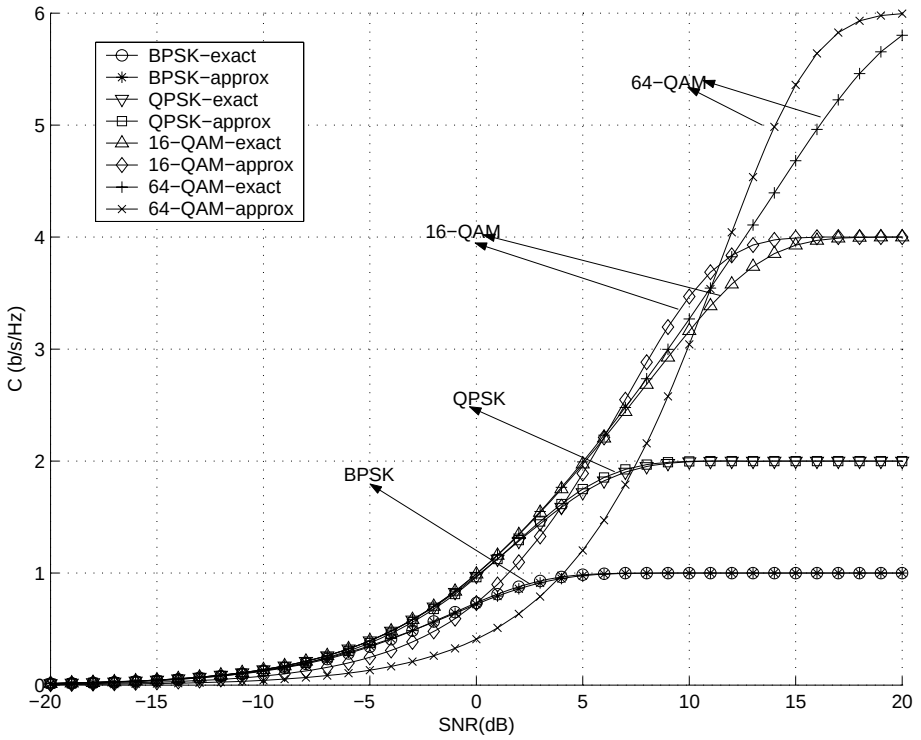

Fig. 29. Exact and appromixate capacities for BPSK, QPSK, 16-QAM and 64-QAM

from different constellations is possible from different subchannels. The goal is to maximize sum information rate subject to a power constraint, which again turns out to be an optimization problem. Also assume that the transmitter can send only the same number of symbols from each subcarrier for a given codeword. (Variable-rate schemes are still possible as different constellations can be transmitted from different subchannels.) The sum information rate, given by:

$$I_{CMM}(\Gamma|\alpha) = \sum_{m=1}^{M} a_m(1 - \exp^{-\frac{b_m \gamma_m \alpha_m^2}{N_o}}) \tag{6.8}$$

has to be maximized subject to the power constraint in Eqn. (6.3). (N_o is the PSD of AWGN noise and is equal to $2\sigma^2$ in the previous section). Note that different subchannels can transmit from different constellations. Solutions for this optimization problem through the Lagrange method [58] can be shown to take the form (derived in Appendix A):

$$\gamma_m = \frac{N_o}{b_m \alpha_m^2} \left(\log \mu - \log(\frac{N_o}{\alpha_m^2 a_m b_m}) \right)^+, \tag{6.9}$$

where μ is chosen such that Eqn. (6.3) is satisfied.

For a fixed constellation, at very low SNRs, this power-allocation is very similar to Gaussian waterfilling, however for higher SNRs it deviates from it. The main reason for this behavior is that for a fixed constellation, there is no advantage in adding more power into the best channel beyond the SNR where it saturates to its maximum rate a. The transmitter can gain in sum-rate transferring that extra power into a different subchannel which is starved for power. This is evident from the above expression where there is an extra $1/\alpha_m^2$ outside the expression $\left(\log \mu - \log(\frac{N_o}{\alpha_m^2 a_m b_m}) \right)^+$.

It is a very challenging problem to design a single code which will perform well (in terms of BER) over a large spectrum of code-rates (by puncturing or shortening).

This is the reason why there is a constraint on the average code-rate supported by the subchannels to be between R_{min} and R_{max}. Theoretically, for the parallel subchannel system, sum-rate can be maximized if every subchannel trasmits from the highest constellation available (denote it as C_h). This constellation will have the least penalty from unconstrained sum-rate and hence will have the highest sum-rate. However, for some set of the sub-channel values α (and esp. for lower SNRs), the average code-rate of all subchannels will be very small ($< R_{min}$) if all the subchannels transmit from C_h. Since this is not feasible, a better idea would be for all the sub-channels to transmit from the next lower-order constellation available, C_{h-1}. This will make the overall code-rate higher, however, some of the subchannels might not provide the maximum rate that they can support with C_h. This is because, with C_{h-1}, the maximum rate supported is lower and it is possible that some subchannels are almost saturated in this constellation. Hence, it is always better to transmit using a mixture of constellations from different subchannels based on what rate each subchannel can support.

As stated before, rate-adaptation across subchannels is obtained by transmitting different constellations from different subchannels. In order to decide which constellation can be supported on each sub-channel such that the overall code-rate constraint is satisfied ($R_{min} < R_{avg} < R_{max}$) and what is the best sum-rate achievable, an algorithm has been designed which is described below. This algorithm maximizes the sum-rate by changing the constellation of each subchannel subject to a constraint imposed on the code-rates of the individual subchannels (shown below). Define C_m as the dimension or constellation number of m-th subchannel. It can be 0 - BPSK, 1 - QPSK, 2 - 16-QAM or 3 - 64-QAM. Let R_{pr} stand for the sum-rate obtained in the previous iteration and R is the sum-rate obtained in the current iteration. One iteration of Loop1 determines the power-allocation for each subchannel subject to its

given constellation which is decided by the corresponding C_m. The breaking condition is when the current sum-rate R is less than R_{pr} which ensures that the sum-rate is maximized. Loop2 ensures that the code-rate constraint is satisfied *i.e.* m-th subchannel transmits over a constellation which can support a code-rate, R_m less than R_{max}. This condition will make sure that the rate supported on a given subchannel is not close to the saturation point for the corresponding constellation. In other words, if the code-rate supported is close to 1, then that subchannel can support a better code-rate if the next higher-order constellation is used instead.

- Initialization:

  $R_{pr} = 0, flag = 1, C_m = 0 \quad m = 1, 2, \ldots, M$

- Loop1: $while(flag == 1)$

$$
\begin{aligned}
& flag = 0; \\
& \gamma_m = \frac{N_o}{b_m \alpha_m^2} \left(\log \mu - \log(\frac{N_o}{\alpha_m^2 a_m b_m}) \right)^+ \\
& \text{s.t.} \frac{1}{M} \sum_{m=1}^{M} \gamma_m \leq \mathbf{P}, \\
& R_m = (1 - \exp^{-\frac{b_m \gamma_m \alpha_m^2}{N_o}}) \\
& R = \sum_{m=1}^{M} R_m a_m \\
& \text{if} \quad (R < R_{pr}) \\
& \qquad \text{break;}
\end{aligned}
$$

  - Loop2 over m:

$$
\begin{aligned}
& \text{if} \quad (R_m > R_{max}) \ \ \& \ \ (C_m < 3) \\
& \qquad flag = 1; C_m = C_m + 1;
\end{aligned}
$$

$$\text{if} \quad (0 < R_m < R_{min}) \;\; \& \;\; (C_m > 0)$$
$$flag = 1; C_m = C_m - 1;$$

  - end Loop2

- $R = R_{pr}$

- end Loop1

Note that a_m and b_m take on values according to C_m, the constellation allocated to the m-th subchannel. This algorithm is a suboptimal and greedy one (since it searches over roughly half the total number of constellations suited for each subchannel) which determines the constrained capacity of this system within some reasonable error caused by the exponential approximations. This also provides the near-optimum power and rate allocation scheme to approach the limit for constrained constellations which is considered in the next subsection. For very low SNRs ($E_s/N_o < 0$dB) depending also on the values of the subchannel states, the average code-rate (average of R_m) supported by the system might become lower than R_{min}, the rate of the mother-code. In that case, an outage can be declared and there will be no transmission. For some realizations of α and $\mathbf{P}$, the algorithm might provide an average code-rate less than R_{min} and declare an outage, even though with a different choice of constellations over the subchannels, it might be possible to obtain an average code-rate higher than R_{min}. This is a very rare event and was never observed in the simulations.

1. Proposed Coding Scheme

As stated before, a single code is used for practical reasons. Variable rate is achieved through different constellations from different subchannels. Hence the average rate

of the channel code is:

$$R_{avg} = \frac{\sum_{m=1}^{M} a_m R_m}{\sum_{m=1}^{M} a_m} \tag{6.10}$$

The mother-code can be punctured to give this rate. As stated before, equal number of symbols (can be from different constellations) are transmitted from each subchannel. Denote this length as L_s. Assume that L_b is the length of the punctured codeword in bits. With the above rate of the mother-code, L_s is given by:

$$L_s = \frac{L_b}{\sum_{m=1}^{M} a_m}, \tag{6.11}$$

If $l_{b,m}$ is the number of bits transmitted from the m-th subchannel, then:

$$l_{b,m} = L_s a_m \tag{6.12}$$

If however, multiple codebooks are allowed to be used at the transmitter, then the corresponding channel code-rate of each of the subchannels should be R_m. Instead of using M codes for M subchannels, lesser number of codebooks (say 2 or 3) can also be used for comparable performance. Each of the codebooks can take care of subchannels that are within a certain code-rate range and these subchannels can be grouped together and encoded with that codebook. This can have comparable performance as using M separate codebooks too.

From (6.9), it is obvious some of the subchannels may not get any power assigned to them. In summary, the proposed scheme uses a single code with a rate determined by the subchannel states. However, it is a variable-rate scheme as the constellation is different from subchannel to subchannel and also a variable-power scheme as the power is varied across subchannels and all this obtained in spite of using a single-code.

All the processing mentioned above to obtain the rate of the code, the length of the codeword in bits, the total number of symbols transmitted and the constellations

used from different subchannels are done at the transmitter. However, in practice, this processing has to be done concurrently at the transmitter as well as the receiver (which have knowledge of the fade magnitude values for the current block) to obtain knowledge of parameters such as L_s, L_b, R_{avg}, C_m and the puncturing ratio so that the receiver can decode the block.

E. Tighter Power and Rate Allocation

In the previous section, power and rate allocation methods based on the approximate constrained capacity expressions (Eq. (6.7)) were discussed. These expressions are very simple and very easy to implement in a practical system in which the channel is changing from one code-block to the next. They are also good approximations as can be seen from Figure 29 especially for lower-order constellations such as BPSK and QPSK. We have observed that tighter expressions for constrained capacity can be obtained by applying sum of exponentials for higher-order constellations such as 16-QAM and 64-QAM. As seen from Figure 30, sum of two and three exponentials for 16-QAM and 64-QAM respectively makes the constrained capacity approximation very tight.

$$C_{16-QAM}(SNR) \approx \sum_{i=1}^{2} a_i \left(1 - \exp^{-b_i SNR}\right)$$
$$C_{64-QAM}(SNR) \approx \sum_{i=1}^{3} a_i \left(1 - \exp^{-b_i SNR}\right) \tag{6.13}$$

Following the steps in the previous section, the resulting power allocation will satisfy the condition that weighted sum of exponentials is a constant.

$$\sum_{i=1}^{K} \frac{a_i b_i \alpha_i^2}{\sigma^2} \exp^{\frac{-b_i \gamma_m \alpha_i^2}{\sigma^2}} = \text{constant} \tag{6.14}$$

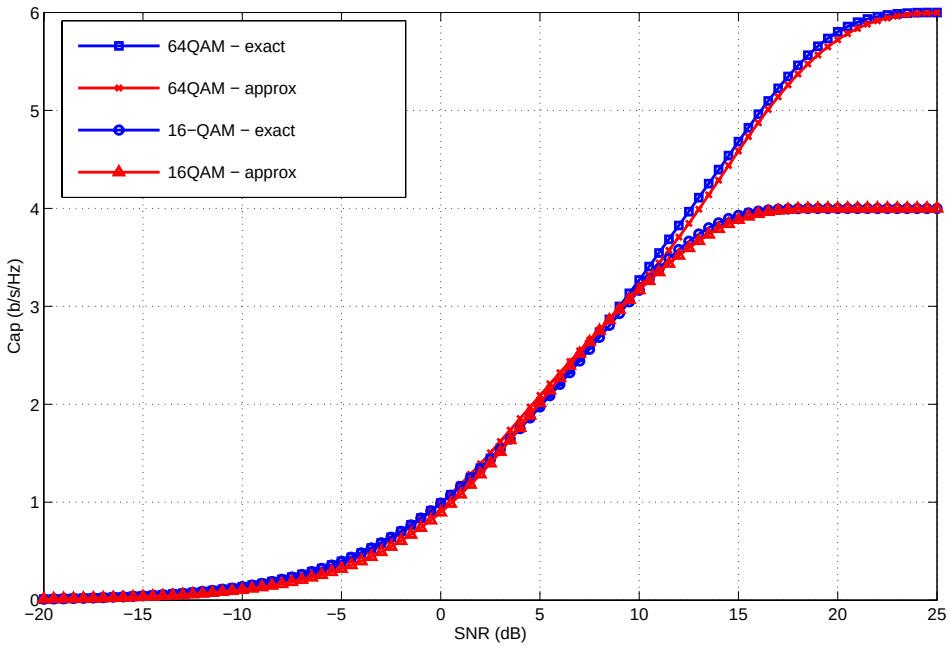

Fig. 30. Exact and tighter capacities for 16-QAM and 64-QAM

where K is equal to 2 for 16-QAM and 3 for 64-QAM and higher for higher-order constellations. There is no closed-form solution for this power allocation expression. Numerical methods are required to optimize the power allocation in order to maximize the sum-information rate. However, since the left-side of (6.14) is a sum of exponentials which is a monotonously decreasing function of γ_m, the solution can be easily obtained through Newton-Raphson method within a few iterations. In some practical systems, this method can be implemented for power allocation as it has minimal complexity.

However, the main objective of this section is to obtain a tight approximation to the sum-information rate and the sum-constrained capacity, as well as to determine the best performance of an LDPC coded system with this set of tighter power allocation values. The best performance possible with the LDPC code will provide an idea of how close the approximate power allocation method in the previous section is.

Concurrently, [59] has considered power allocation methods with arbitrary input constellations. In their work, they apply the result that the derivative of mutual information is mean-squared error (MSE) [60] and derive the curves for MSE through numerical integration for any input constellation. The resulting power allocation is through numerical optimization techniques with the aid of the MSE curves for different constellations, where the curves need to be stored. This may not be very practical as it requires a large amount of resources. In our scheme, through Lagrange multipliers, we obtain Eqns. (6.9) and (6.14). The LHS of these equations are derivatives of mutual information with respect to SNR, γ_l (assume that σ^2 is a constant) which is in fact the minimum MSE in estimating the transmitted value, x given the received value, y. Hence the exponential approximation (Eq. (6.7)) results in a closed-form approximation for the MMSE as well as the power allocation which is tight for BPSK and QPSK. With the aid of sum of exponentials, MMSE expression for 16-QAM

and 64-QAM can be tightened but the resulting power allocation is not a closed-form expression. However, due to presence of closed-form expression for MMSE, the optimization is still very simple as the MSE curve values do not have to be stored contrary to the scheme in [59]. Simplicity of the power allocation is very important for a scheme where the channel realizations change quickly from block to block and the power-allocation has to adapt itself.

F. Multiple Antennas

1. System Description

Consider a MIMO channel as shown in Figure 31. It is easier to represent the MIMO

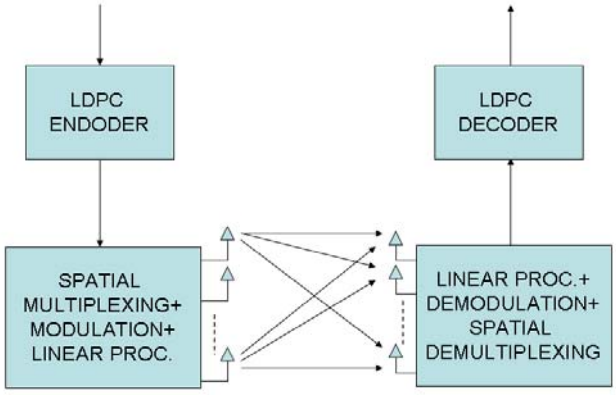

Fig. 31. MIMO system description

channel in terms of vectors and matrices rather than scalars. The relationship of this setup to the above method may not be clear at this point however, it will be clarified

in the coming subsections. Let complex valued matrices of size $r \times t$ be represented as $C_{r\times t}$. Assume a vector of size $t \times 1$, $\mathbf{x}$ is incident on a flat fading channel with an channel matrix $\mathbf{H} \in C_{r\times t}$ (r is the number of receiver antennas and t is the number of transmit antennas) and the output of the channel is $\mathbf{y}$. The channel is assumed to be flat-fading channel with AWGN $\mathbf{n}$. Both $\mathbf{y}$ and $\mathbf{n}$ belong to $C_{r\times 1}$. Then:

$$\mathbf{y} = \mathbf{H}\mathbf{x} + \mathbf{n} \tag{6.15}$$

The problem statement is as follows: which is the best power allocation scheme among the different elements of $\mathbf{x}$ that can achieve the capacity on this channel when $\mathbf{H}$ is known both at the transmitter as well as the receiver (CSITR). As shown in the next sub-section the power-allocation for the case when $\mathbf{x}$ is Gaussian distributed is straighforward to obtain [61]. However, the problem for constrained constellations is unsolved and is difficult to obtain. In the following sub-sections, we derive an expression for the constrained maximum sum-information-rate and the corresponding power-allocation with constraints on $\mathbf{x}$ being a linear transformation of QAM symbols. The advantage of this scheme is that a BICM system based on LDPC codes where the coded bits are mapped to QAM symbols and linearly transformed into the transmitted signals $\mathbf{x}$ can be used to perform close to capacity. This will become clear in the following sub-sections.

2. Gaussian Constellation

For the Gaussian constellation, this problem has already been solved by Telatar [61]. We will re-derive the capacity expression as this derivation will be required for the constrained constellation too. Assume a channel model given by (6.15). $\mathbf{x}$ has a power constraint given by $E[\mathbf{x}'\mathbf{x}] \leq \mathbf{P}$, where $()'$ stands for Hermitian. $\mathbf{n}$ is assumed to be AWGN with $E[\mathbf{n}\mathbf{n}'] = \sigma^2\mathbf{I}_{\mathbf{r}\times\mathbf{r}}$, where $\mathbf{I}_{\mathbf{r}\times\mathbf{r}}$ is the identity matrix of size rxr. The

power-allocation problem can be solved by performing a singular value decomposition (SVD) of $\mathbf{H}$. Eqn. (6.15) can be rewritten as:

$$\mathbf{y} = \mathbf{UDV'x} + \mathbf{n} \tag{6.16}$$

where $\mathbf{U} \in C_{r\times r}$ such that $\mathbf{U'U} = \mathbf{I_{r\times r}}$ and $\mathbf{V} \in C_{t\times t}$ and $\mathbf{V'V} = \mathbf{I_{t\times t}}$. Also $\mathbf{D}$ is a diagonal matrix of size $r \times t$ containing the singular values of $\mathbf{H}$, i.e. $\mathbf{D}_{r\times t} = diag(\lambda_1, \lambda_2, \ldots, \lambda_{min(r,t)})$. Eqn. (6.16) can be further simplified by left-multiplying it by $\mathbf{U'}$ which results in:

$$\tilde{\mathbf{y}} = \mathbf{D}\tilde{\mathbf{x}} + \tilde{\mathbf{n}}, \tag{6.17}$$

where $\tilde{\mathbf{x}} = \mathbf{V'x}$, $\tilde{\mathbf{n}} = \mathbf{U'n}$, and $E[\tilde{\mathbf{x}}'\tilde{\mathbf{x}}] \leq \mathbf{P}$ and $E[\tilde{\mathbf{n}}\tilde{\mathbf{n}}'] = \sigma^2\mathbf{I_{r\times r}}$. Since the transformations applied were linear and one-one, $I(\mathbf{x};\mathbf{y}) = I(\tilde{\mathbf{x}};\tilde{\mathbf{y}})$. Eqn. (6.17) represents a set of parallel Gaussian channels and mutual information is maximized when $\tilde{\mathbf{x}}$ is Gaussian distributed with power allocation given by water-filling distribution.

$$\tilde{y_i} = \lambda_i\tilde{x_i} + \tilde{n_i} \qquad\qquad i = 1, \ldots, min(r,t) \tag{6.18}$$

is the the set of parallel Gaussian channels. The overall capacity can be obtained by a power-allocation function,

$$P(i) = (\mu - \lambda_i^{-2})^+ \tag{6.19}$$

where μ is chosen such that $\sum_i^{\min(r,t)} P(i) = \mathbf{P}$ and,

$$I(\mathbf{x};\mathbf{y}) = \sum_i \log(\mu\lambda_i^{-2})^+ \tag{6.20}$$

3. Constrained Constellation

Similar approach as above can be applied to constrained constellations too. Eqn. (6.16) is a good starting-point for the constrained constellation.

$$\mathbf{y} = \mathbf{UDV}'\mathbf{x} + \mathbf{n} \tag{6.21}$$

Transmit a vector $\mathbf{x}$ given by:

$$\mathbf{x} = \mathbf{V}\tilde{\mathbf{x}} \tag{6.22}$$

where the elements of the vector, $\tilde{\mathbf{x}}$ are generated independently from one of the standard constellations as 64-QAM, 16-QAM, QPSK or BPSK (i.e. the coded bits of the channel code can be mapped to one of the four modulation symbols which form the elements of $\tilde{\mathbf{x}}$). As shown before, the power constraint on $\tilde{\mathbf{x}}$ directly translates from the same power constraint on $\mathbf{x}$ *i.e.* $E[\mathbf{x}'\mathbf{x}] \leq \mathbf{P} \Rightarrow E[\tilde{\mathbf{x}}'\tilde{\mathbf{x}}] \leq \mathbf{P}$. This is because $\mathbf{V}$ is a Hermitian matrix.

Left-multiplying equation (6.21) with $\mathbf{U}'$ leads to:

$$\tilde{\mathbf{y}} = \mathbf{D}\tilde{\mathbf{x}} + \tilde{\mathbf{n}} \tag{6.23}$$

This problem has the same characteristics as the single-antenna case discussed in the previous sections as $\mathbf{D}$ is a diagonal matrix *i.e.* there are $min(r, t)$ parallel subchannels given by Eqn. (6.23). Hence, we have simplified the multiple antenna case to the single-antenna case with multiple sub-channels. Coding approaches similar to the ones discussed for the single-antenna case, based on a single mother-code under the same set of constraints, can be applied here. This approach can be further extended to a MIMO-OFDM system with multiple sub-channels very easily. Note that $\mathbf{x}$ does not conform to any standard constellations and the problem where $\mathbf{x}$ conforms to

a standard constellation is a difficult one to solve. The advantage of the proposed system is that a BICM system based on an LDPC code where the coded bits are mapped directly to QAM symbols $\tilde{\mathbf{x}}$ can be used.

G. Results for Single Antenna System

In this section, we present simulation results for the single-antenna system with an LDPC code assuming the transmission of different constellations from different subchannels. The number of subchannels is fixed as $M = 8$ for simulation purposes. Two code-word lengths of the LDPC codes were chosen for simulations - 12288 and 393216. We choose the LDPC mother code to be of rate $R_{min} = 1/3$ and optimized for the AWGN channel. R_{max} is chosen as 0.8 in the optimization algorithm in Section D. The mother code will be punctured to obtain higher rates as and when required from block to block to equal the average of the code-rates supported on the subchannels. At the detector, we use a MAP-demodulator followed by a sum-product decoder. The mapping is chosen to be Gray for all the modulations (since the mapping is Gray, iterations between demodulator and decoder do not help very much, hence iterative demodulation is not used).

The performance of the proposed power and rate allocation method is determined by the average gap of the LDPC code simulation (averaged over channel realizations) from the sum-rate capacity of the Gaussian constellations as well as the constrained constellation as shown in Figure 32. For each channel realization, the LDPC code is simulated until the Bit Error Rate (BER) is less than 10^{-4} and the gap is determined. The channel is assumed to be independent from one frame to the next and hence averaging over channel realizations will give an estimate of the throughput (independence assumed only for simulation purposes).

We have also obtained the sum-rate of the constrained system and a comparison of this rate to the unconstrained system is shown in Figure 32. As it can be seen, simulation of the coded system for the longer codeword length of 393,216 performs within 1.5 dB of the unconstrained sum-rate limit. For the shorter length, the performance is within 2 dB of the unconstrained limit. This is good performance in spite of the fact a single-code once designed for the whole system has been punctured to obtain rate-compatibility. The reason for the slight difference of 0.5dB between unconstrained and constrained sum-rate capacities is because of the inaccuracies of the exponential approximation and also because of the inherent difference between constrained and unconstrained capacities. It can be concluded from the figure that the proposed scheme is a very robust power/rate-allocation scheme which performs very close to the theoretical limits and can be also easily implemented in real-time (keeping track of the changes in the fade magnitudes from block to block) as the power-allocation procedure is a very simple operation.

Figure 33 presents the comparison of tighter power allocation method with the approximate power allocation method. As can be seen from the figure, the gain of tighter power allocation is less than 0.5dB and most of the gain is in the higher SNR regime. This is due to the fact that in this region, 16-QAM and 64-QAM is chosen more often than BPSK and QPSK and since the approximation for the constrained capacity for 16-QAM and 64-QAM with a single exponential is loose, the approximate power allocation is farther than the tighter power allocation. However, as pointed out earlier, the tighter approximation is more complex to implement.

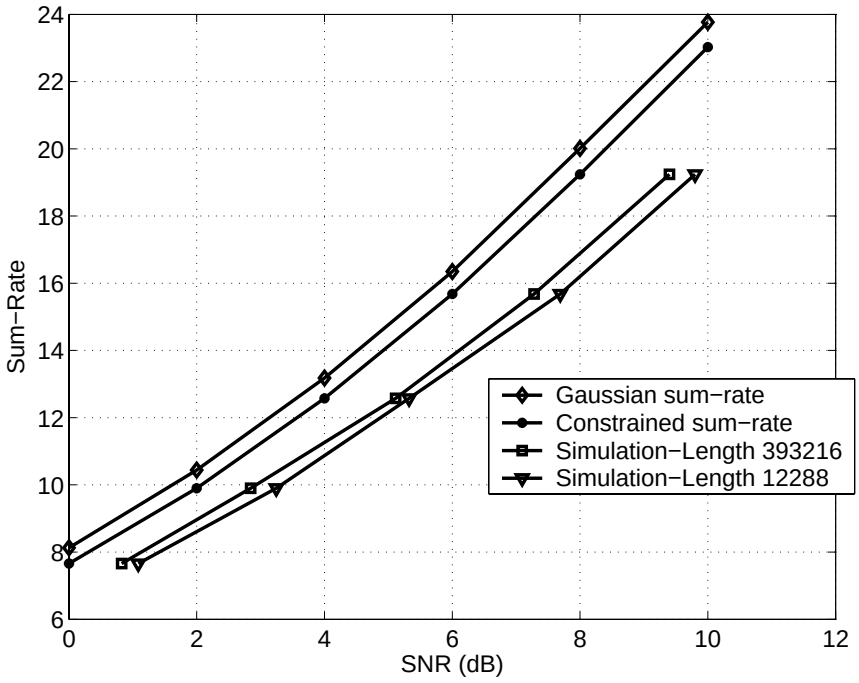

Fig. 32. Comparison of constrained and unconstrained information rate (bits per channel use) and simulation results for the single antenna system with $M = 8$

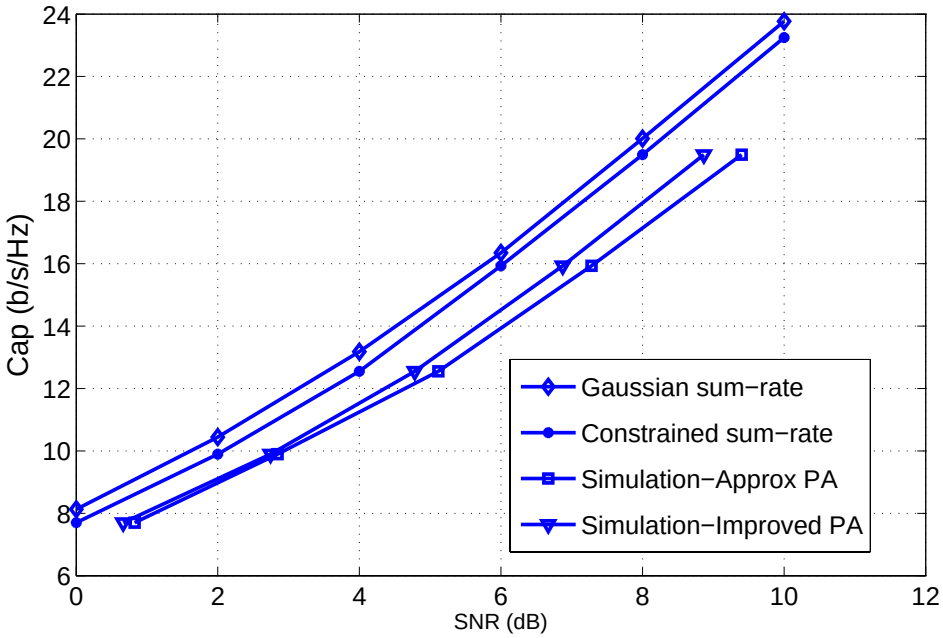

Fig. 33. Comparison of the tight power allocation and approximate power allocation through simulation for the single antenna system with $M = 8$ and code-length 393216

H. Results for MIMO System

The same LDPC mother-code used for the single antenna case was used here for two different lengths of 393216 and 12288. The MIMO system assumed was a 4x4 system (4 transmit and 4 receive antennas) which implies that M equals 4. A graph similar to Figure 32 was obtained. Figure 34 shows the results for the MIMO case. As can be seen, similar to the single antenna case, the simulation of the proposed scheme with LDPC code performs within 1.5dB for the longer codeword length and within 2dB for the shorter length of the unconstrained sum-rate and hence is robust for multiple antennas too.

As in the single antenna case, Figure 35 presents the comparison of tighter power allocation method with the approximate power allocation method. As can be seen from the figure, the gain of tighter power allocation is less than 0.5dB and most of the gain is again in the higher SNR regime.

When the channel state is known to the transmitter as well as the receiver, Gaussian waterfilling (which is optimal for Gaussian codebooks) is not optimal for the constrained constellations. Hence we have derived a near-optimal power/rate-allocation method for the constrained case for a single antenna case. The resulting power-allocation expression is very simple and it can implemented on-the-fly at the transmitter to keep up with the changes in the fade values from block to block. We further extend these principles to a practical MIMO system. We have also demonstrated the practical capability of the proposed resource allocation method by simulating with a single LDPC mother-code optimized for the AWGN channel and punctured to obtain higher rates. Through these simulations, we show that the coding scheme performs close to the theoretical limit.

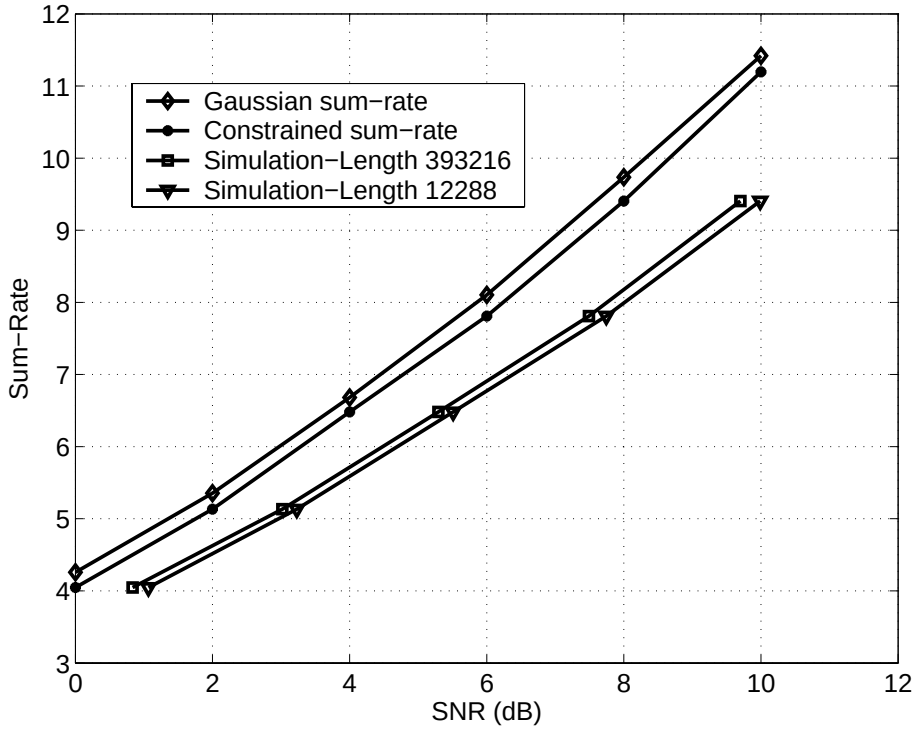

Fig. 34. Comparison of constrained and unconstrained information rate (bits per channel use) and simulation results for the 4 x 4 MIMO system

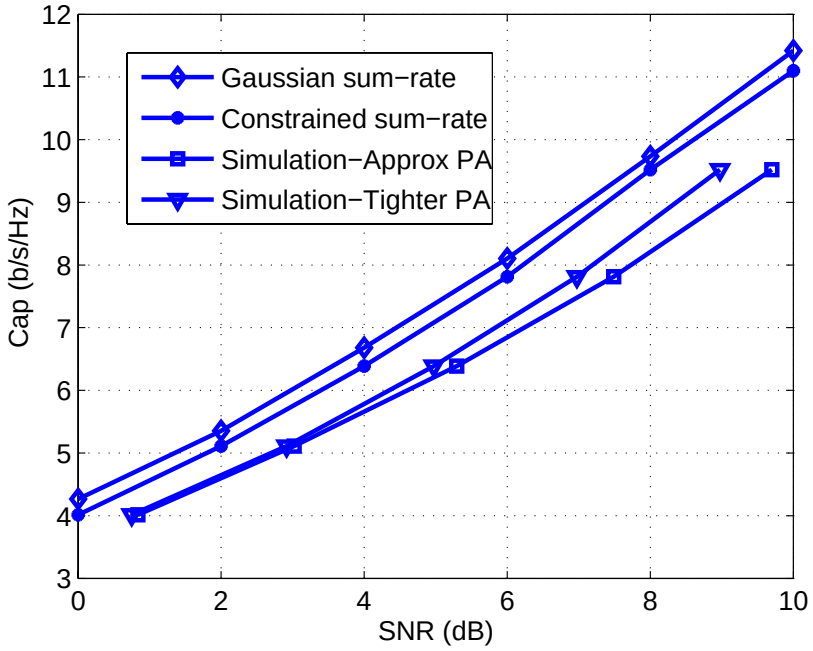

Fig. 35. Comparison of the tight and approximate power allocation simulation results for the 4x4 MIMO system and code-length 393216

CHAPTER VII

MEMORY-SAVING LDPC CODES*

Carefully designed irregular low-density parity-check (LDPC) codes [23], [16], [24] perform very close to capacity on additive white gaussian noise (AWGN) channels and can achieve capacity on the binary erasure channel (BEC) [25]. However, one disadvantage of LDPC codes is that the message passing decoder requires a lot of memory (number of fixed point numbers that need to be stored). The memory requirement at the decoder increases linearly with the number of edges in the graph of LDPC codes, which could turn out to be a bottleneck in many cases. In this work [14], we propose a variation of the message-passing decoding algorithm, which is memory-efficient and analyze this algorithm. Recently, similar decoding scheme has appeared in [62]. The proposed algorithm performs almost as well as the conventional LDPC code with sum-product decoding, in terms of bit-error rate. The main idea is to split the LDPC code in two sub-codes and decode them in a turbo fashion instead of applying the message passing algorithm to the entire graph. In splitting, we consider a semi-random approach which is explained in detail later. We then analyze the performance of LDPC codes with the proposed decoding algorithm and show how to design good LDPC codes for the proposed scheme. We then show that LDPC codes designed for conventional sum-product decoding are asymptotically optimal for this scheme also and they perform very close to each other.

A. Proposed Decoding Algorithm

The object of the proposed decoding algorithm is to reduce memory requirements. This has been accomplished by splitting the graph in a semi-random fashion into two subgraphs and then applying sum-product decoding algorithm on each of the subgraphs.

1. Proposed Splitting

1. Divide the check nodes into 2 halves (call them Half-1 and Half-2) such that the two halves contain approximately the same number of check nodes of each degree.

2. In connecting variable nodes to check nodes two possibilities arise:

   - If the degree of a variable node is even, distribute the edges of this node equally between Half-1 and Half-2
   - If, on the other hand, the degree is odd, divide the edges among them in such a way that one of the halves gets one edge more than the other. For successive odd-degree variable nodes, the extra edge can be connected to different halves, so as to ensure that each half has approximately the same number of edges. This construction can be better understood from Figure 36.

3. In each of the halves, the edges between the bit nodes and check nodes are placed at random, subject to the degree profile limitations.

4. Denote the degree of the variable node i in Half-1 as $\nu_i^{(1)}$ and that in Half-2 as $\nu_i^{(2)}$.

5. For better performance, it must be ensured that the degree-2 variable nodes of the overall graph (Half-1+Half-2) do not form any loop of small lengths as far as possible.

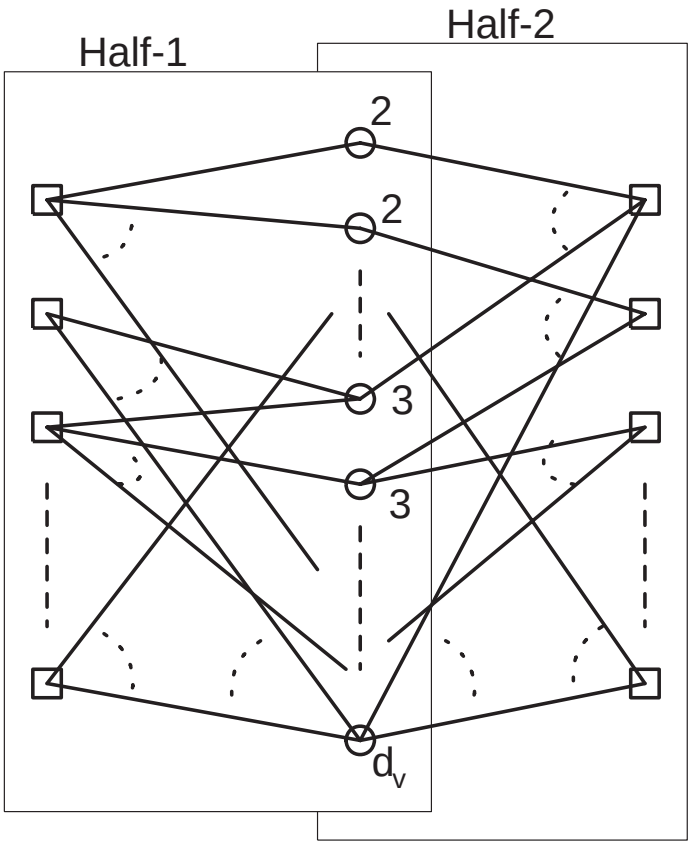

Fig. 36. LDPC code under the new semi-random construction: circles represent variable nodes and squares check-nodes. The numbers on the variable-nodes denote their overall degrees

The recently proposed concatenated Gallager codes [63] can be seen to be a special case of this scheme.

2. Decoding

Assume transmission of bits with binary phase shift keying (BPSK) modulation over an additive white Gaussian noise (AWGN) channel. If $\underline{X} = (x_0, x_1, \ldots, x_{n-1})$ is the transmitted codeword (after modulation) and $\underline{Y} = (y_0, y_1, \ldots, y_{n-1})$ is the received word, then clearly,

$$y_k = x_k + n_k \tag{7.1}$$

where n_k is the noise sample which is a zero-mean, Gaussian random variable with variance σ^2. The decoding is done in the following fashion: sum-product decoding is run on one of the halves for a fixed number of iterations (call these *sub-iterations*). Denote this fixed number of sub-iterations as Q_1. The extrinsics on each of the variable nodes are obtained. Sum-product decoding is run on the other half with these extrinsics as *a priori* information. These steps are repeated a fixed number of times (call these *super-iterations* and let there be Q_2 super-iterations) and the result on the nodes is declared. This scheme is similar to turbo decoding. Note that when a new set of sub-iterations is started on a half, the edge-LLRs(log-likelihood ratios) are initialized to zero. So, over each sub-iteration of the decoding, there are just half the number of active edges as there are in conventional sum-product decoding and, hence, the memory requirement is reduced in half.

The algorithm is explained below in more detail. Let $L_{c\to v,l}^{(m,q,h)}(x_{i,v})$ denote the LLR passed from check to variable along the lth edge incident on the ith variable node during the mth super-iteration, qth sub-iteration and in Half-h($h = 1$ or 2). Similarly, let $L_{v\to c,j}^{(m,q,h)}(x_{i,v})$ denote the LLR passed from variable to check node along the jth edge on the ith variable node during the m-th super-iteration, (q)th sub-iteration and in Half-h ($h = 1$ or 2). Let us denote the extrinsics passed from Half-h

to the other half, Half-$(3-h)$ $(h = 1, 2)$ at the mth super-iteration as $L^{m,h}(x_i)$ $(L^{0,h}(x_i) = 0\ \forall i)$. Also assume without loss of generality that the decoding starts on Half-1. The iterative procedure is given by:

- Initialization: Set $L^{1,2}(x_i) = L_{ch}(x_i) = -2y_i/\sigma^2$
- For $m = 1$ to Q_2
  - For $h = 1$ to 2
  - Set edge LLRs to zero: $L_{c\to v,l}^{(m,0,h)}(x_{i,v}) = 0$ for $h = 1, 2$
    - For $q = 1$ *to* Q_1
    - Bit node update:

$$L_{v\to c,j}^{(m,q,h)}(x_{i,v}) = L^{m+h-2,(3-h)}(x_i) + \sum_{l=0,l\neq j}^{\nu_i^{(h)}-1} L_{c\to v,l}^{(m,q-1,h)}(x_{i,v}) \tag{7.2}$$

    - Check node update:

$$\tanh\left(\frac{|L_{c\to v,l}^{(m,q,h)}(x_{k,c})|}{2}\right) = \prod_{j=0,j\neq l}^{\eta_k-1} \tanh\left(\frac{|L_{v\to c,j}^{(m,q,h)}(x_{k,c})|}{2}\right) \tag{7.3}$$

    - end q
  - The extrinsics passed on to the other half $(3-h)$ is given by

$$L^{m,h}(x_i) = L_{ch}(x_i) + \sum_{l=0}^{\nu_i^{(h)}-1} L_{c\to v,l}^{(m,Q_1,h)}(x_{i,v}) \tag{7.4}$$

  - end h
- end m
- Final LLRs:

$$L(x_i) = L^{Q_2,1}(x_i) + \sum_{l=0}^{\nu_i^{(2)}-1} L_{c\to v,l}^{(Q_2,Q_1,2)}(x_{i,v}) \tag{7.5}$$

which are used to make a hard decision on transmitted bit, x_i.

3. Quantifying Memory Savings

Let N_1 represent the total number of edges in the overall graph (Half-1+Half-2) and let the length of the code be $N (N = N_1 \sum_{i=1}^{d_v} \lambda_i / i)$. Then:

a. Memory Required for Sum-product Decoding

From Section II, it can be observed that in an iteration, $L^{(q)}_{c \to v,l}(x_i)$ must be stored. Since each edge has an LLR associated with it, this amounts to N_1 fixed-point values. Apart from these, the channel extrinsics have to be stored, which account for N fixed-point values. So, the memory required from iteration to iteration is:

$$\begin{aligned} M_1 &= N_1 + N_1 \sum_{i=1}^{d_v} \frac{\lambda_i}{i} \\ &= N + \frac{N}{\sum_{i=1}^{d_v} \frac{\lambda_i}{i}} \text{ fixed-point numbers.} \end{aligned} \tag{7.6}$$

b. Memory Required for the Proposed Scheme

Using the same argument as for conventional sum-product decoding, we need $N_1/2$ fixed-point values for storing the edge-LLRs (instead of N_1 fixed-point numbers as in the conventional scheme; this is where the memory-saving comes in). We need another $2N$ fixed-point numbers for storing the N extrinsics $L^{m,h \to (3-h)}$ which need to be passed between halves and N channel LLRs. Therefore, memory required is:

$$\begin{aligned} M_2 &= N_1/2 + 2N_1 \sum_{i=1}^{d_v} \frac{\lambda_i}{i} \\ &= \frac{N}{2 \sum_{i=1}^{d_v} \frac{\lambda_i}{i}} + 2N \text{ fixed-point numbers.} \end{aligned} \tag{7.7}$$

Therefore, the memory saving is

$$\mu = 1 - \frac{M_2}{M_1} = 1 - \frac{1 + 4\sum_{i=1}^{d_v} \frac{\lambda_i}{i}}{2 + 2\sum_{i=1}^{d_v} \frac{\lambda_i}{i}}. \tag{7.8}$$

It is worthy to note at this point that the proposed construction can result in more savings because the size of the address mapping of the LDPC code (connects variable nodes to check nodes) required at a time is reduced by half. Though it is not quantified here, this could turn out to be considerable in some cases. Hence, effectively μ can be greater than $1 - M_2/M_1$. It is also possible that $\mu < 0$ (when $\sum_{i=1}^{d_v} \lambda_i/i > 0.5 \Rightarrow \lambda_1 > 0$).

B. Analysis and Optimization

In this section, we analyze the proposed sum-product decoding on an AWGN channel based on the Gaussian approximation [26] for the semi-random construction described earlier. Since it is not clear whether the proposed decoding algorithm performs close to actual sum-product decoding or not, this analysis is important in understanding the new scheme better.

1. Modified Degree Profiles

Let $\lambda(x)$ represent the variable node profile from the edge perspective of the overall LDPC code (Half-1+Half-2). It has a corresponding node perspective representation which we represent as $\tilde{\lambda}(x)$. It is straight-forward to determine the node- and edge-perspective variable node profiles of each of the halves for the semi-random construction. Since both halves are symmetric, it is also safe to assume that they have the same profiles - represent this profile in the node-perspective as $\tilde{\lambda}'(x)$.

It can be easily observed that for:

(i) d_v even:

$$\tilde{\lambda'}_i = \frac{\tilde{\lambda}_{2i-1}}{2} + \tilde{\lambda}_{2i} + \frac{\tilde{\lambda}_{2i+1}}{2} \qquad i = 1, 2, \ldots, d_v/2 - 1$$
$$\tilde{\lambda'}_i = \frac{\tilde{\lambda}_{2i-1}}{2} + \tilde{\lambda}_{2i} \qquad i = d_v/2 \tag{7.9}$$

(ii) d_v odd:

$$\tilde{\lambda'}_i = \frac{\tilde{\lambda}_{2i-1}}{2} + \tilde{\lambda}_{2i} + \frac{\tilde{\lambda}_{2i+1}}{2} \qquad i = 1, 2, \ldots, \frac{d_v - 1}{2}$$
$$\tilde{\lambda'}_i = \frac{\tilde{\lambda}_{2i-1}}{2} \qquad i = \frac{d_v + 1}{2} \quad . \tag{7.10}$$

These equations stem from the fact that a degree-i variable node in one of the halves can arise out of only 3 cases - a variable node degree of $2i-1, 2i$ or $2i+1$ in the overall LDPC code. If the overall degree is $2i-1$, half of these nodes will contribute to degree-i in a half. If it is $2i$, all those nodes will contribute to degree-i. If it is $2i+1$, again half of these nodes will contribute to degree-i.

Represent the corresponding λ-profile in the edge-perspective of each of the halves obtained from $\tilde{\lambda'}(x)$ as $\lambda^{'}(x)$. Let $d_v^{'}$ be the maximum degree of $\tilde{\lambda'}(x)$ and hence of $\lambda^{'}(x)$.

For the sake of simplicity of notation, assume that d_v is even from here on. The optimization discussed here can be very easily extended to odd d_vs too. Define a $K_1 \times K_2 (K_1 = \frac{d_v}{2}, K_2 = 3)$ matrix $\lambda^{(\mathbf{c})}$ as:

$$\lambda^{(\mathbf{c})} = \begin{bmatrix} \lambda_{\mathbf{1}}^{(\mathbf{c})} & \lambda_{\mathbf{2}}^{(\mathbf{c})} & \ldots & \lambda_{\frac{\mathbf{d_v}}{\mathbf{2}}}^{(\mathbf{c})} \end{bmatrix} \tag{7.11}$$

where:

$$\lambda_{\mathbf{i}}^{(\mathbf{c})} = \begin{bmatrix} \frac{\tilde{\lambda}_{2i-1}}{2} & \tilde{\lambda}_{2i} & \frac{\tilde{\lambda}_{2i+1}}{2} \\ \tilde{\lambda'}_i & \tilde{\lambda'}_i & \tilde{\lambda'}_i \end{bmatrix} \qquad i = 1, 2, \ldots, d_v/2 - 1$$
$$\lambda_{\mathbf{i}}^{(\mathbf{c})} = \begin{bmatrix} \frac{\tilde{\lambda}_{2i-1}}{2} & \tilde{\lambda}_{2i} & 0 \\ \tilde{\lambda'}_i & \tilde{\lambda'}_i & \end{bmatrix} \qquad i = d_v/2 \quad . \tag{7.12}$$

Let $\lambda_{i,k}^{(c)}$ represent the kth (1,2,... , K_2) element of the vector $\lambda_i^{(c)}$. Note that in each half, a variable node of degree i can be connected only to a variable node of degree $i-1$, i or $i+1$ in the other half. The kth component of the vector, $\lambda_i^{(c)}$, namely, $\lambda_{i,k}^{(c)}$ represents the fraction of nodes of degree i in any one half h that are connected to nodes of degree $i+1$, i and $i-1$ respectively in the other half.

2. Evolution of Pdfs

As in [26], we assume that the output of every bit node and check node is a random variable with a Gaussian distribution. Due to the irregularity, the overall pdf of the messages passed from bit node to check node, vice versa and between the two halves is a mixture of Gaussian densities. We assume that the right degree is concentrated (all the check nodes are either of the same degree or are of degree i and $i+1$). Due to this, it is reasonable to assume that the messages passed from the check node to the bit node have a Gaussian pdf rather than a mixture of Gaussian pdfs. A discussion of the notation used in this subsection is in order here:

- $f_0 = \mathcal{N}(m_0, 2m_0)$ - pdf of the LLRs from the channel, where $m_0 = 2/\sigma^2$
- $m_{c,j}^{(m,q,h)}$ - mean of the message passed from a check node of degree j to a variable node during the mth super-iteration and the qth sub-iteration in the Half-h.
- $f_c^{(m,q,h)} = \mathcal{N}(m_c^{(m,q,h)}, 2m_c^{(m,q,h)})$ pdf of the message passed from a check node to a variable node during the mth super-iteration and the qth sub-iteration in the Half-h. Note that the mean of the messages is $m_c^{(m,q,h)} = \sum_j \rho_j \; m_{c,j}^{(m,q,h)}$.
- $f_{v,i,k}^{(m,q,h)}$ - kth component of a Gaussian mixture pdf passed from a variable node of degree i to a check node during the mth super-iteration and qth sub-iteration in Half-h.

- $\tilde{f}_i^{(m,h)}$ - pdf of the messages passed from half h to the other half $(3-h)$ during the mth super-iteration at a variable node of degree i in a half

- $m(\ )$ - represents the means of the messages

Consider the qth sub-iteration during the mth super-iteration in Half-h. The pdf of the message arriving at a node of degree i (including the contribution of the channel and the extrinsic information from the other Half-$(3-h)$) is given by

$$f_i^{\prime(m,h)} = \sum_{k=1}^{3} \lambda_{i,k}^{(c)} \ \tilde{f}_{i+k-2}^{(m,3-h)} \tag{7.13}$$

for the proposed scheme. The above expression results since a bit node of degree i in one half is connected to a bit node of degree $i-1$, i or $i+1$ with probability $\lambda_{i,1}^{(c)}$, $\lambda_{i,k}^{(c)}$ and $\lambda_{i,k}^{(c)}$, respectively.

The pdf of the messages at the output of a variable node of degree i that is passed to the check nodes is $f_{v,i}^{(m,q,h)}$ can be computed as follows:

$$\begin{aligned} f_{v,i}^{(m,q,h)} &= f_i^{\prime(m,h)} \mathcal{N}[m_0 + (i-1)m_c^{(m,q-1,h)}, 2(m_0 + (i-1)m_c^{(m,q-1,h)})] \\ &= \sum_{k=1}^{3} \lambda_{i,k}^{(c)} \ \mathcal{N}\left(m_{v,i,k}^{(m,q,h)}, 2m_{v,i,k}^{(m,q,h)}\right), \end{aligned} \tag{7.14}$$

where

$$m_{v,i,k}^{(m,q,h)} = (i+k-2)m_c^{(m-1,Q_1,3-h)} + m_0 + (i-1)m_c^{(m,q-1,h)}. \tag{7.15}$$

where $m_c^{(m-1,Q_1,3-h)}$ is the mean of the messages from the check nodes to bit nodes during the $(m-1)$th super-iteration, Q_1th sub-iteration and in half $(3-h)$, and represents convolution. The distribution at the input of a check node is then mixture

of Gaussians given by:

$$f_v^{(m,q,h)} = \sum_{i=1}^{\frac{d_v}{2}} \lambda_i^{'} \sum_{k=1}^{3} \lambda_{i,k}^{(c)} \mathcal{N}\left(m_{v,i,k}^{(m,q,h)}, 2m_{v,i,k}^{(m,q,h)}\right). \tag{7.16}$$

The output mean on an edge connected to a check node of degree j is:

$$m_{c,j}^{(m,q,h)} = \phi^{-1}\left(1 - \left[1 - \sum_{i=1}^{\frac{d_v}{2}} \lambda_i^{'} \sum_{k=1}^{3} \lambda_{i,k}^{(c)} \phi(m_{v,i,k}^{(m,q,h)})\right]^{j-1}\right), \tag{7.17}$$

where $\phi(x) = E[\tanh(u/2)]$, u being a Gaussian random variable with mean x and variance $2x$.

Then, the mean of the message passed from the check nodes to bit nodes is given by:

$$m_c^{(m,q+1,h)} = \sum_{j=1}^{d_r} \rho_j \, m_{c,j}^{(m,q,h)}. \tag{7.18}$$

The distribution of the messages passed from the check nodes to the bit nodes is

$$f_c^{(m,q+1,h)} = \mathcal{N}(m_c^{(m,q+1,h)}, 2m_c^{(m,q+1,h)}). \tag{7.19}$$

The distribution of the message passed from half h to the other half $3-h$ at the end of the Q_1th sub-iteration at a node of degree i in half h is given by:

$$\tilde{f}_i^{(m,h)} = \mathcal{N}\left(im_c^{(m,Q_1,3-h)}, 2im_c^{(m,Q_1,3-h)}\right), \quad i = 1, 2, \ldots, d_v/2. \tag{7.20}$$

The threshold of an LDPC code is the SNR (Signal-noise ratio) above which the mean $m_c^{(m,q+1,h)} \to \infty$ as the super-iterations progress. This can be easily determined for a given $\lambda(x)$ using the above equations. Nonlinear optimization techniques such as *fmincon* in MATLAB can be used for finding the best λ-profiles for a given rate once the threshold can be calculated.

C. Results

Two sets of comparisons are presented here:

1. the optimum left degree profiles for a rate-1/2 LDPC code with a constant right degree $j = 9$ was designed as explained in the previous section for the semi-random case for $Q_1 = 3$, $Q_1 = 5$ and $Q_1 = 7$. The best profiles that could be obtained for all these cases turned out to be the same and is:

$$\lambda(x) = 0.21596x + 0.17317x^2 + 0.02281x^4 + 0.19311x^5 + 0.39495x^{19} \quad (7.21)$$

$$\rho(x) = x^8. \quad (7.22)$$

The threshold for this profile with the semi-random scheme is 0.4dB for the case mentioned above and is the same for the scheme with conventional sum-product decoding. Also, the threshold for this profile with conventional sum-product decoding is the same as that of the best LDPC code with maximum left degree 20 and right nodes concentrated in one degree that was designed in [26]. This suggests that the decoding scheme proposed here is just a minor variation of actual sum-product decoding and performs very close to it.

For the conventional scheme, a code of length $N = 10667$ (number of edges is approximately 48000) was constructed at random corresponding to the profile given above. For the proposed semi-random scheme, a bipartite graph was constructed as explained in Section IV. The 5334 check nodes were split into two (each half getting $5334/2 = 2667$ nodes) and then Half-1 and Half-2 were constructed. A total of 75 iterations were used for both types of decoding (for the proposed construction $Q_1 = 5$ and $Q_2 = 75/5 = 15$ was used). The BER plot of the new semi-random and the conventional schemes have been compared

in Figure 37. The same figure shows comparison of the schemes at lower number of total iterations of 25 ($Q_1 = 5$, $Q_2 = 5$) and 50 ($Q_1 = 5$, $Q_2 = 10$) also. It can be observed that the proposed scheme performs as well as conventional sum-product decoding and reaches a BER of around 10^{-6} with 75 iterations though the convergence is slower for the proposed scheme. The focus of this work is on memory-saving and is aimed at applications which have reasonable computational capability and can tolerate slower convergence. It is evident from the simulation that the proposed algorithm is robust in terms of BER while resulting in memory-savings. However, depending on the implementation of the decoder and other factors like length of the code, amount of hardware available, number of iterations and target BER, the amount of savings in memory or whether there is any savings at all can change.

Same set of comparisons for the same code have been shown in Figure 38 for a shorter block length of $N = 2000$. This figure shows that the proposed scheme is robust for shorter blocklengths too.

2. In order to show that the proposed decoding technique can be used with regular LDPC codes also, we have shown simulation results for a $(3, 6)$ regular LDPC code of rate-1/2 and length $N = 16000$ in Fig. 39 with the proposed semi-random construction and for the original code. Again, it can be seen that the proposed construction and decoding algorithms provide almost the same performance as conventional sum-product decoding.

For the particular LDPC codes experimented with above, memory-saving (μ) is at least 23% for irregular case and at least 12.5% for the regular case. Note that this does not include the savings in memory from the address mapping of the LDPC code.

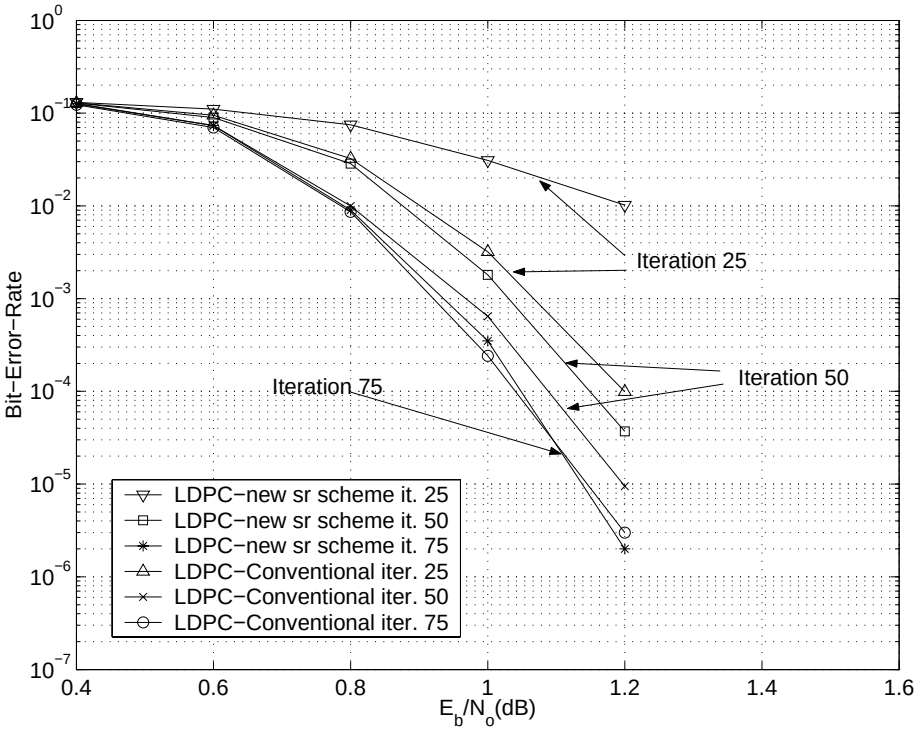

Fig. 37. BER plot comparing the new semi-random (sr) scheme with conventional LDPC (irregular) rate=0.5, N=10667

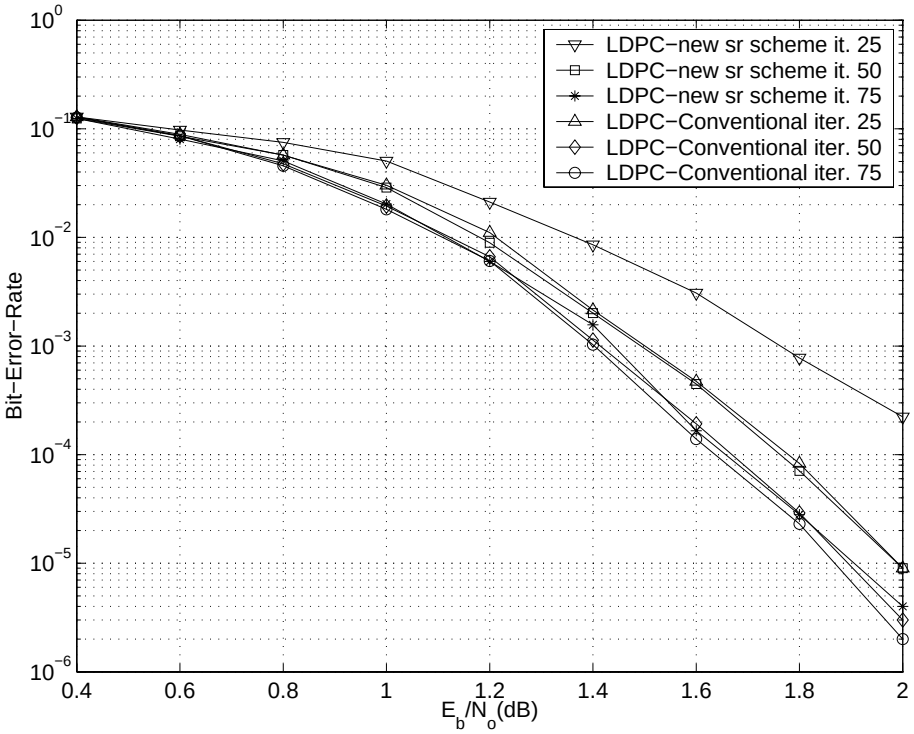

Fig. 38. BER plot comparing the new semi-random (sr) scheme with conventional LDPC (irregular) rate=0.5, N=2000

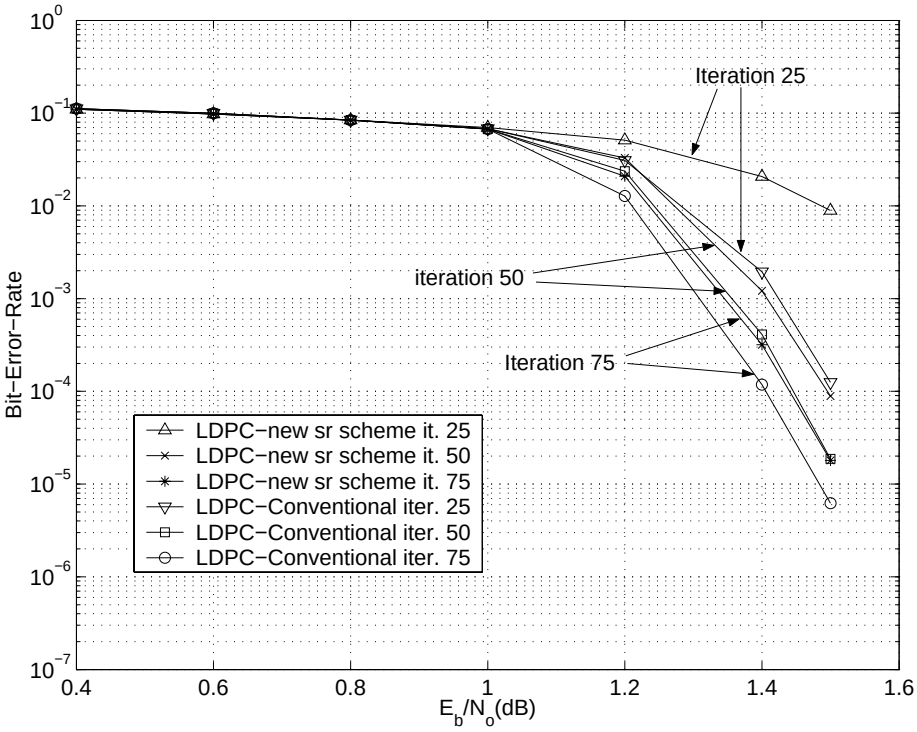

Fig. 39. BER plot comparing the new semi-random(sr) scheme with conventional LDPC (regular (3,6)) rate=0.5, N=16000

The new scheme implemented here leads to savings in memory with little sacrifice in performance. The analysis leads us to conclude that the proposed decoding scheme is just a minor variation of actual sum-product decoding as the thresholds are the same and the same deductions can be obtained from simulations. Even though the convergence is slightly slower for the proposed scheme, the focus of this work is on memory-saving. This scheme will especially come in handy in instances where memory at the receiver is a bottle-neck and complexity is not the issue, as in DSP applications. Splitting the graph into more than two halves will result in more memory-saving, but the resulting decoding algorithm will be more sub-optimal as correlated information will have to be exchanged between the subcodes. This has been considered in [62].

CHAPTER VIII

CONCLUSION AND FUTURE WORK

A. Conclusion

In this dissertation, we presented coding schemes for near-optimum performance over wireless channels. We classified the code-design problem into three categories:

1. Channel State Information (CSI) is available only to the receiver (CSIR).
2. CSI is not available to either the transmitter or the receiver and it has to be estimated from pilots which we denote as Partial CSI (PaCSI).
3. CSI is available to both the transmitter and the receiver (CSITR).

and designed robust coding schemes for each scenario separately. We designed coding schemes for high-order constellations when CSIR is available, based on bit-interleaved coded-modulation (BICM) and low-density parity-check (LDPC) codes. Multi-level coding with multi-stage decoding (MLC/MSD) achieves the capacity of this system, however, as we show through our work, finite-length performance can be quite different from infinite-length near-capacity performance. For the same complexity and latency, we show that LDPC codes used with a BICM scheme has an advantage of bit-error rate (BER) performance over MLC owing to higher overall code-length and thereby better error-exponents. This advantage is retained even when the code-length used for the scheme increases beyond a few tens of thousands. Thus BICM is not merely a pragmatic scheme, as often thought, but also a more optimal scheme for short code-lengths.

We further characterize the rate-diversity tradeoff of MIMO and MIMO-OFDM systems for a fixed constrained constellation (the tradeoff implicitly assumes CSIR and has significance only when CSIR is available). It is proved in our work that for SISO-OFDM systems, there is no tradeoff in rate in order to achieve all the frequency-diversity present in the system. Any good code with minimum distance more than a factor of L, the number of taps in the channel, can take advantage of all the frequency-diversity present in the system and the code-rate of such a code can tend to 1. For MIMO systems, the rate-diversity tradeoff has already been well-characterized and a scheme with LDPC codes as the outer-code and serial-parallel mapper as the inner code has been proved to achieve this rate-diversity tradeoff. ML decoder for this coding scheme is however a requirement to achieve the tradeoff. We show through simulations that with an iterative decoder for this scheme, performance very close to the tradeoff curve is obtainable. We also prove for a MIMO-OFDM system that if the coding scheme described above achieves a diversity of order N_d over the basic MIMO system, it will achieve diversity of order N_dL where L is the number of independent taps in the channel. This proof is valid asymptotically in the length of the LDPC code with an ML decoder. Through simulations, we show that this coding scheme performs very close to the predicted rate-diversity tradeoff for MIMO-OFDM systems with an iterative decoder and for finite lengths of the LDPC code.

Code design for PaCSI is performed on flat-fading channels where some pilots are transmitted to aid in decoding as well as obtaining CSI at the receiver. The object of this work is to minimize the amount of pilots as much as possible as pilots are expensive in terms of power and bandwidth. Instead, the strength of the code (here we use a non-systematic Irregular Repeat Accumulate (IRA) code) is used to derive and improve the CSI at the receiver with the help of an iterative decoding and channel estimation algorithm. For frequency-selective channels, OFDM can be used

to convert the channel into parallel flat-fading channels. We further design the code such that its EXIT chart is matched on an average (*i.e.* in ergodic sense) to that of the channel + channel estimator. The proposed scheme performs close to the receiver which has CSIR and also using a matched IRA code. The scheme is robust to changes in number of taps and time-delay profile of the channel and requires a very simple channel estimator.

For the case with CSITR, we consider a system with parallel flat-fading subchannels for transmission of data, similar to a multicarrier system. Here the sub-channel states are known perfectly to both the transmitter and the receiver. The results presented so far in literature for this system, have only considered maximizing the sum-rate with Gaussian constellations, which is not realizable in practice. We consider practical QAM constellations for transmission instead, the size of which can be varied across subchannels. Under this constraint, we derive the maximum sum-information-rate of the overall system and the power/rate allocation algorithm to achieve it, which has not been attempted before. A practical MIMO system can be resolved into parallel subchannels and we then extend the allocation algorithm to a MIMO case. We further constrain the system to use a single overall codebook which is more practical and optimize the proposed power/rate allocation algorithm under this constraint. The simulations with an LDPC code show that the proposed power/rate allocation method is very robust and the code performance is within 2dB of even the unconstrained Gaussian sum-rate limit for both cases.

B. Future Work

The future work can focus on the following areas:

1. LDPC Codes for High-Order Constellations

In Chapter III, we focussed on designing LDPC codes for a BICM scheme which also has properties of multi-level coding owing to the inherent unequal protection present in LDPC codes. Here the code-profiles were optimized separately for different constellations. In practice, for wireless communication systems, it is desirable to have rate-compatible coding schemes. The receiver usually estimates the channel and feeds back the modulation-coding scheme (MCS) that can be supported over the channel for the current channel state (unless reciprocity is present and the transmitter can estimate the channel and determine the MCS for the subsequent transmissions). For these different MCS formats, it is desirable to use the same LDPC code (but punctured for different code-rates) over different constellations, as requested in the MCS. It was observed in this work that the overall profiles of the LDPC code for different constellations for the same code-rate were not substantially different but only the sub-profiles were different for different bits in the mapped word. Thus a scheme can be devised where different bits of the same LDPC code are allocated to different bits in the mapped word of the constellation with the overall profile remaining the same. This problem again turns out to be an optimization problem. This proposed scheme can be further extended to OFDM systems where the relative SNRs of different subchannels is known to the transmitter and different bits of a single LDPC code have to allocated to these subchannels.

2. Rate-Diversity Tradeoff

Chapter IV discussed coding schemes for achieving the rate-diversity tradeoff of MIMO and MIMO-OFDM systems. It was shown that a coding scheme with LDPC as an outer code and a simple serial to parallel converter as an inner code can achieve

this tradeoff. However, an ML decoder for the overall scheme is required to achieve the tradeoff. We showed in the same chapter that performance very close to the tradeoff can be achieved with a sub-optimal iterative decoder. (i) It is an interesting problem to study the effect of using the sub-optimal iterative decoder and whether it leads to any penalties in performance. It would also be interesting to study if those penalties diminish as the length of the LDPC code-word increases. Also for some regions of the code-rates, higher diversity was observed for finite SNRs than what is available asymptotically. It is an interesting problem to learn if this occurence is due to the sub-optimal iterative decoder apart from the presence of many high-ranked codewords than low-ranked ones for those code-rates. The low-ranked codewords dominate at high SNRs and result in the diversity predicted by the tradeoff. (ii) Another question to be answered is: it was shown in the proofs that asymptotically in length of the LDPC code, all the frequency diversity present in the system is obtained for free at no expense of the code-rate - are there any finite-length LDPC codes which provably achieve the frequency-diversity at no expense of the code-rate. Because simulations of finite-length LDPC codes perform very close to the tradeoff it seems plausible that provably good finite-length LDPC codes with some structure can be found which achieve the tradeoff. (iii) can it be proved for this scheme that the coding gain obtained is greater than some number with very high probability - this will establish these schemes to be superior to any scheme presented so far in literature. Again, through simulations presented in this work, it can be conjectured that the coding gain is "good" for this coding scheme.

3. CSITR

a. Multi-user Information Theory

Multi-user information theory has a direct effect on the operation of cellular mobile systems. Design of efficient coding schemes, bandwidth and power allocation schemes are essential to maximize the overall throughput of these multi-user systems. The capacity regions of multiple access channels and broadcast channels have been characterized with Gaussian inputs. However, constrained inputs can change the overall capacity with CSI at the receiver as well as the transmitter. The power and rate-allocation schemes in this dissertation work in Chapter VI, apply to single-user case with CSITR where the channels are easily parallelized and power and rate can be allocated independently across the parallel subchannels. These algorithms have to be rederived when there are multiple-users in the system. Under the constraint of a practical constellation to transmit from, the problem is to maximize the overall throughput or a weighted throughput (with some degree of fairness guaranteed to each user). The solution to this type of problems is not as straightforward as a single-user case, as the cost function need not be convex. It is an interesting problem to design coding schemes and the associated signal processing at transmitter and receiver to maximize the overall information rate of the multi-user system with constrained constellations to transmit from.

b. Effect of Channel Uncertainty on Practical Wireless Systems

In practical wireless systems, perfect CSI is not available and CSI has to be estimated in order to improve the overall throughput of the system. There is always a certain amount of uncertainty in the CSI owing to noise in channel estimation algorithms. Resources in the form of transmit power and bandwidth have to be allocated to

estimate CSI. Needless to say, these resources are expensive and they have to be used efficiently. CSI at the receiver is obtained through pilots transmitted along with data. CSI at transmitter can be obtained through different methods. In TDD systems, the forward and reverse channels can be assumed to be the same (reciprocity) and the estimate obtained for one direction can be used for the other. In this case, energy and bandwidth spent for pilots is sufficient to obtain channel estimates in both directions. In some other systems such as FDD systems, reciprocity does not hold and hence the channel estimates at the receiver have to be fed back to the transmitter. CSI to be fed back, can be compressed using a source-code and then channel-coded for protection against errors in the channel. Feedback requires additional bandwidth and power apart from those allocated to the pilots. The quality of channel estimates is a direct function of the resources allocated to the pilots and feedback, as well as the channel estimation and source-coding algorithms. The use of power and bandwith for CSI determination in turn reduces the resources available for transmission of data-traffic which results in reduced throughput. Hence there is a tradeoff between channel uncertainty and the overall throughput of the system which has to be optimized. The optimal point in this tradeoff is also a function of the specific channel estimation algorithm applied, feedback strategy, and the transmitter rate and power allocation algorithms if present. Thus there is the need to characterize and understand the effect of channel uncertainty in wireless systems. There is also the fundamental question of when CSI at the receiver and/or the transmitter can improve the overall performance of the system, which has to be addressed. For some values of CSI, there can be tremendous increase in the overall throughput while for some others there will be negligible gain.

c. Outage Calculation

A by-product of the exponential expressions used to approximate constrained capacity in Chapter VI is to use them in determining the outage probabilities with constrained constellations to transmit from, when CSIR is available, over both SISO and MIMO systems. The problem of outage determination for constrained constellations with CSIR is complicated and can only be determined through simulations. These approximations for capacity can result in closed-form expressions for the outage probability with constrained constellations.

REFERENCES

[1] H. Bolcskei and A. J. Paulraj, "Space-frequency coded broadband OFDM systems," in *Proc. IEEE WCNC 2000*, Chicago, IL, Sept. 2000, vol. 1, pp. 1–6.

[2] C.E. Shannon, "A mathematical theory of communication," in *Bell System Technical Journal*, July/Oct. 1948, vol. 27, pp. 611–644 and 623–656.

[3] H. Sankar, N. Sindhushayana, and K.R. Narayanan, "Design of LDPC codes for high order constellations," in *Proc. IEEE Globecom '04*, Dallas, TX, Nov. 2004, vol. 5, pp. 3113–3117.

[4] U. Wachsmann, R.F.H. Fischer, and J.B. Huber, "Multilevel codes: Theoretical concepts and practical design rules," *IEEE Trans. Inform. Theory*, vol. 45, no. 5, pp. 1361–1391, July 1999.

[5] G. Caire, G. Tarrico, and E. Biglieri, "Bit-interleaved coded modulation," *IEEE Trans. Inform. Theory*, vol. 44, no. 5, pp. 927–946, May 1998.

[6] H.-F. Lu and P. Vijay Kumar, "Rate-diversity tradeoff of space-time codes with fixed alphabet and optimal constructions for psk modulation," *IEEE Trans. Inform. Theory*, vol. 49, no. 10, pp. 2747–2751, Oct. 2003.

[7] H. Sankar and K.R. Narayanan, "Design of variable-rate variable-diversity space-time and space-frequency-time systems with low-density parity-check codes," in preparation.

[8] H. Sankar and K.R. Narayanan, "Design of IRA codes for OFDM with partial CSI," in *Proc. WCNG Conf.*, Austin, Texas, Oct. 2003, vol. 1, pp. 120–125.

[9] H. Sankar and K. R. Narayanan, "Design of IRA codes for OFDM with partial CSI," *IEEE Trans. Wireless Commun.*, vol. 4, no. 5, pp. 2491–2497, Sept. 2005.

[10] S. ten Brink and G. Kramer, "Design of repeat-accumulate codes for iterative detection and decoding," *IEEE Trans. Signal Processing*, vol. 51, no. 11, pp. 2764–2772, Nov. 2003.

[11] K. R. Narayanan, D. N. Doan, and R. V. Tamma, "Design and analysis of LDPC codes for turbo equalization with optimal and sub-optimal soft output equalizers," in *40th Allerton Conference*, Monticello, IL, USA, Oct. 2002, pp. 236–240.

[12] H. Sankar and K.R. Narayanan, "Design of low density parity check codes for adaptive modulation with practical constraints," in *Proc. IEEE ICC*, Istanbul, Turkey, June 2006, to appear.

[13] G. Caire, G. Taricco, and E. Biglieri, "Optimum power control over fading channels," *IEEE Trans. Inform. Theory*, vol. 45, no. 5, pp. 1468–1489, July 1999.

[14] H. Sankar and K. R. Narayanan, "Memory-efficient sum-product decoding of LDPC codes," *IEEE Trans. Commun.*, vol. 52, no. 8, pp. 1225–1230, Aug. 2004.

[15] R. W. Chang, "Synthesis of band-limited orthogonal signals for multichannel data transmission," *Bell Systems Technical Journal*, vol. 45, pp. 1775–1796, Dec. 1966.

[16] D. J. C. MacKay and R. M. Neal, "Near Shannon limit performance of low-density parity-check codes," *Electron. Lett.*, vol. 32, pp. 1645–1646, Aug. 1996.

[17] J. Proakis, *Digital Communications*, third edition, McGraw-Hill, Singapore, 1995.

[18] G. L. Stuber, *Principles of Mobile Communications*, Kluwer Academic Publishers, Cambridge, MA, 1996.

[19] V. Tarokh, N. Seshadri, and A. R. Calderbank, "Space-time codes for high data rate wireless communications: Performance criterion and code construction," *IEEE Trans. Inform. Theory*, vol. 44, no. 2, pp. 744–765, Mar. 1998.

[20] L. Zheng and D. Tse, "Diversity and multiplexing: A fundamental tradeoff in multiple antenna channels," *IEEE Trans. Inform. Theory*, vol. 49, no. 5, pp. 1073–1096, May 2003.

[21] D. Tse and P. Viswanath, *Fundamentals of Wireless Communication*, first edition, Cambridge University Press, New York, 2005.

[22] J. W. Cooley and J. W. Tukey, "An algorithm for the machine calculation of complex Fourier series," *Mathematics Computing Journal*, vol. 19, pp. 297–301, 1965.

[23] R. G. Gallager, *Low-Density Parity Check Codes*, MIT Press, Cambridge, MA, 1963.

[24] N. Wiberg, "Codes and decoding on general graphs," Ph.D. dissertation, Dept. Elec. Eng. Linkoping Univ., Linkoping, Sweden, 1996.

[25] T. Richardson and R. L. Urbanke, "The capacity of low-density parity-check codes under message-passing decoding," *IEEE Trans. Inform. Theory*, vol. 47, no. 2, pp. 599–618, Feb. 2001.

[26] S. Y. Chung, T. J. Richardson, and R. L. Urbanke, "Analysis of sum-product decoding of low-desity parity-check codes using a Gaussian approximation," *IEEE Trans. Inform. Theory*, vol. 47, no. 2, pp. 657–670, Feb. 2001.

[27] H. Sankar, N. Sindhushayana, and K.R. Narayanan, "Design of low density parity check codes for high order constellations," in preparation.

[28] J. Hou, P.H. Siegel, L.B. Milstein, and D. Pfister, "Capacity-approaching bandwidth-efficient coded modulation schemes based on low-density parity-check codes," *IEEE Trans. Inform. Theory*, vol. 49, no. 9, pp. 2141–2155, Sept. 2003.

[29] R. Narayanaswami, "Coded modulation with low-density parity-check codes," M.S. thesis, Texas A&M Univ., College Station, Texas, June 2001.

[30] C. Berrou, A. Glavieux, and P. Thitimajshima, "Near Shannon limit error-correcting coding and decoding: Turbo codes," in *Proc. IEEE International Conference on Communications*, Geneva, Switzerland, May 1993, pp. 1064–1070.

[31] J. Hou, P.H. Siegel, L.B. Milstein, and D. Pfister, "Multilevel coding with low-density parity-check component codes," in *Proc. IEEE Globecom '01*, San Antonio, TX, USA, Nov. 2001, vol. 2, pp. 1016–1020.

[32] Y. Wang, R. Omrani, K. M. Chugg, and P. Vijay Kumar, "Low-density parity-check space-time codes: Performance analysis and code construction," in *Proc. IEEE Sym. on Information Theory (ISIT)*, Chicago, IL, USA, June/July 2004, p. 156.

[33] Z. Liu, Y. Xin, and G. B. Giannakis, "Space-time-frequency block-coded OFDM with subcarrier grouping and constellation precoding," in *Proc. IEEE ICASSP '02*, Oct. 2002, vol. 3, pp. 2205–2208.

[34] H. Bolcskei and A. J. Paulraj, "Space-frequency coded MIMO-OFDM with variable multiplexing-diversity tradeoff," in *Proc. IEEE ICC 2003*, Anchorage, AK, May 2003, vol. 4, pp. 2837–2841.

[35] A. Ashikhmin, G. Kramer, and S. ten Brink, "Extrinsic information transfer functions: model and erasure channel properties," *IEEE Trans. Inform. Theory*, vol. 50, no. 11, pp. 2657–2673, Nov. 2004.

[36] H. El Gammal, A. R. Hammons Jr., Y. Liu, M. P. Fitz, and O. Y. Takeshita, "On the design of space-time and space-frequency codes for MIMO frequency-selective fading channels," *IEEE Trans. Inform. Theory*, vol. 49, no. 9, pp. 2277–2292, Sept. 2003.

[37] H. Jin, A. Khandekar, and R. McEliece, "Irregular repeat-accumulate codes," in *Proc. IEEE International Symposium on Turbo Codes*, Brest, France, Sept. 2000, pp. 1–8.

[38] N. Varnica and A. Kavčić, "Optimized low-density parity-check codes for partial response channels," *IEEE Communications Letters*, vol. 7, no. 4, pp. 168–170, Apr. 2003.

[39] D. N. Doan and K. R. Narayanan, "Some new results on code design for inter-symbol interference ISI channels with turbo equalization," in *Proc. IEEE International Conf. on Comm.*, New York, NY, May 2002, vol. 3, pp. 1873–1877.

[40] Y. Li, N. Seshadri, and S. Ariyavisitakul, "Channel estimation for OFDM systems with transmitter diversity in mobile wireless channels," *IEEE J. Select. Areas Commun.*, vol. 17, no. 3, pp. 461–471, Mar. 1999.

[41] Y. Li, L. J. Cimini Jr., and N. R. Sollenberger, "Robust channel estimation for

OFDM systems with rapid dispersive fading channels," *IEEE Trans. Commun.*, vol. 46, no. 7, pp. 902–915, July 1998.

[42] A. Grant and C. Schlegel, "Differential turbo space-time coding," in *Proc. Information Theory Workshop 2001*, Cairns, Australia, Sept. 2001, pp. 120–122.

[43] L. H.-J. Lampe and R. Schober, "Bit-interleaved coded differential space-time modulation," *IEEE Trans. Commun.*, vol. 50, no. 9, pp. 1429–1439, Sept. 2002.

[44] J. Li, "Low complexity capacity approaching schemes: Design, analysis and applications," Ph.D. dissertation, Texas A&M University, College Station, USA, 2002.

[45] Y. Yao and M. M. K. Howlader, "Serial concatenated single differential space-time coded OFDM system," in *Proc. IEEE ICC 2003*, Anchorage, AK, May 2003, vol. 5, pp. 3150–3154.

[46] M. K. Simon and M. S. Alouini, *Digital Communication over Fading Channels*, John Wiley and Sons, New York, NY, 2000.

[47] G. Caire and S. Shamai, "On the capacity of some channels with channel side information," *IEEE Trans. Inform. Theory*, vol. 45, no. 6, pp. 2007–2019, Sept. 1999.

[48] A. Goldsmith and P. P. Varaiya, "Capacity of fading channels with channel side information," *IEEE Trans. Inform. Theory*, vol. 43, no. 6, pp. 1986–1992, Nov. 1997.

[49] H. Sankar and K.R. Narayanan, "Design of low density parity check codes for adaptive modulation with practical constraints," in preparation.

[50] P. S. Chow, J. M. Cioffi, and J. A. C. Bingham, "A practical discrete multitone transceiver loading algorithm for data transmission over spectrally shaped channels," *IEEE Trans. Commun.*, vol. 43, no. 3, pp. 773–775, Feb. 1995.

[51] Enzo Baccarelli, Antonio Fasano, and Mauro Biagi, "Novel efficient bit-loading algorithms for peak-energy-limited ADSL-type multicarrier systems," *IEEE Trans. Signal Processing*, vol. 50, no. 5, pp. 1237–1247, May 2002.

[52] A. Goldsmith and P. P. Varaiya, "Variable-rate variable-power MQAM for fading channels," *IEEE Trans. Commun.*, vol. 45, no. 10, pp. 1218–1230, Oct. 1997.

[53] S. Vishwanath and A. Goldsmith, "Adaptive turbo coded modulation for flat fading channels," *IEEE Trans. Commun.*, vol. 51, no. 6, pp. 964–972, June 2003.

[54] J. Zheng, "Analysis of coded OFDM system over frequency-selective fading channels," M.S. thesis, Texas A&M Univ., College Station, Texas, June 2003.

[55] T.M. Cover, *Elements of Information Theory*, John Wiley & Sons, Inc., New York, 1991.

[56] G. Ungerboeck, "Channel coding with multilevel/phase signals," *IEEE Trans. Inform. Theory*, vol. 28, no. 1, pp. 55–67, Jan. 1982.

[57] J. Zheng and S. L. Miller, "Performance analysis of coded OFDM systems over frequency-selective fading channels," in *Proc. IEEE Globecom '03*, San Francisco, CA, USA, Dec. 2003, vol. 3, pp. 1623–1627.

[58] S. Boyd and L. Vandenberghe, *Convex Optimization*, Cambridge University Press, Cambridge, UK, 2004.

[59] A. Lozano, A. Tulino, and S. Verdu, "Mercury/waterfilling: Optimum power allocation with arbitrary input constellations," in *Proc. IEEE Sym. on Information Theory (ISIT)*, Adelaide, Australia, Sept. 2005, pp. 31–35.

[60] D. Guo, S. Shamai, and S. Verdu, "Mutual information and minimum mean-square error in Gaussian channels," *IEEE Trans. Inform. Theory*, vol. 51, no. 4, pp. 1261–1283, Apr. 2005.

[61] I. E. Telatar, "Capacity of multi-antenna Gaussian channels," in *European Trans. on Telecommunications*, Nov. 1999, vol. 10, no. 6, pp. 582–595.

[62] N. R. Shanbhag M. M. Mansour, "Memory-efficient turbo decoder architectures for LDPC codes," in *Proc. IEEE SIPS 2002*, Oct. 2002, pp. 120–124.

[63] H. Behairy and S. Chang, "Parallel concatenated Gallager codes," *IEE Electronic Letters*, vol. 36, no. 24, pp. 2025–2026, Nov. 2000.

APPENDIX A

POWER ALLOCATION WITH CONSTRAINED CONSTELLATION

The maximization of sum-information rate in Chapter VI is considered under the approximation of the constrained capacity by a single exponential function. The optimization problem can be stated as follows:

$$I_M(\Gamma|\alpha) = \sum_{m=1}^{M} a_m \left[1 - \exp\left(-\frac{b_m \alpha_m^2 \gamma_m}{\sigma^2}\right)\right] \tag{A.1}$$

where $I_M(\Gamma|\alpha)$ is the sum-rate, γ_m is the power allocated to the m-th subchannel, subject to the power constraint:

$$\frac{1}{M}\sum_{m=1}^{M} \gamma_m \leq \mathbf{P}. \tag{A.2}$$

Define:

$$J = \sum_{m=1}^{M} a_m \left[1 - \exp\left(-\frac{b_m \alpha_m^2 \gamma_m}{\sigma^2}\right)\right] - \frac{1}{\mu'}\left(\frac{1}{M}\sum_{m=1}^{M} \gamma_m - \mathbf{P}\right) \tag{A.3}$$

Setting $\frac{\partial J}{\partial \gamma_m} = 0$ results in the solution to the constrained optimization problem. This implies:

$$\frac{a_m b_m \alpha_m^2}{\sigma^2} \exp\left(-\frac{b_m \alpha_m^2 \gamma_m}{\sigma^2}\right) - \frac{1}{\mu' M} = 0 \tag{A.4}$$

Denote $\mu' M = \mu$. Solution to Eqn. (A.4) can be easily obtained to be:

$$\gamma_m = \frac{\sigma^2}{b_m \alpha_m^2}\left[\log \mu - \log \frac{\sigma^2}{a_m b_m \alpha_m^2}\right]^+ \tag{A.5}$$

VITA

Hari Sankar received the B.S. degree in electrical engineering from the Indian Institute of Technology, Madras (IIT-M), India, in 2000. He received his Ph.D. degree in electrical engineering at Texas A&M University, College Station in August 2006. His research interests include channel coding schemes for wireless communications with emphasis on low-density parity-check (LDPC) code iterative detection and decoding techniques, near-capacity performing adaptive modulation schemes, and multiple-input multiple-output (MIMO) systems.

Address:

c/o Dr. Krishna R. Narayanan,

Dept. of Electrical Engineering,

Texas A&M University,

College Station, TX 77843.